COMPREHENSIVE PLANNING OF URBAN DRAINAGE FOR FLOOD CONTROL

Submitted in partial fulfilment of the requirements
for the award of the degree of

DOCTOR OF PHILOSOPHY
in
CIVIL ENGINEERING

by

B. ANEESHA SATYA

(Roll No: 716001)

Supervisor

Dr. M. Shashi

DEPARTMENT OF CIVIL ENGINEERING

NATIONAL INSTITUTE OF TECHNOLOGY

WARANGAL- 506004 INDIA

January 2023

NATIONAL INSTITUTE OF TECHNOLOGY

WARANGAL

CERTIFICATE

This is to certify that the thesis entitled "**COMPREHENSIVE PLANNING OF URBAN WATER DRAINAGE FOR FLOOD CONTROL"** being submitted by **Ms B. Aneesha Satya** for the award of the degree of **DOCTOR OF PHILOSOPHY** to the Faculty of Engineering and Technology of **NATIONAL INSTITUTE OF TECHNOLOGY, WARANGAL** is a record of bonafide research work carried out by her under my supervision and it has not been submitted elsewhere for award of any degree.

Dr. M. Shashi
Thesis Supervisor
Associate Professor
Department of Civil Engineering
National Institute of Technology Warangal
Warangal – INDIA

APPROVAL SHEET

This Thesis entitled "**COMPREHENSIVE PLANNING OF URBAN WATER DRAINAGE FOR FLOOD CONTROL**" by **Ms B. Aneesha Satya** is approved for the degree of Doctor of Philosophy.

Examiners

_____

_____

_____

Supervisor

_____

Chairman

_____

Date: _____

DECLARATION

This is to certify that the work presented in the thesis entitled **"COMPREHENSIVE PLANNING OF URBAN WATER DRAINAGE FOR FLOOD CONTROL"** is a bonafide work done by me under the supervision of **Dr. M. Shashi, Associate Professor, Department of Civil Engineeirng,** was not submitted elsewhere for the award of any degree. I declare that this written submission represents my ideas in my own words and where other ideas or words have been included, I have adequately cited and referenced the original sources. I also declare that I have adhered to all principles of academic honesty and integrity and have not misrepresented or fabricated or falsified any idea / data / fact /source in my submission. I accept that any breach of the aforementioned will result in disciplinary action by the Institute, as well as legal action from the sources that have not been correctly referenced or from whose permission has not been obtained when necessary.

_____

(**B. Aneesha Satya**)

(Roll No: **716001**)

Date: _____

Dedicated To

My family who supported me throughout the journey

ACKNOWLEDGEMENTS

With great pleasure and proud privilege, I manifest my heartier thankfulness to my research supervisor, **Dr. M. Shashi**, Department of Civil Engineering, for his valuable suggestions, sagacious guidance, scholarly advice and comprehensive critical remarks in bringing out this research work with artistry. I am very much honoured to work under him and I will be grateful to him for my whole life.

I am also thankful to my mentor, well-wisher Prof Deva Pratap, Department of Civil Engineering for his valuable suggestions and comments throughout my Ph.D. program. I am perspicuous to divulge my sincere gratitude to Dr Gunneswara Rao T. D, Head, Department of Civil Engineering and Chairman and member of my Doctoral Scrutiny Committee for his enlightening guidance and immense help rendered in bringing out this work.

I am grateful, and I express my deep sense of gratitude, my sincere and heartfelt thanks to the members of the Doctoral Scrutiny Committee, in the Department of Civil Engineering, Dr. K. V. R. Ravi Shankar, Associate Professor, Department of Civil Engineering; Dr. S. Ravi Chandra, Professor in the Department of Computer Science and Engineering, National Institute of Technology, Warangal for their guidance and help during the investigation.

I am also thankful to the other faculty members of Remote Sensing and GIS, Professor Dr. K.Venkata Reddy, Dr. Manali Pal for the moral support given during the period of research work.

I thank my friends and fellow research scholars Mr. Kumarapu Kumar, Mr. Allu Ayappa Reddy Ayyapa, Mr. P V S Sylesh, Ms Tharani Kotrike, Mr. Buri Eswar Sai, Ms. Loukika K N, Mr. Kopparavuri Rambrahmam, Ms. Sri Lakshmi Sesha Vani Jayanthi, Mr. Nagireddy for their support during the period of my research work.

Finally, I thank everyone, who contributed either directly or indirectly in the successful completion of this work.

- **B. Aneesha Satya**

ABSTRACT

Pavements and concrete slabs are examples of the impermeable layers that have been added to naturally occurring land surfaces because of urbanization. Changing natural water systems, such as habitat modification, increasing runoff volume and rate, lowering infiltration, and raising flood hazards, are all examples of hydrological impact of urbanization. Storm drainage systems, which receive runoff from these types of impervious surfaces, are unable to process greater amounts of rainfall, resulting in more intense floods. Stormwater runoff from impermeable areas and water bodies can cause negative consequences in the urban areas if the drainage capacity is not adequate. A city's population density also affects the way land use and cover (LULC) evolve over time. Modeling techniques such as Artificial Intelligence can be used to handle the issue of LULC conversion and modification, which has become a major focus in recent years. Satellite imagery is said to have been stressed as a powerful tool for analyzing and understanding earth systems because of LULC change. Most of the rivers and streams have seen significant changes in the past that have a significant impact on urban drainage. Although the impacts of LULC change on urban runoff have been previously explored, the study combined the current stream changes and projection of LULC change is not explored.

Personal Computer Storm Water Management Model (PCSWMM) is a dynamic hydrological and hydraulic model capable of simulating runoff quantities areas in urban and rural that can be used for urban drainage infrastructural design and management. Several Structural and non-structural methods of flood control are in use to reduce the risk of flooding. Structural measures involve engineered or manufactured systems, whereas non-structural solutions include insurance policies, land-use restrictions, source controls and proper maintenance. The risk of flooding can be greatly reduced by the

reduction of excess runoff at the source by implementing the Sustainable Drainage Systems (SuDS). SuDS reduce the impact of new and existing developments with respect to water in both rural and urban areas by replicated natural systems. According to this study, SuDS strategies in developing cities are to be evaluated for their effectiveness in reducing flood risk. As a result, the anticipated SuDS hydrological consequences were simulated and examined using hydrological simulation models powered by strong engines.

CONTENTS

LIST OF TABLES

LIST OF FIGURES

LIST OF ABBREVIATIONS

1D	One Dimension
2D	Two Dimension
AHP	Analytical Hierarchical Process
AMRUT	Atal Mission for Rejuvenation and Urban Transformation
ANN	Artificial Neural Networks
BMPs	Best Management Practices
CN	Curve Number
DEM	Digital Elevation Model
FHI	Flood Hazard Index
GIS	Geographic Information System
GPM	Global Precipitation Measurement
IDF	Intensity Duration Frequency
LID	Low Impact Development
LR	Logistic Regression
LULC	Land Use Land Cover
MCDA	Multi-Criteria Decision Analysis
ML	Maximum Likelihood
PCSWMM	Personal Computer Storm Water Management Model
RIW	Relative Importance Weights
RS	Remote Sensing
SCP	Sponge City Program
SuDS	Sustainable (Urban) Drainage Systems
USGS	United States Geological Survey
WMC	Warangal Municipal Corporation
WSUD	Water Sensitive Urban Design

CHAPTER 1
Introduction

1.0 General

Natural disasters caused by climate change and environmental degradation have regularly influenced humans, and their influence has considerably grown in recent decades. Flooding is one such disaster, and in cities, it is defined as "the submergence of normally dry areas by a substantial amount of water caused by unexpected extreme rainfall, an overflowing river or lake, melting snow, or an exceptionally high tide." Moradi et al. (2019) say that the growing trend of urban flooding is a worldwide problem that poses a big challenge to city managers and urban planners everywhere. The issues associated with urban floods range from minor to severe incidents, with cities being inundated for a few hours to several days. Because of this, there can be a wide range of effects, such as people moving away temporarily, damage to public facilities, a drop in water quality, and the possibility of diseases.

A hazard is a harmful physical phenomenon that can end up in causing death or injury, damage to property or the environment, and social or economic loss. The hazard of flooding can be categorized into three groups: primary dangers, which happen when people encounter water; secondary dangers, which happen because of the flooding, like service interruptions; health effects, like famine and disease; and tertiary effects, like shifting river channels. Changes in land-use planning, the use of specific flood-proofing measures, the creation of emergency response plans, and other steps can help people be more ready. Flood Hazard mapping is an important part of planning how to utilize land in areas that are likely to flood. The flood hazard maps make it easier to find areas at risk of flooding and help prioritise efforts to prevent and deal with flooding (Bapulu & Sinha, 2005). Flood hazard assessment can be made even more detailed by looking at specific risks based on the social and economic factors (like industrial activities, population density, and land use) of the areas that are at risk. For example, areas that are likely to need to be evacuated can be found and evacuation routes can be planned ahead of time so that local people know what to do in case of an emergency. In order to reduce the risk of flooding in cities, each city's flood prevention measures (like floodplains, river basins, surface water, etc.) should be firmly built into the city's overall land use policy and master planning.

1.1 Flood a natural disaster

Changes in land use and floodplains during urban development affect flooding in many ways. The transition from a natural to an artificial landscape during urbanization considerably alters rainwater circulation and storage at ground level within a particular watershed. Three of the most essential components of planning that increase the area's imperviousness are encroachments that result in filling up natural drainage, ignoring storm water drains, and concreting open space. Water cannot penetrate paved impervious surfaces naturally, which reduces the rate of infiltration, possibly causing soil erosion and floods (Dingman 2015). Many waterbodies have vanished or dried up because of construction that has gone in the direction of natural drainage. When the rate of precipitation exceeds the maximum rate of infiltration, the excess precipitation is released as runoff into a local water system. Storm water drains, which are frequently placed close to the edge of the road, collect rainwater from impermeable surfaces including pavement, roadways, and rooftops. Typically, the annual maximum discharge in a stream, in comparison to the annual maximum discharge in rural areas, will increase as urban development occurs. Early studies used historical field measurements from river gauges and rainfall gauging stations to link to the severity and frequency of urban flooding (Moscrip and Montgomery 1997). Modern nonstationary flood-frequency models have been employed in times that are more recent to demonstrate that urbanization has a statistically significant impact on the increasing magnitude and frequency of floods (Villarini et al. 2009; Prosdocimi et al. 2015). Over the last few years (CRED, 2016), there has been an increasing trend of urban flood disasters in India, with major cities being badly hit: Hyderabad in 2000, Ahmedabad in 2001, Delhi in 2002 and 2003, Chennai in 2004, Mumbai in 2005, Surat in 2006, Kolkata in 2007, Jamshedpur in 2008, Delhi in 2009, and Guwahati and Delhi in 2010. Srinagar in 2014 and Chennai in 2015 are among the most notable.

1.2 Urban Storm Water Management

Due to urban land cover, impermeable surfaces, and the interruption of natural runoff, huge q uantities of peak runoff discharge are created, altering the natural hydrological pattern and cy cle therefore causing localized flooding. An extreme runoff load event leads storm water to c ombine with sewage and flow into natural stream and river systems.Cities are reinventing, res toring, and releasing natural hydrological systems, including rivers, natural drains, and wetlan ds, for environmental and social benefits. Thus, the drainage system and stormwater management should be adjusted to offset the negative consequences of the new hydrological

circumstances of precipitation and runoff in urban areas. Urban stormwater extreme events are considered a threat to urban infrastructure, the urban economy, and the urban ecosystem when not planned and managed properly. Urban stormwater management is a tool to provide flow rate control. Some urban stormwater management technologies are already in place that control the runoff quantity at or near the source (decentralized technologies). These stormwater management methods integrate quality, quantity, social and economic views at the source and are named differently in a few parts of the world: Low Impact Development (LID) or Best Management Practices (BMPs), Water Sensitive Urban Design (WSUD), Sustainable Urban Drainage Systems (SuDS), and the Sponge City programme (SCP) (Hoang and R.A. Fenner, 2016). Urban hydrology is essential to the system for managing stormwater in cities. The combined effects of land use patterns, climate change, ecology, waste reuse and its treatment, socioeconomic factors must all be taken into account in order to get the best results. Urban drainage systems must be robust and sustainable in order to handle rainwater more effectively.

1.3 Flood mitigation measures using sustainable drainage systems

Keeping the built-up area away from floodplains and areas with high flood hazards is one strategy to reduce the probability of flooding. In locations where building has already encroached, flood control measures must be taken into consideration. New construction in flood-prone areas must be constantly monitored and supervised. Despite the fact that mitigation measures are often associated with construction operations, it is possible to distinguish between non-structural and structural flood control strategies. Structural measures are projects that alter the structure in order to sustain or improve runoff. Non-structural mitigation approaches, such as standards, norms, and technical suggestions, are used to prepare organisations and citizens for the adoption of these standards. In addition to reducing flood hazards, these systems help recharge groundwater and store water for dry seasons. It only makes sense to invest in making our cities robust so that, in the event of a disaster, we can resume normal operations with the fewest possible fatalities and losses of property. Numerous nations found that the outdated urban drainage system was improperly managed, operated, and maintained. Initiatives from the Indian government, such as the Sponge Cities mission and the Atal Mission for Rejuvenation and Urban Transformation (AMRUT), can significantly aid local governments in planning cities with flood risks in mind.

Drainage systems in the cities are increasingly recognised and encircled by the new idea of SuDS, which integrates urban expansion and environmental adaptation, a water-supply

strategy, and flood control. SuDS considered is a practice that use or mimic natural processes that result in the infiltration, evapotranspiration or use of stormwater in order to protect water quality and associated aquatic habitat. When a natural environment is created, a large portion of the surfaces, such as buildings, roads, and parking lots, become impervious. As a result, previously infiltrated water now flows through the area, necessitating the need to pick, transfer, and pour the natural environment at precise spots. It also prevents rain from penetrating the ground and replenishing aquifers. It is desired that the hydrological response of a developed region be as close to where it was in its original state as possible through the deployment of SuDS. Considering not just the necessity of evacuating rainfall, but also the necessity of doing so in a sustainable manner, with reduced peak flows and adequate quality is what describe the SuDS. SuDS approaches utilize soils, vegetation, and rainwater harvesting techniques to preserve, restore, and generate green space at both the site and regional scales. Along with the government adopting these actions, there need to be public education regarding the risks associated with purchasing real estate near floodplains or in low-lying areas. Although such actions might not provide immediate benefits, they might in the future produce noticeable results. Stormwater runoff peak and volume have received the most credit for the hydrological impacts of SuDS policies. Despite widespread acceptance that SuDS techniques may successfully manage storm runoff, their flood control capabilities at broad scales are little understood. A case study in Warangal Municipal Corporation was used to demonstrate the use of SuDS strategies in an urban watershed to prevent flooding. This study intends to provide a more complete view to assist municipalities and metropolitan districts in their efforts to manage urban flooding.

1.4 Motivation for the study

One of the most densely populated areas of Warangal city is the Warangal Municipal Corporation (WMC). Warangal's water supply, irrigation, and drinking water all come from the Kakatiya Canal. A number of different sources, including chain tanks, which are fed by rains during the season, supplements the city’s drinking water supply. The area receives an average of 800 mm of rain each year, with the heaviest rainfall occurring in July, August, and September. As part of the unplanned development along the Kakatiya canal watercourse, encroachments have become a major problem in the study region. Increased imperviousness and lower infiltration rates have been caused by these encroachments, which are responsible for sealing natural drainage. Storm water has overflowed roadways due to changes in waterways caused by urban construction. Moreover, owing to the changes in land use, the

increasing areas of the impermeable cover change the run-off mode and reduce the capacity of water storage and penetration. Thus, the study's first focus is on flood risk assessment and the response phase of flood disasters via simulation methodologies and technology. The effective management of stormwater runoff is essential in order to prevent urban flooding in the future. There was a need for a concept known as SuDS that would link the implementation of SuDS with the existing stormwater drainage system based on current climatic variables, such as rainfall and land usage.

This research work presents an approach to understand and model the urban flooding, which can help in the planning and effective management of flood mitigation measures. From the detailed literature review, it is clear that there is a research gap in modelling of the urban flood due to its complex nature. A framework is developed to study hydraulic and hydrological characteristics of the flood in urban area. The study also compares different scenarios to understand the mitigation of the flood.

1.5 Thesis Organization

The complete thesis is organized as per the following chapters:

i. **Chapter 1** of the thesis motivates the necessity of this study and discusses: a) Impact of urbanization on urban floods; b) Sustainable urban drainage; c) Flood mitigation measures, details the scope and objectives of the investigation.

ii. **Chapter 2** reviews the literature on the gaps in the literature are summarized.

iii. **Chapter 3** details the scope and objectives of the investigation.

iv. **Chapter 4** includes the mapping of flood hazard in the study area.

v. **Chapter 5** explains the future LULC prediction analysis.

vi. **Chapter 6** demonstrates the integrated runoff modelling of the storm water drainage network.

vii. **Chapter 7** presents the evaluation of SuDS for flood control reduction.

viii. **Chapter 8** presents the conclusions and the scope for further study.

CHAPTER 2

Review of Literature

2.0 General

In the previous chapter, the concept of urban flood and its risk, urban flood modeling, and the need to mitigate the issues in urban stormwater management were addressed. In the present chapter, the details of the extensive research of the studies that were reported earlier with regard to the study of urban flooding are discussed. A brief report of the literature study is presented below.

2.1Review of literature on urban flood and its risk

Meyer and Messner (2006), contributed to the current challenge in flood risk data analysis, which is to improve knowledge of the interactions and social-economic dynamics of flood risk, For the flood damage assessment, vulnerability, preparedness by flood management a contemporary design of flood damage analysis and flood risk management is delivered in the research.

Grimm et al. (2008), talked about how the ecology of cities is changing globally. Production and consumption change land use, biodiversity, and hydrosystems on a local to regional scale. However, in cities, local changes in the environment are more important than global changes in the environment. In a world where urbanisation brings both environmental problems and solutions, urban ecology employs both natural and social sciences to investigate these drastically altered local habitats and their regional and global consequences.

Zevenbergen and Gersonious (2008), attempts to manage water and flood risk in a more integrated way. In a resilient approach, the goal is to deal with flood waters while minimizing their effects and getting back to normal quickly. Spatial solutions (differentiating levels for different land uses based on how vulnerable they are) may be important ways to reduce flood damage, while making buildings flood-proof improves the system's ability to recover. In this paper, it is argued that cities play a big role in the transition from traditional flood management methods to ones that are more flexible and adaptable at different spatial and temporal scales.

Estoque and Murayama (2015), compared spatial urbanisation and landscape changes using remote sensing and GIS. Understanding the intensity and spatial pattern of urban land changes

(ULCs), or changes from non-built-up to built-up lands, is crucial to understanding human–environment interactions.

M. J. Hammond et al. (2015), reviewed the most recent research on flood impact assessments in urban settings, describing their use and its drawbacks. They described the ways for integrating them as well as approaches for coping with various sorts of consequences. The article will also point out potential future directions for advancement in the methods. Changes in the socioeconomic and climatic conditions may worsen these effects. For city planners and decision-makers, resilience thinking has emerged as a crucial tool for managing flood risks. The idea that flood resilient cities are less affected by extreme flood disasters persists despite diverse definitions of resilience. To create flood-resistant cities, planners and experts in flood risk need to understand the effects of flooding.

Apel et al. (2016) looked at both fluvial and pluvial flood risks separately and came up with a way to look at both. This combined fluvial and pluvial flood risk analysis was carried out at CanTho, which is the largest city in the Mekong Delta in Vietnam. In this tropical area, the annual monsoon caused the Mekong River to flood. This happened at the same time that there was a lot of convective rain, so there was both fluvial flooding and pluvial flooding. The peak flow is estimated based on local rain gauge data and a random rainstorm generator was used to figure out the pluvial hazard. The chances that both types of flooding will happen at the same time were calculated by assuming that the two types of flooding are independent and by taking seasonality and the chance of coincidence into account.

Tengan (2016), studied flooding in Ghana, which happens every year and is in the capital city, Accra, where people and things are destroyed. Even though there have been many ideas for how to stop these floods, they still happen a lot in Ghana. The study found that the single-dimensional approach to flood mapping, the lack of adequate funding, the poor attitude of residents (Ghanaians) toward the environment and sanitation, and the ad-hoc approach to flood management were all major problems when it came to dealing with floods. It is suggested that flood problems could be solved by making flood management more sustainable, tackling flood problems as a whole, and educating people.

Kundzewicz et al. (2019), investigated Flood risk (composed of hazards, exposure, and vulnerability) from the global to the local scale. It discusses observed data, noting an increase in flood damage. There are numerous factors that influence flood hazards and risk, and our assessments, particularly future projections, are fraught with uncertainty. Furthermore, this

study evaluates flood risk reduction options at multiple spatial scales, ranging from the global framework to regional and local scales. In order to search for changes that influence flood hazard and flood risk in river basins, updated records of flood-related indices must be examined on a regular basis.

2.2 Review of literature on LULC change studies

Duran et al. (2006), studied the historical peninsula of Istanbul, the largest province in Turkey, which has undergone a temporal assessment of land cover changes using remotely sensed data and GIS. The acquisition and analysis of land-use distribution between 1963 and 2000 are the study's main objectives. Several digitized maps of various scales, IRS 1C images were used.

Reis & Selçuk (2008), investigated erosion, land planning, global warming, and other applications that require regional-scale LULC mapping. Remote Sensing and GIS are used to study LULC variations in Rize, North-East Turkey. Maximum likelihood is used to classify six reflecting bands of two Landsat images using ground truth data from 1973 and 2002 aerial photographs. The second part analyzed land use land cover changes using change detection comparison (pixel by pixel). In the third section of the study, GIS functions assess land cover changes by slope and altitude.

Dewan & Yanaguchi (2009), evaluated LULC change in Makkah and Al-Taif, Saudi Arabia, from 1986 to 2013 using Landsat images. LULC maps were created using object-oriented classification and maximum likelihood. With the use of GIS and post-classification comparison, the change detection was carried out. According to the findings, urban areas have grown by about 174% in Makkah and 113% in Al-Taif throughout the course of the study period. Because of the shifting average precipitation in this climate, analysis of the vegetation cover over the research region revealed a varying distribution from year to year. The link within Zimbabwe's Midlands Province may be quantified and understood using the information provided by satellite remote sensing. They blamed the Land Reform and Resettlement Program for the rise in land use modifications. In this study, the rate of land-cover change in the Shurugwi district since 1990 was calculated. Geographic Information Systems (GIS) and remote sensing methods were used to achieve this. The study also made an effort to identify the causes influencing changes in land use and land cover, and it did so by conducting semi-structured interviews with significant respondents.

Yu et al. (2011), used a system dynamics model to analyze and simulate the long-term LULC change in Daqing City. Three key factors, including population increase, land use planning, and socioeconomic policies, were identified as the primary drivers for the change in the analysis's trend.

Rafael (2013), used satellite images of the same region of the earth, spread out over time, and computational tools in GIS to draw comparisons using the temporal dimension as a quality of data. This function of remote sensing for the analysis of temporal phenomena is known as detection of changes in LULC rating or time. This study aims to perform an analysis of the temporal and spatial landscape of the city of Bom Retiro do Sul, located in the north-eastern state of Rio Grande do Sul. The results showed that forest areas were increasing and agricultural areas were decreasing in the city.

Halmy et al. (2015), used a Markov-cellular automata (CA) integrated technique to identify the LULC changes of Egypt's northern desert in order to anticipate future changes. It is possible to project a variety of various future scenarios by utilizing a spatially distributed land use change modeling approach, such as the Markov-CA approach.

Naboureh et al. (2017), looked at land-use/land-cover (LULC) dynamics from a scientific point of view and studied how LULC changes over space and time because of urban growth and land-use planning. They worked with local decision-makers and officials to examine the complicated Wuhan metropolitan area. To analyze and project LULC changes, this study used a logistic-MCE-CA-Markov model using a geographic information system (GIS). Additionally, the simulation took into account sites of interest, GDP, population density, closeness to urban centers, and accessibility to transportation lines. The findings demonstrated that natural landscape patches would fragment and multiply as human disturbance intensity rose, resulting in a rise in spatial variability. The simulation results could improve land use planning and management and track upcoming LULC trends for local decision makers.

2.3 Review of the literature on hydrological models used in simulating floods

GAO et al. (2010), explains how the most recent iteration of the variable infiltration capacity (VIC) model works. VIC, a semi-distributed macroscale hydrological model, is used to balance the water and surface energy within the grid cell. The VIC model stands out for its subgrid variability in the land surface vegetation, soil moisture and storage capacity. Drainage from the lower soil moisture zone (base flow) and the inclusion of topography enables precipitation and

temperature lapse rates leading to more realistic hydrology in mountainous regions. To mimic the streamflow, VIC employs a different routing model based on a linear transfer function. In VIC, modifications to the routing model are put into place to represent the effects of reservoir operation, irrigation diversions, and return flows.

Grillakis et al. (2010), illustrated the HBV (Hydrologiska Byrns Vattenbalansavdelning) which is a conceptual distributed hydrological model. With satisfactory findings, the model was calibrated and verified using historical rainfall-runoff events, resulting in values of the Nash-Sutcliffe coefficient ranging from 0.82 to 0.96. The model is validated by using the Spatio temporal precipitation from a rain gauge. The model successfully predicted three of the five basin outputs. When this method is used in conjunction with radar data and operational high resolution short range weather forecast models, the added value is used in peak discharge estimation and event interpretation of flash flood warning system for the study area.

Okirya et al. (2012) used HEC HMS software to perform hydrological modelling. After defining the catchment basin model (325 km2) with HEC GeoHMS, the meteorological model was filled with design storm data, and control specifications have been assigned. Using the HEC RAS software, hydraulic modelling was done. Flood hazard maps were created from the results of the HEC RAS model's output to ArcGIS, where they were used to figure out which areas were likely to flood.

Scharfenberg (2013), investigated the impact of land-use and land-cover change (LULCC) on water balance using the HEC-HMS modelling approach. The processing of digital data for coupling with the model was made easier by the use of HEC-GeoHMS. The hydro-climatic data and the physical properties of the basin contributed to the creation of a geospatial database for the HEC-HMS model. Using the SCS Curve-Number and the Soil Moisture Accounting (SMA) loss methodologies, we examined baseline and future scenario changes for the years 1980–2016. The Hargreaves evapotranspiration method was combined with SMA. The goal of the model calibration was to replicate the basin runoff hydrograph.

Balica et al. (2013), Flooding is one of the most common and widespread natural hazards to life and property. There is a need to identify the risk in flood-prone areas in order to support risk management decisions ranging from high-level planning proposals to detailed design. There are numerous methods for conducting such studies. The most widely accepted and thus widely used method is computer-based inundation mapping. In contrast, the parametric

approach to vulnerability assessment is becoming more popular. Each of these approaches has advantages and disadvantages for decision makers, and this paper compares how they are used. It is concluded that the parametric approach, in this case the FVI, is the only one that evaluates flood vulnerability; whereas the deterministic approach, while limited in its evaluation of vulnerability, has a stronger scientific foundation.

Mandal and Chakrabarty (2016) explained the basin model, meteorological model, control specifications, and time-series data manager as the four important components of the HEC-HMS model. The hydrograph is created after the model has run, and it can be used alone or in conjunction with other programmes to conduct studies on water availability, urban drainage, bird forecasting, the effects of future urbanisation, reservoir spillway design, food damage reduction, foodplain regulation, and system operation.

Maryam (2017), today, with the growth and expansion of agricultural activities, is faced with changes in natural ecosystems and water resources. Hydrological modeling techniques can be used to identify the watersheds payment. Soil and Water Assessment Model (SWAT), which is applicable in ArcGIS tools for hydrological studies, water quality, sediment, effects of climate, change. This model is founded on land use data layers, slope and soil in GIS environment to create a Hydrological Unit Response (HRU). The model uses data Climatology and some other information. Hydrological process simulation model, including rain, snow, storage pothole, surface runoff, infiltration, precipitation, evapotranspiration, infiltration, surface flow, shallow and deep groundwater flow. The SWATCUP model has a link through the PARASOL, MCMC, SUFI2 and GLUE to calibrate and validate the model deals. In this study the hydrological model SWAT, calibration and validation of the model is discussed.

Vinay et al. (2018) developed flood inundation and flood risk maps using a coupled 1D-2D flood modelling approach to identify flood-prone locations. Using the storm water management a 1D model is created for the pilot region is combined with 2D model (SWMM). The current network information are georeferenced using a web-based GIS tool called INPPINS and exported to a 1D SWMM model. The model simulates an extreme flood event that has taken place in the past. The simulation run results show prepared risk maps, flood inundation maps, and overflowing drainage nodes.

Abdessamed and Abderrazak (2019), used a coupled HEC-RAS and HEC-HMS rainfall-runoff modelling, specifically in Ain Sefra city, Ksour Mountain, and SW Algeria for design periods of 10,100, and 1000 years. HEC-HMS is a physical-based and conceptual semi-

distributed model that is intended to simulate complete watershed hydrologic processes such as rainfall-runoff processes. The purpose of this research is to examine the inundation behaviour of Ain Sefra city during extreme food events, both with and without concrete retaining walls built by local authorities. The Ain Sefra watershed crosses completely urbanised areas where it was prone to many inundations, resulting in numerous losses, both economic and human life, because of population growth. The simulations also revealed that the downtown area is the most affected by the flood.

Hossain et al. (2019), stated that each modelling technique has its strengths. EPA-SWMM is a popular hydrological processes model. The US Environmental Protection Agency (US EPA) introduced SWMM1 in 1971 and has upgraded it to SWMM2, SWMM3, SWMM4, and SWMM5.

2.4 Review of literature on Urban Stormwater Management

Fang et al. (2006), made a 1D-2D integrated hydraulic simulation model to simulate how storm water flooding and drying happen in urban areas with complicated drainage systems. Flood risk information is obtained from the model. The model was used in Beaumont, Texas, and checked against the rainfall and runoff data from Tropical Storm Allison. There was good agreement between the two.

Semadeni Davies et al. (2008), used drainage simulations to investigate the effects of climate change and urbanization on stormwater flows to a suburban stream in Helsingborg, south Sweden. City expansion during heavy rains will raise peak flow volumes and flood risks. Then, the new stormwater management regime called for sustainable urban drainage systems that use natural, cost-effective techniques to reduce urbanization's environmental impact.

AnnaPalla and IlariaGnecco (2015), demonstrated the effectiveness of LIDs in the modeling results. The peak reduction is mostly impacted by the effective impervious area (EIA) reduction. To see a notable change in hydrologic conditions, an EIA drop greater than 5% is needed. EIA reduction percentages rise linearly with hydrologic performance. When the return period is increased from two to ten years, the peak reduction decreases by 0.14.

Jha et al. (2011), gave a thorough and easy-to-understand look at the state of the art in managing flood risk in cities within the Global Handbook. It gives technical experts, people in

charge of making decisions, and other interested people in the private and public sectors an introduction to integrated urban flood risk management. It talks about the causes, likelihood, and effects of floods as well as the steps that can be taken to manage flood risk by balancing structural and non-structural solutions. It also talks about how these steps can be paid for, put into action, and their progress tracked and evaluated. The Handbook gives a systematic guide on how to deal with the risk of flooding in areas where cities are growing quickly and the climate is changing.

Ellis et al. (2014), found "critical drainage areas" to measure "hot spot" flood and pollution risks from urban surface runoff during extreme events. This methodological need is met by describing an innovative 1D-2D modeling analysis based on GIS and a drainage assessment tool. The modeling approach also uses a tool called SUDSLOC from the Sustainable Urban Drainage System (SUDS) to make a surface water management framework that is easy for all stakeholders to understand. The performance effectiveness of the chosen SUDS controls is looked at, and the usefulness of the animated graphical outputs is talked about. While the SUDS controls show large reductions (>57%) in total discharge volumes for storms with return periods up to 1:30 years, there aren't many volumetric reductions for storms with return periods longer than 1:30 years.

Seith and Butler (2017), developed an approach for evaluating Urban Drainage System performance under a wide range of random functional failure scenarios (severe rainfall) with varied amplitude, duration, and spatial distribution. The functional resilience index calculates the residual functionality of the system for each rainy block-loading scenario. Using the established technique, an existing UDS in Kampala, Uganda, was tested and characterised for functional resistance to high rainfall. The study discovered that (1) short-duration, high-intensity rainfall events, as well as spatial rainfall variation during extreme rainfall conditions, have a significant impact on UDS functional resilience, and (2) future resilience enhancement strategies should use spatially distributed rainfall inputs to help size potential adaptation strategies.

Kourtis et al. (2018), intend to compare Low Impact Development (LID) methods to traditional stormwater solutions and quantify the effect of LID practices in reducing peak runoff and runoff volume. The Storm Water Management Model was the hydrologic-hydraulic model that was utilized (SWMM 5.1). Green roofs and permeable pavements were the two LID practices that were modelled. The design of a detention pond and the widening of the sewer

were the two typical techniques that each LID was tested against independently. Results indicated that LID procedures are equally effective as traditional approaches in preventing flooding during minor storm occurrences. In general, the design process should consider minor storms.

Panos et al. (2018), explained how infill development has an impact on how much water flows off in Denver, Colorado. For multiple potential redevelopment scenarios, design storms and summer rainfall periods were simulated using a calibrated, high-resolution Personal Computer Stormwater Management Model (PCSWMM). According to the findings, an increase in impervious area of 1% caused by redevelopment will result in a 1.63 percent increase in surface runoff volume for a 2-year, 24-hour design storm and a 0.91 percent increase for a 100-year, 24-hour design storm. This indicates that there is a higher relative danger of flooding with lesser storms. Results highlight the limitations of the current storm sewer system, the likelihood of future flooding, and potential beneficial uses for stormwater.

2.5 Summary of the Literature Review

From a detailed literature review carried out for the study, it can be concluded that

i. The rising interest in urban flood risk management can be attributed to the problems that are affecting the human environment. The failure to improve drainage infrastructure in conjunction with the expansion of cities was the primary contributor to the overstressing of urban drainage systems.
ii. The fact that flooding is responsible for an increase in economic and social losses around the world is evidence that changes in land use have had a significant impact on the hydrology of watersheds.
iii. It is necessary to have an efficient urban flood control system in place in order to reduce the likelihood of damage caused by urban flooding.
iv. PCSWMM's capabilities to model urban drainage has recently made it more accessible to a wider range of users.
v. Because urban flooding is unpredictable and difficult to control, it is essential to make use of the technologies that are intended for the purpose.

vi. The best way to fix the damage done to urban drainage is to first determine the relationship between the magnitude of the flood and then transition from conventional drainage systems to sustainable urban drainage systems.

vii. Sustainable urban drainage system, also known as Low impact development, is a technique that makes use of natural drainage in conjunction with various technologies and policies. The effectiveness of several urban drainage scenarios will be examined.

CHAPTER 3

Scope and Objectives of Investigation

3.0 General

This research work presents an approach to understand and model the urban flooding, which can help in the urban flood management. From the detailed literature review, it is clear that there is a research gap in modeling of the urban flood due to its complex nature. A framework is developed to study hydraulic and hydrological characteristics of the flood in urban area. The study also compares different scenarios to understand the mitigation of the flood.

3.1 Scope of the Present Investigation

i. The research scope includes determining the study area's hydrological and hydraulic parameters.
ii. Develop a framework to estimate the urban flood and to model different SuDS scenarios.

3.2 Research Significance

As a natural disaster, urban flooding cannot be avoided however, the losses caused by flooding can be managed with proper flood mitigation planning. As a result, appropriate flood hazard estimation for different flow conditions is required. The problem associated with the present study area is encroachment filling up the drainage (both natural and storm water) resulting in urban floods. Excess runoff flowing over stormwater drainage is one type of urban flood that is being debated in policy circles and academia. Despite an increase in research on these terms, an integrated review on urban flooding in stormwater drainage and using remote sensing and GIS has yet to be produced. Based on previous studies a critical review is provided for modeling the urban flood. Hence, the research evaluates the integrated planning of flood management. Future research directions are also suggested to help readers better understand the concepts behind urban floods and improve urban flood hazard management strategies.

3.3 Objectives of the research

i. Identification and mapping of flood hazard zones in the study area.

ii. To predict and analyses the future Land Use Land Cover

iii. To simulate an integrated 1D-2D runoff for the stormwater drainage network.

iv. To develop a model for flood control using the Sustainable Urban Drainage.

3.4 Research Methodology

The overall methodology of the research is given in a flow as shown in the Figure 3.1. In order to achieve the objectives of the study, detailed experimental work is planned in four phases. In the first phase, a geospatial approach is used to generate a flood hazard map of Warangal Municipal Corporation. Zones with high vulnerability to flood are identified. In the second phase the multi-temporal transition in LULC from past to future is analysed to understand the variations occurring in the landscape of the study area. This phase has its own importance as the LULC has direct impact on the urban floods especially in our study area WMC. In the third phase, hydrological and hydraulic modelling of flood inundation is carried to obtain the information on flood characteristics and accurate flow path. Identification of flood inundation has become increasingly significant, especially for urban area like WMC, as the reasons to urban floods are area specific. The flood inundation in an urban area is simulated using coupled 1D-2D rainfall runoff modelling. The fourth phase is to develop a model to incorporate SuDS as a part of urban flood management in the vulnerable areas and to analyse their effect on runoff reduction to minimize damages caused by urban flooding.

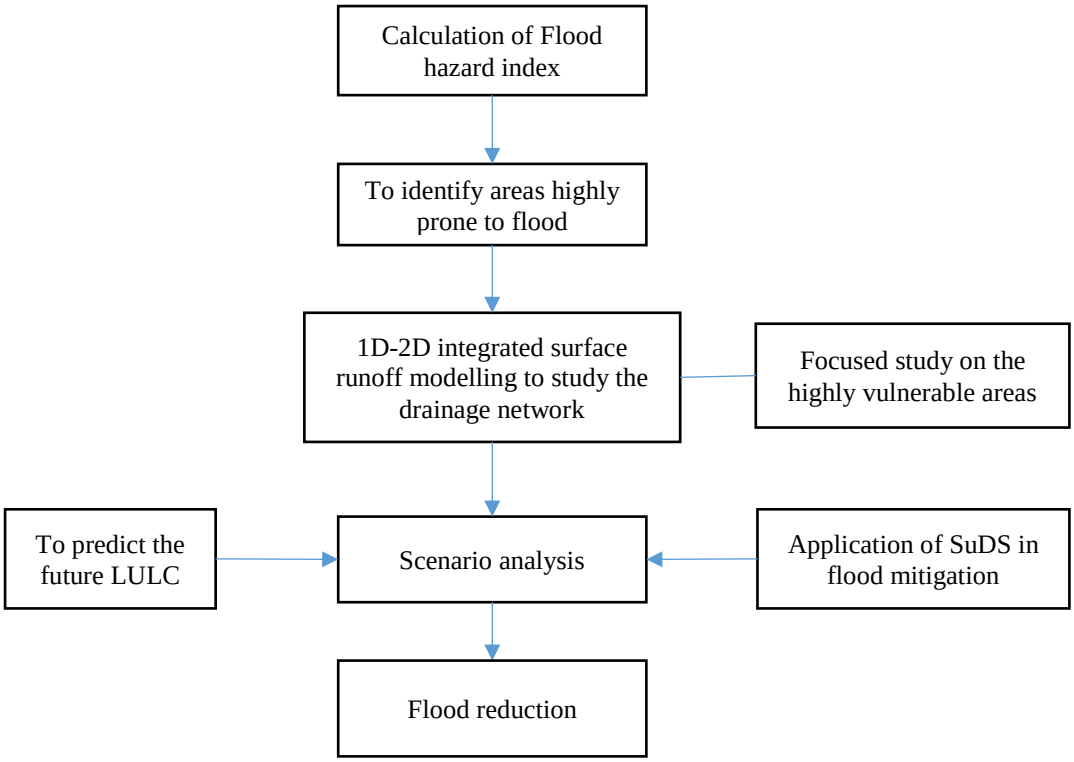

Figure 3.1 Schematic diagram of the research work

Chapter 4
Flood hazard mapping

4.0 General

Floods are commonly regarded as the most prevalent natural disaster worldwide (Stefanidis & Stathis 2013). Significant damages to urban infrastructure demonstrate the critical need for flood control and prevention (Pradhan et al. 2014). Therefore, comprehensive flood hazard analysis is a crucial component of risk management for estimating flood-prone areas (Meyer et al., 2008). Recent improvements in the effectiveness of Remote Sensing (RS) and Geographic Information System (GIS) technologies have resulted in a shift in the study of hydrology, particularly in flood management, which can meet all requirements for flood forecasting, preparation, prevention, and damage assessment. The probabilities of flooding are determined in order to generate flood hazard maps. Hazards can include latent conditions that may represent future threats and can have different origins: natural (geological, hydrometeorological, biological and those induced by human processes (environmental degradation and technological hazards). Each hazard is characterized by its location, intensity, and probability. The flood hazard assessment needs to be presented using a simple classification such as indicating high, medium, low hazard. The inundation or hazard mapping is an essential component of emergency action plans; it assists policymakers and decision-makers in allocating resources, conducting flood forecasts, conducting ecological studies, and planning for significant land use in flood-prone areas. Among different GIS-based flood models presented in the literature, multi-layered feed forward network (Kar et al., 2015), decision trees (Tehrany et al. 2013), and Analytical hierarchical process (AHP) (Zhu et al., 2015) has been broadly utilized in the GIS environment for generating flood hazard maps, with a decent level of precision. AHP is a semi-quantitative, multi-criteria technique used to depict the hierarchy of a decision-making issue, and it has found widespread application in flood hazard estimation.

This chapter presents the first element of flood risk management, i.e., the identification of flood hazard areas in Warangal Municipal Corporation (WMC). The objective of this chapter is to map the Flood Hazard index (FHI) for the vulnerable sites to urban flood, using GIS and spatial data sources available, where mitigation measures are to be taken. A hierarchical structure through AHP method is implemented to evaluate the factors considered whereas the analysis

of the data, preparation of the urban flood-hazard map is carried out in the GIS environment to develop an integrated approach for the urban case study.

4.1 Methodology

The application of Geographic Information Systems and AHP for flood hazard mapping in the research area includes three stages: (1) Collection of the data inputs; (2) Determining the causative factors of flood (3) development of flood hazard map using the AHP method.

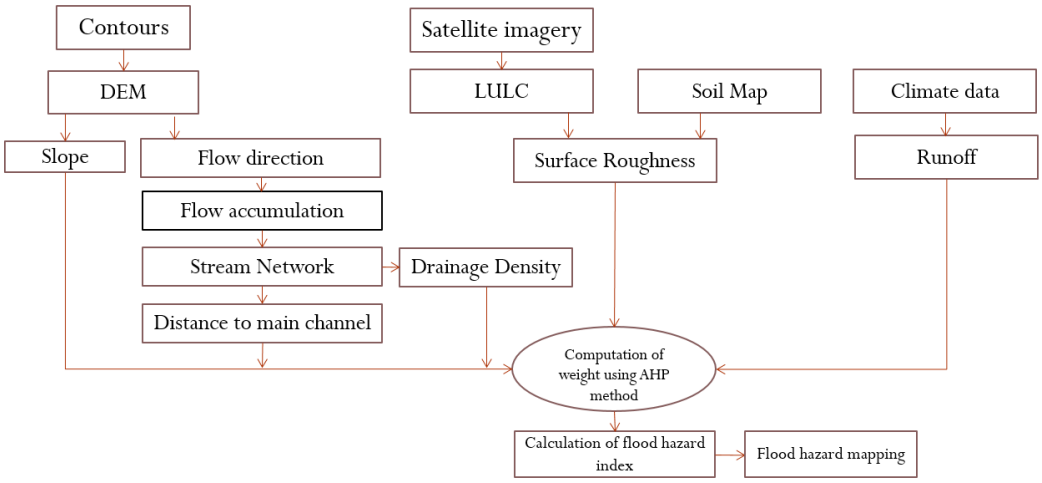

Figure 4.1. Flow chart of the proposed methodology for flood hazard mapping

4.1.1 Study area

Warangal Municipal Corporation (WMC), is a highly urbanized part of the Warangal Urban district, which lies between 17^0 46' and 18^0 13' (Figure 4.2), with a population of 746594 as per 2011 census. The area, for the most part, has a tendency to be dry without real changes in the temperature ranging from 34^0C to 42^0C. It gets very warm amid the mid-year periods of April, May and June. The stormy season sets in the Warangal city with the start of south-west rainstorm in the later bit of June month, and completes in the long extend of September with the finish of the south-west tempest. The normal yearly rainfall of the region is 800mm, with most extreme precipitation recorded in the long stretches of July, August and September consistently. Kakatiya canal is the main water supply source for irrigation and drinking water to the whole Warangal city. Rain encouraged tanks, wells and lakes, which require enough of showers in the season, are some of the other sources of water supply in the city. Surface drainage shapes an essential viewpoint about WMC but the improper design or blockage to the natural drainage pattern resulted in unhygienic conditions in the town, severe water logging

and vulnerability risk.

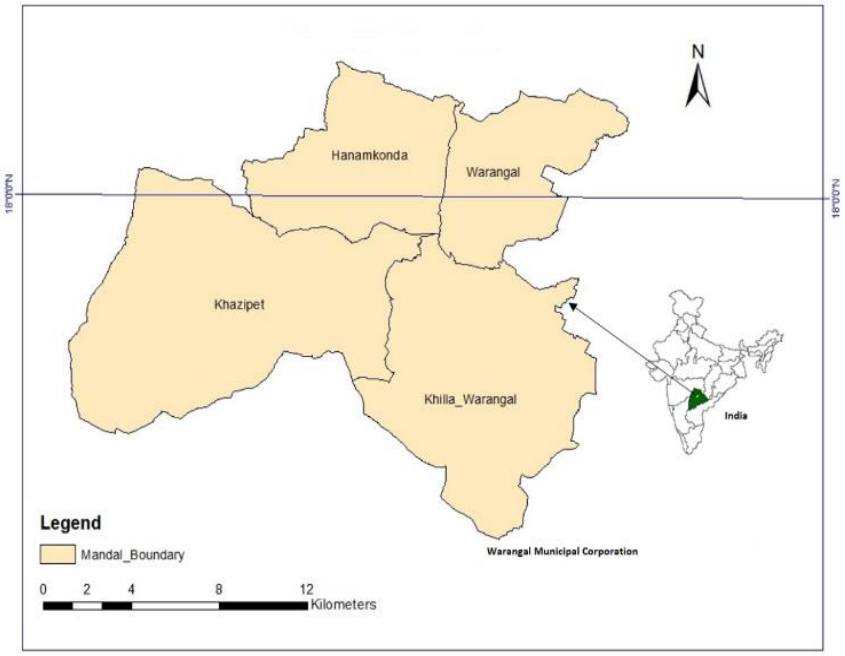

Figure 4.2 Location map of the study area

4.1.2 Data Sets

The Survey of India (SOI) collateral dataset, which includes toposheets 56N12 and 56O09 at a scale of 1:50,000, were used to make the base maps for this study. Rainfall monthly data for the years 20555 to 2016 was collected from the Irrigation & CAD Department, Warangal, and Government of Telangana. The Landsat 8 OLI multispectral data for the year 2016 was downloaded from United States Geological Survey (USGS). The Chief Planning Office, Warangal, provided important LULC change drivers such as population and soil data. GPS data was used to find the training sites, check the ground truth in the image classification and to figure out how accurate the results were. To categorize and validate a satellite image, it is advised to use at least 30 training sites per class (Congalton and Green, 2008). 50 GPS points were used in total for the investigation to verify the LULC classification.

4.2 Causative factors considered in the flood hazard mapping

Likelihood of an event within a given time period of a potentially damaging phenomena and area is characterized as a Hazard. At the point when flood happens, the damage relies upon the factors affecting flood, varying from one study area to another. Based on past investigations and reliable expert opinions seven causative factors were chosen in the present study due to their significance in causing flood. The factors considered are; Elevation and slope distance to

main channel, soil type, LULC, Surface roughness, runoff, drainage density. The chosen factors have been demonstrated to be powerful for mapping and are handled in a GIS environment; later the thematic maps are visualized independently.
The following are the factors used in the flood hazard mapping.

4.2.1 Elevation Surface and Slope

In this study, contours were digitized at 10 m intervals and contour map is generated (Figure 4.3 a) from Survey of India topographical maps. The elevation surface called Digital Elevation Model (DEM) (Figure 4.2 b) is created from the contour map. The slope map was prepared from slope generation tools using the DEM (Figure 4.2c). The amount of surface drainage reaching a site is greatly influenced by the slope direction. Highly vulnerable sites to flood occurrences have low gradient slopes when compared to high gradient slopes (Ouma & Tateishi, 2014). The slope has a dominant role in influencing water velocity, flood strength, and infiltration (Das, 2020). The DEM created has the elevations of the terrain varying from 250 to 330 m while the slope is displayed in percentage and is classified into five classes' values range from 0.002 to 4. Classes of slope are assigned a higher rank with less value as they refer to flat terrain, while the ones with maximum value were ranked lower due to relatively high runoff (Kumar et al., 2014). Furthermore, (Ho and Umitsu et al., 2011) stated that in areas with the same elevation and landform, flooding does not always coincide due to the slope of the terrain and the water level flood.

The extraction of watershed features from DEM is considered an important task in hydrological study. Flow direction is given as an input to the create stream network (Figure 4.3(d)). Basin function is created from the stream network to derive all the connected cells that come from the same drainage basin. The entire study area is divided into 4 sub basins and the basin map is shown in the (Figure 4.3 (f)). The raster gives the course in which inlet water will flow out of a cell concerning its prompt surrounding cells, showing the steepest heading from a cell to the surrounding cells.

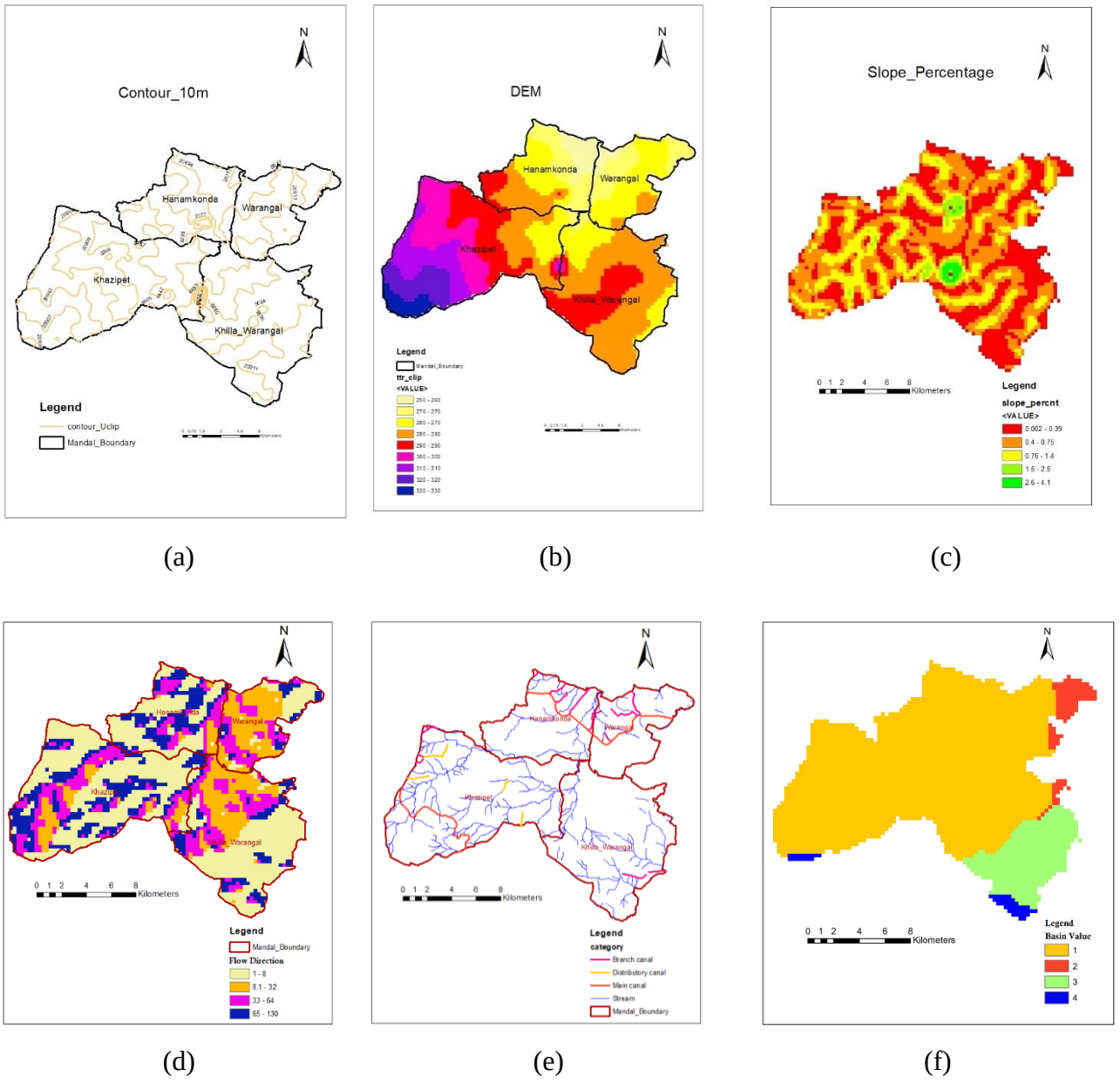

(a) (b) (c)

(d) (e) (f)

Figure 4.3 (a). Contour map, (b). DEM, (c). Slope map showing the percentage of slope (d) Flow direction map , (e)Streams network ,(f) Basins in the study area

4.2.2 Distance to the main channel-Kakatiya canal

A property, open space domain or roadway is subject to flooding if the flow carrying capacity of a nearby drain or roadside drainage channel is frequently exceeding to overflow. Often the inundation emanates from riverbeds and expands in the surroundings. Therefore, areas located close to the main channel and flow accumulation path are more susceptible to flooding. By considering the drainage network of our study area, the main channel Kakatiya canal, which has the maximum stream order, causes great damage. Euclidian Distance method is used to calculate the distance from the main channel and to identify zones that are near to the main

channel. The distances in the study were categorized within a range of 0 to 8500m. As the distance of the floodwater to reach the channel increases, time to reach the channel also increases and hence the infiltration capacity increases. As shown in (Figure 4.4), the villages falling under parts marked in blue of range 7700 to 8500m are at high risk as the runoff in that area takes a long time to reach the main channel. The areas falling under parts marked in yellow within the range of 0 to 2500m are at low risk of flooding.

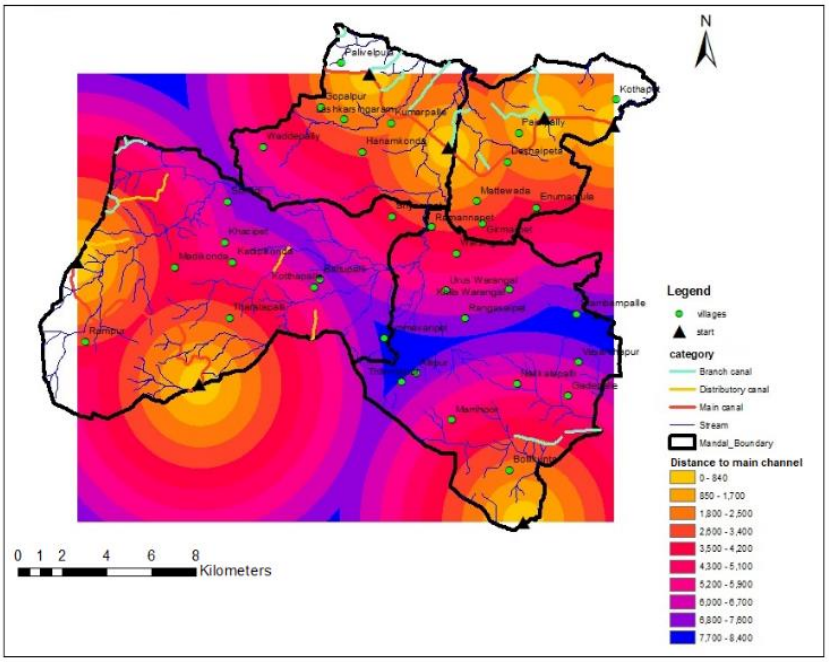

Figure 4.4. Distance to the main channel

4.2.3 Soil type

Soil texture is one of the critical components of soils, posing a great effect on flooding. As per (Ouma and Tateishi, 2014) the sandy soil absorbs water quickly, resulting in less runoff. On the other hand, the clay soils are less permeable and hold water longer than sandy soils. This suggests that areas characterized by clay soils are more influenced by flooding. As per the Public health department, soil types found within the WMC are divided into three categories (Figure 4.5): sandy loam (good drainage), sandy clay loam (medium drainage) and clay loam (poor drainage).

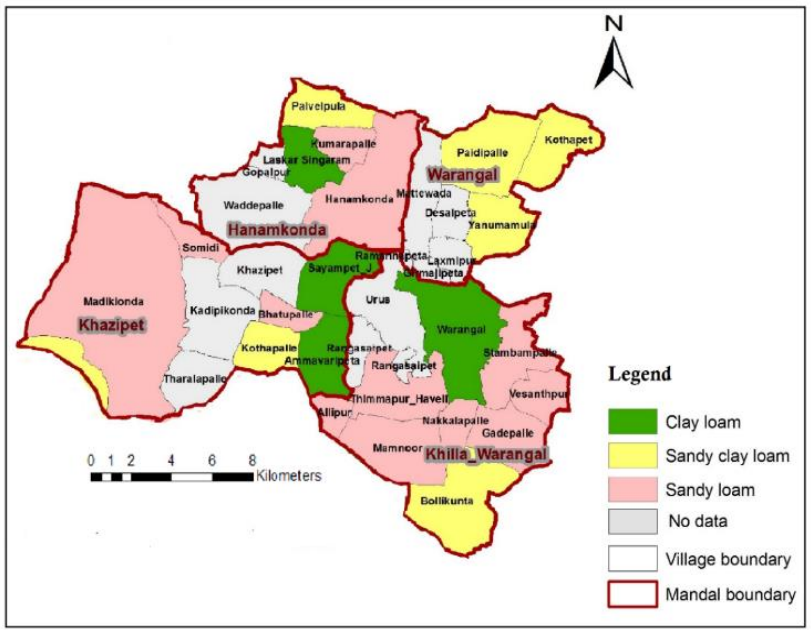

Figure 4.5. Soil map of the study area

4.2.4 Classification of Land Use Land Cover

LULC mapping of WMC urban catchment is carried out using Landsat 8 OLI satellite image for the year 2016, September. Maximum likelihood algorithm was used for supervised classification of the images, per-pixel signatures are assigned to the satellite data and the area is differentiated into four classes such as built-up, agricultural land, wasteland and water bodies of the area based on the corresponding Digital Number (DN) value of different landscape elements. The classified LULC map is shown in (Figure 4.6). The results of the classification, i.e., the area and the percentage are given in Table 4.1. The observations made after classification of the study area (WMC) are that built-up area is 11%, agricultural land is about 82 % followed by Wasteland occupies 4.12 % and water bodies covers 2.316 % of the area. LULC portrays the appearance of the landscape, which reflects its utilization, condition, development and occasional phenology. LULC, like vegetation cover of soils, has an important impact on the ability of the soil to act as a water store event; hence, it is one of the crucial factors in deciding the probabilities of flood occurrence event. Rainwater resulting in the runoff is substantially more likely on barren fields than those with a decent crop cover. Then again, built up area(impermeable surfaces), for example, concrete, ingests no water by any means and acts as a resistant cover, lessening the water hold up time, increasing the peak discharge of water that enhances a peak flooding.

.

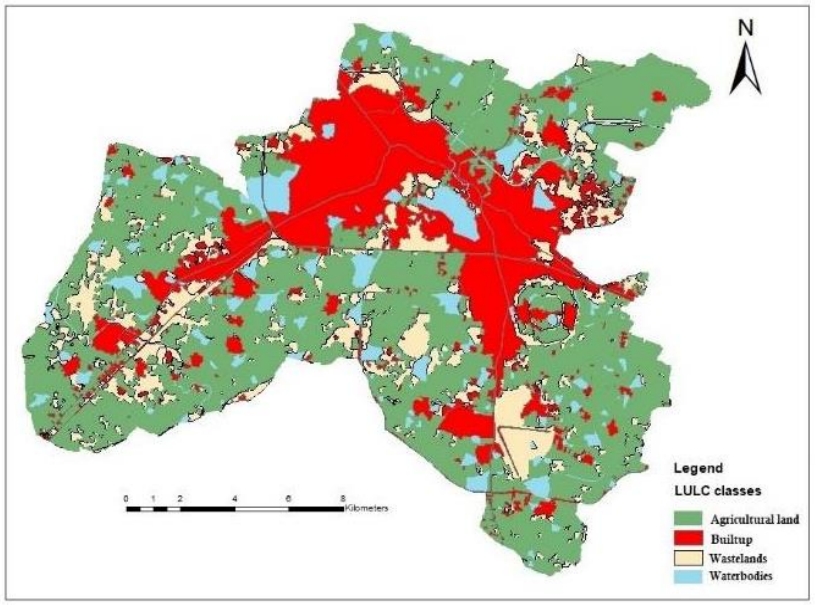

Figure 4.6. LULC derived for the study area

Table 4.1. Table showing different LULC Classes and their respective areas

Classes	Area (Sq. m)	Percentage (%)
Built up	11,085	11.085
Agricultural land	82,388	82.388
Wastelands	4,129	04.129
Waterbodies	2,316	02.316
TOTAL	99,918	99.91

4.2.5 Estimation of surface roughness

The roughness of the earth's surface (e.g., roads, ground) and the objects here (e.g., buildings, vegetation) in terms of hydrodynamic friction is considered one of the essential inputs for flood simulations. Inundation area by flood increases as channel surface roughness becomes higher (Helen Dorn et al., 2014). During the hydrodynamic simulation of the study, the roughness parameter is defined through Manning's formula CHOW (1959). The Manning's roughness coefficient (n) is given a CN lookup table (Table 4.2) commonly used to represent surface roughness. The appropriate Manning's 'n' value for each polygon of the soil-land map is assigned according to The two multiple feature layers, i.e., the soil raster and the LULC raster, are merged as input features in ArcGIS to combine the polygons and a roughness map is created as shown in (Figure 4.7).

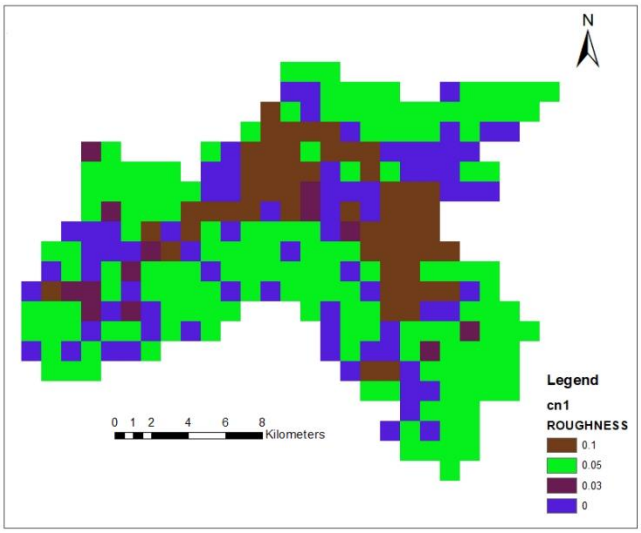

Fig 4.7. Surface roughness map

Table 4.2 Estimated land use and surface roughness values for the study area

Classes	Manning's Roughness Coefficient
Built up	0.10
Agricultural land	0.05
Wastelands	0.03

4.2.6 Simulation of Runoff

SWAT is a watershed model capable of simulating long and short period yields to find the effect on land management practices. In the present study, surface runoff in QSWAT is determined using SCS-CN (Soil Conservation Service Curve Number) method while the potential evapotranspiration is determined by Penmen-Moneith method. The central part of the SWAT model is water balance, the basic equation 4.2 is

$$WYLD = PREC - SURQ - GW - PET - ET - SW \qquad \text{Equation 4.1}$$

Where,

WYLD = Water yield (mm of H_2O)
PREC = Amount of Precipitation (mm)
SURQ = Amount of Surface runoff on day (mm)
GW = Groundwater Contribution (mm)
PET = Potential Evapotranspiration (mm)
ET = Actual Evapotranspiration (mm)
SW = Soil water content (mm)

To derive runoff parameters, before simulation there are some pre-requisite requirements to be prepared that are to be available in the QSWAT directory. All the spatial data (DEM, Land use and Soil raster) are projected into a geographic coordinate system, WGS 1984 with datum UTM

Zone 44N. Derived Land use and Soil look up tables are prepared. Climate data such as precipitation, solar radiation, wind speed and relative humidity are considered for the years 2005 to 2016. Once the data is prepared, the whole drainage basin is delineated into 100 sub-catchments (Figure 4./8) are linked together.

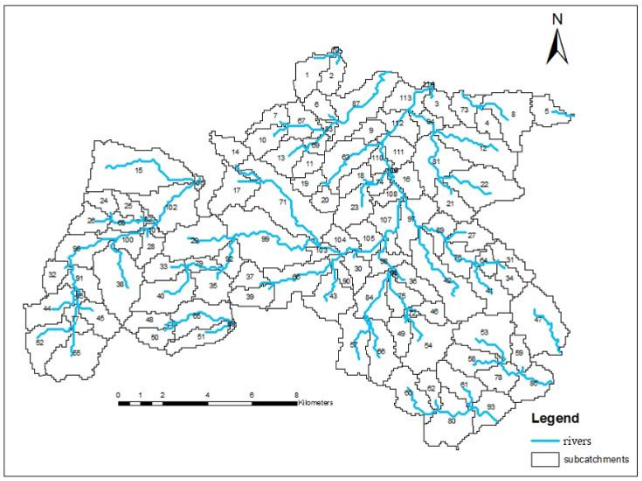

Figure 4.8 Derived subcatchments of the drainage

i. Computing subbasin parameters by using QSWAT and Run-off model description

The study area is classified into four classes' namely agricultural land, Wastelands, Built up and Water bodies (Figure 4.6). Using QSWAT Ref 2012.mdb file, SWAT Code was assigned to each Land-use and copied to excel file Watershed_Landuse.xls file. Similarly, from the soil type raster an excel file Watershed_soils.xls file is created. The weather data such as precipitation (mm), Temperature (^{0}C), Wind velocity (m/s) and solar radiation (MJ/m^2) for stations nearby study area was downloaded from (*SWAT | Soil & Water Assessment Tool*). Then all the results are copied to the WGEN_WatershedGan.xls file. The simulated results are obtained, once the SWAT is run successfully. It gives all hydrological components like average amount of Precipitation, potential evapotranspiration, actual precipitation, Groundwater contribution, Surface runoff, Soil water content, Water yield for each sub basin and Curve number (CN). For each subbasin, a Curve Number value that is a part of yielding runoff volumes is assigned based on class of LULC and hydrological soil type. Based on combinations of Soil Conservation Service (SCS) Land-use data and Soil data for urban catchments (National Engineering Handbook, 1972) CNs are listed in Table 4.3.

Table 4.3. List of Curve numbers for urban catchments.

Land use group	Hydrological group			
	A	B	C	D
Built up	47	65	76	82
Agricultural land	64	75	82	85
Wasteland	77	86	94	98

For the meteorological modeling, QSWAT run is carried out using a monthly time series for the years 2005 to 2016 as the event has occurred in the month of September 2016, which has the peak rainfall during the year 2016, as shown in the (Figure 4.9).

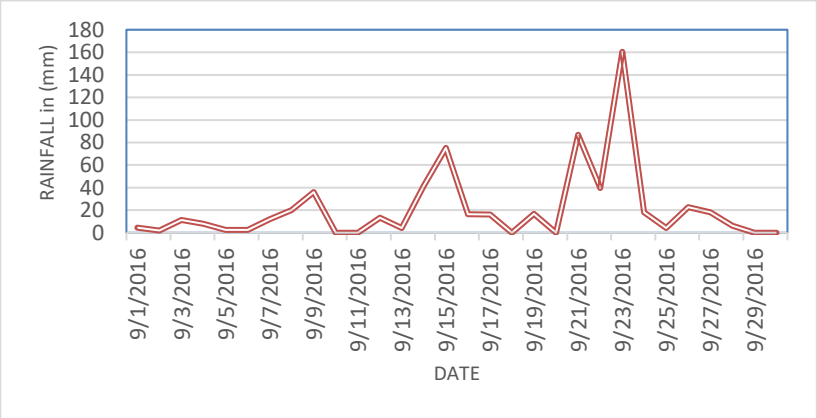

Figure 4.9. Average Rainfall from in the month of September from gauge (mm) 2016

ii. Sensitivity analysis

Sensitivity analysis for the given model considered 13 parameters among which the surface water parameters were more sensitive to stream flow and are highly influencing hydrological parameters for the simulation. Calibration for water balance and stream flow is carried out for monthly data simulation. It was indicated by the base flow technique that about 60 % of the total water yield at the outlet was found to be contributed by the surface runoff. 12 most sensitive flow parameters were considered for calibration and their values differed iteratively inside the admissible extents until a satisfactory agreement is achieved between measured and simulated streamflow, which in turn improve the model efficiency significantly. When compared to measured flow data, the thorough hydrologic calibration came about great SWAT predictive efficiency at the monthly time step of the study area. It was found that the model after validation has strong predictive capability with r^2, E_{NS} and D values of 0.65, 0.69 and 3.00, respectively.

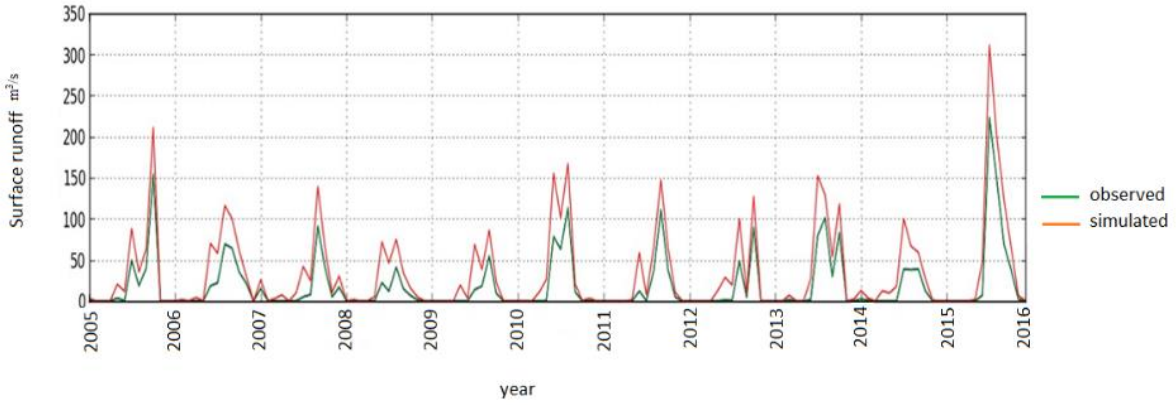

Figure 4.10. Surface runoff generated in sub catchment 4 during time step

As per the output, the sub catchment 4 has the highest value of surface runoff. The subcatchment 4 falls in the Wasteland in LULC with a CN value of 96.5, it has a peak precipitation of 471.6mm and a peak surface runoff of 309.289mm as shown in the (Figure 4.10).

4.2.7 Drainage Density

The runoff from all the parts of the drainage basin is accumulated by streams and is dependent on the stream length. Watershed with high drainage density indicates that more precipitation quickly joins streams whereas low density means more precipitation traveled as surface runoff, through flow and base flow. High-density values are favored in land surfaces with weak infiltration, where rainfall does not readily sink, therefore causing a high amount of runoff. The drainage density determines water outlets and rock structures. Statistically, drainage density is the ratio of the total stream lengths of all the stream orders within a drainage basin to the area of that basin projected to the horizontal (Dixon et al., 2016). It can be calculated using Equation 4.2). As per the Figure 4.11, the volume of drainage density has its peaks in the subcatchments from 45 to 89. The more the drainage density the more water is accumulated in the above mentioned subcatchment resulting high risk of flood.

$$DD = \frac{\Sigma L_S}{A_w} \qquad \text{Equation 4.2}$$

where

DD = drainage density,
L_s = length of streams, and
A_w = area of watershed

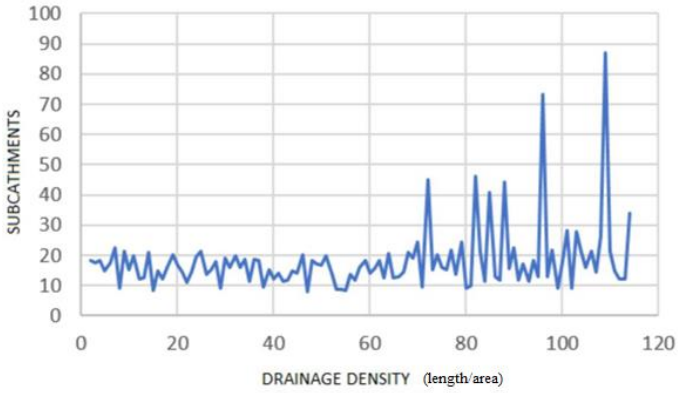

Figure 4.11 Graph between subcatchments and drainage density

4.3 The Analytic Hierarchy Process (AHP)

AHP is an analytical technique is that follows an empirical approach of "multi-criteria decision analysis" (MCDA) (Saaty, 1980). AHP aims to evaluate the relative indicator weight based on paired criteria in achieving a specified target (Carr and Zwick, 2007). A cross-tabulation matrix is used to conduct a structured comparison of all paired combinations of criteria. An AHP transformation equation uses numeric values from the matrix to construct a scale of the relative importance of each criterion based on the pair-wise comparison. In our study, the primary aim of AHP was to determine the relative importance of the spatial inputs considered in defining the spatial extent of flood hazard in the WMC. This needed a global AHP matrix. The following steps made up the application of the AHP approach in this study. The fundamental classification of each causal component into subcategories is the first stage. Each element will be given an arithmetic value between 1 and 7 in the second phase, based on how important that factor is in relation to the other factors that are paired. The importance of the scale, which includes many criteria and values, is expressed by the arithmetic value. A useful aspect of AHP is its capacity to detect errors in judgment when comparing matched criteria in the AHP matrix. AHP was utilized to generate the final flood hazard map by adding the seven input GIS data layers with their individual weights and resulting ranks.

4.4 Flood hazard Mapping

In order to cite the flood hazard zones in WMC, all the causative factors considered were, Slope type of soil, LULC, Surface Roughness, Runoff, Drainage density, and Distance to main channel and the relative weights of the factors are ascertained. The weight of each factor was given based on its estimated significance into the cause of flooding as described in Table 4.4. The overall weight value for each factor is calculated by multiplying each factor's weight by each class of the same factor. Final weighted flood hazard index is created as per

equation 4.3 from an additive model.

$$FHI = \sum_{i=1}^{n}(RIW_{ij}).(RIW_j) \qquad \text{Equation 4.3}$$

Where,

FHI = Flood hazard index
RIW_{ij} = is the weight of class i on variable j
RIW_j = is the weight of variable j
n = 2 (level of decision factors)

The consequences of the pairwise comparison matrix of the analysis is displayed in Table 4.5. Initially a single pair-wise comparison matrix (Elkhrachy, 2015) is made for each criteria considered, by multiplying the values in each row together and calculating the nth base of the said causative factor (here n =7, as 7 criteria are considered). Then, nth root of the factors is standardized to make a priority vector for the fitting weights.

Table 4.4. Causative factors for flood and their corresponding weights

Causative Factor	Weights
Runoff	7
Soil type	6
Slope	5
Drainage density	4
Roughness	3
Distance to main channel	2
LULC	1

Table 4.5 Relative importance weights (RIWs) for factor criteria and Pairwise comparison matrix

Factor Criteria	Runoff	Soil type	Slope	Drainage density	Roughness	Distance to main channel	LULC	Priority Vector
Runoff	1	2	3	4	5	6	7	0.355
Soil type	0.5	1	2	3	4	5	6	0.240
Slope	0.33	0.5	1	2	3	4	5	0.159
Drainage density	0.25	0.33	0.50	1	2	3	4	0.104
Roughness	0.20	0.25	0.33	0.5	1	2	3	0.068
Distance to main channel	0.17	0.20	0.25	0.33	0.5	1	2	0.045
LULC	0.14	0.17	0.20	0.25	0.33	0.5	1	0.030

FHI= (Runoff x 0.355) + (Soil type x 0.240) + (Slope x 0.159) + (Roughness x 0.104) + (Flow Accumulation x 0.068) + (Distance to main channel x 0.045) + (LULC x 0.30)

Table 4.6. Zones, which are affected by flood

FHI range	Hazard classification	No of sub catchments likely to be affected
0.92 - 2.45	Low vulnerable	36
2.46 - 3.37	Moderate	27
3.38 - 4.26	Highly vulnerable	32

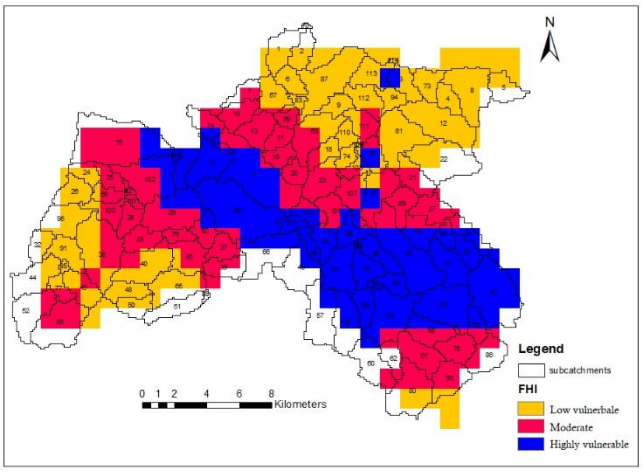

Figure 4.12 Flood vulnerable map for the study area

Once the FHI is calculated, estimations of FHI were characterized into low vulnerable, medium vulnerable, highly vulnerable, thus creating a Flood hazard map as appeared in Figure 4.13. The natural breaks method is used to classify the study area into three classes based on their hazard values. Zonal statistics function is used to define zones likely to be affected by urban flood, and the classification scheme is summarized in Tab. 6 and the results are described as such, about 36 zones are vulnerable to low FH, 27 zones vulnerable to moderate, and 37 zones are highly vulnerable to flood risk. From the (Figure 4.13) and previous considerations it is clear that mostly, the high risk and the moderately risk areas are in a basin with relatively high curve number, drainage density and surface slope.

4.5 Summary

In this investigation, Analytic Hierarchy Process integrated with GIS was effectively connected in simulating the flood hazard zones in WMC. The social and monetary misfortunes because of flood debacles, technological emergencies, as well as worldwide epidemics are developing; requiring more powerful cooperative choice making under vulnerability. In the study, an additive model is used to create the Flood hazard index, with the integration of GIS and spatial data. In developing this model, seven variables were considered (Runoff, Type of soil, Slope percentage, Surface Roughness, Flow accumulation, Distance to main channel in the stream

network, Land use). QSWAT, a 2D hydraulic model has been used to create rainfall-runoff processes with the point of recreating the impacts of considered rainfall situations. AHP process is utilized to build a hierarchical decision approach, in determining the relative weight of flood causative factors to derive a Flood hazard map. Village administrative boundary is then overlaid on the flood hazard map to the villages which are highly prone to flood are obtained. Wadepally, Somidi, Khazipet, Kadipikonda, Battupalli, Kotthapalle, Ammavaripet, ramanapet, Khilla Warangal, nakkalpalli, Vasanthapur fall under high-risk zone. Benefits of the applied technique in the study incorporate precision, practical, advanced yields, and its capacity to be re-keep running for another situation. Because floods are a common occurrence in the research area, the proposed methodology could aid in increasing the accuracy of identifying flood hazard areas as well as improving flood mitigation techniques. The above developed flood hazard map would be useful in administrative planning in WMC. It will be helpful amid post-disaster activities to evaluate harms and misfortunes caused because of surge.

Chapter 5
Prediction of LULC

5.0 General

Human activity and interaction with the earth's surface to obtain necessities of daily life have resulted in the transformation of natural land cover into man-made land cover (Hamad et al. 2018). These activities are regarded as the primary factor in shifting land use from arable to built-up areas and altering the natural environment in both urban and suburban areas (Mallick et al. 2008). Furthermore, the extent of urbanisation influences the pattern of change in land use and land cover. The problem of LULC conversion and modification can be addressed by modelling, which has recently become a focus of international attention due to concerns about issues such as climate change and global warming. Therefore, recently, the knowledge of LULC has become important for many planning and management activities. Effective analysis and monitoring of land cover need a considerable quantity of data concerning the earth surface and therefore the living habitats. Further, in this kind of studies, the analysis is aided by the mathematical and statistical advancement. In the previous chapter, we have seen the flood hazard mapping of the study area. In Warangal, there is a significant unmonitored LULC change due to several reasons such as the illegal occupations and migration of people from rural to urban areas, due climate change. Hence in this chapter analysis and prediction of LULC change from past to future was carried out.

5.1 Methodology

In order to achieve the goal of the study that involves the simulation of LULC change scenarios, satellite imagery from Landsat missions of the years 2004, 2006, and 2018 was used. A flowchart describing the basic components of the modeling in this study is presented in Fig. 5.1. The major steps include (1) database development and classification of images; (2) the application of the CA-Markov model to obtain the prediction of LULC in the years 2052 and (3) validation of the results.

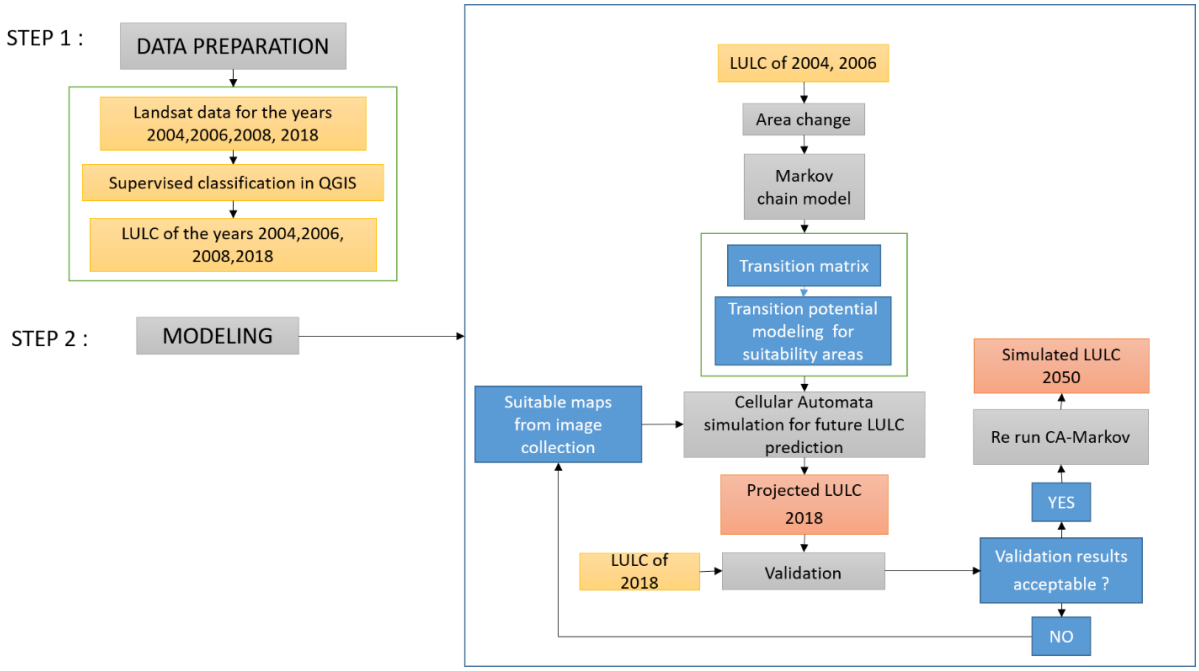

Figure 5.1 Flow chart showing the methodology followed

5.1.1 Study area

Warangal Municipal Corporation (WMC) is located at 18° N and 79.58° E (Fig. 2) with a population of 746,594 as per 2011 census. The city has an average elevation of + 271 m above MSL. The area for the most part has a tendency to be dry without real changes in the temperature ranging from 34 to 42 °C. It gets very warm amid the mid-year periods of April, May, and June. The stormy season sets in the Warangal City with the start of southwest rainstorm in the later bit month of June and completes in the long extent of September with the finish of the south-west tempest. The city comes under Godavari river Basin. The city is sloping towards northern side and all the major nallahs flow towards north direction. There are a number of water bodies within the study area and two of the larger ones serve as summer storage tanks for drinking water supply. Out of the total municipal area of 80 km2, 25% of the total is contributed by canals, river banks, agricultural land, dense scrub, hills etc. with an area of 20.48 km2 and the major portion is occupied by residential area, i.e., 28.84 km2, contributing 37% of the total. The city economy of Warangal is predominantly based on agricultural in nature. Cotton is the major cash crop since the early 1990s. Paddy is the major food crop in the region but most of the farmers grow rice for both subsidence and commerce.

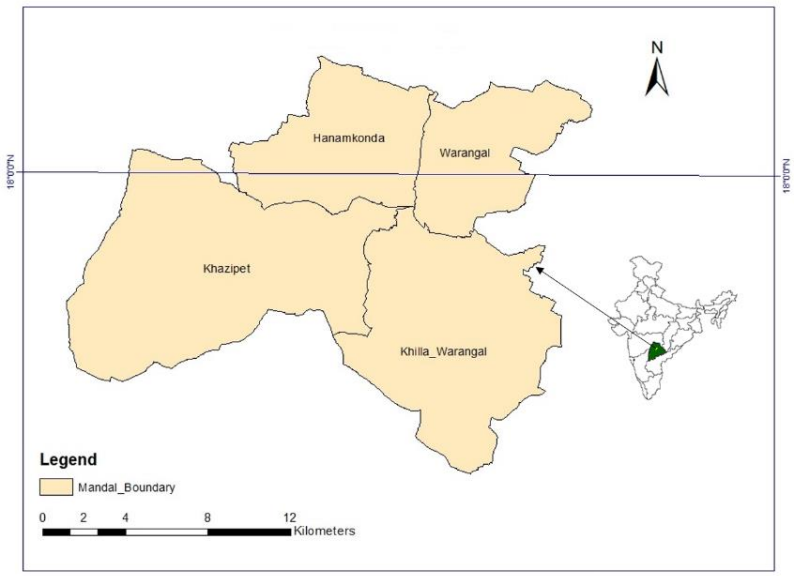

Figure 5.2 Location map of the study area.

5.1.2 Data preparation

For evaluating and modelling of the dynamic LULC change, multi-temporal spatial data were collected. In this study, imagery from Landsat 5 TM and Landsat 8 satellite with a resolution of 30 m, for the years 2004, 2006, and 2018, were used. The detailed information of the data is shown in Table 5.1. All the spatial data are set to the same coordinate system, which is WGS_1984_UTM_Zone_40N. Raster images of the study area were subset as per the administrative boundary. To evaluate the accuracy of the interpreted satellite imagery, Google Earth and field investigation are considered as ground truth check.

Table 5.1 Satellite imagery used in study

Data type	Path and row	Acquisition date	Source
Landsat 5 TM	143 and 48	13/04/2004	USGS
Landsat 5 TM	143 and 48	05/05/2006	USGS
Landsat 5 TM	143 and 48	10/05/2008	USGS
Landsat 8 LDCM	143 and 48	06/05/2018	USGS

Taking into account the rate of socio-economic advancement and the periodic variation of LULC change, temporal range for the simulations cannot be short; hence, the time nodes as input were taken as 2004, 2006, and 2018 to predict the LULC pattern for the year 2052.

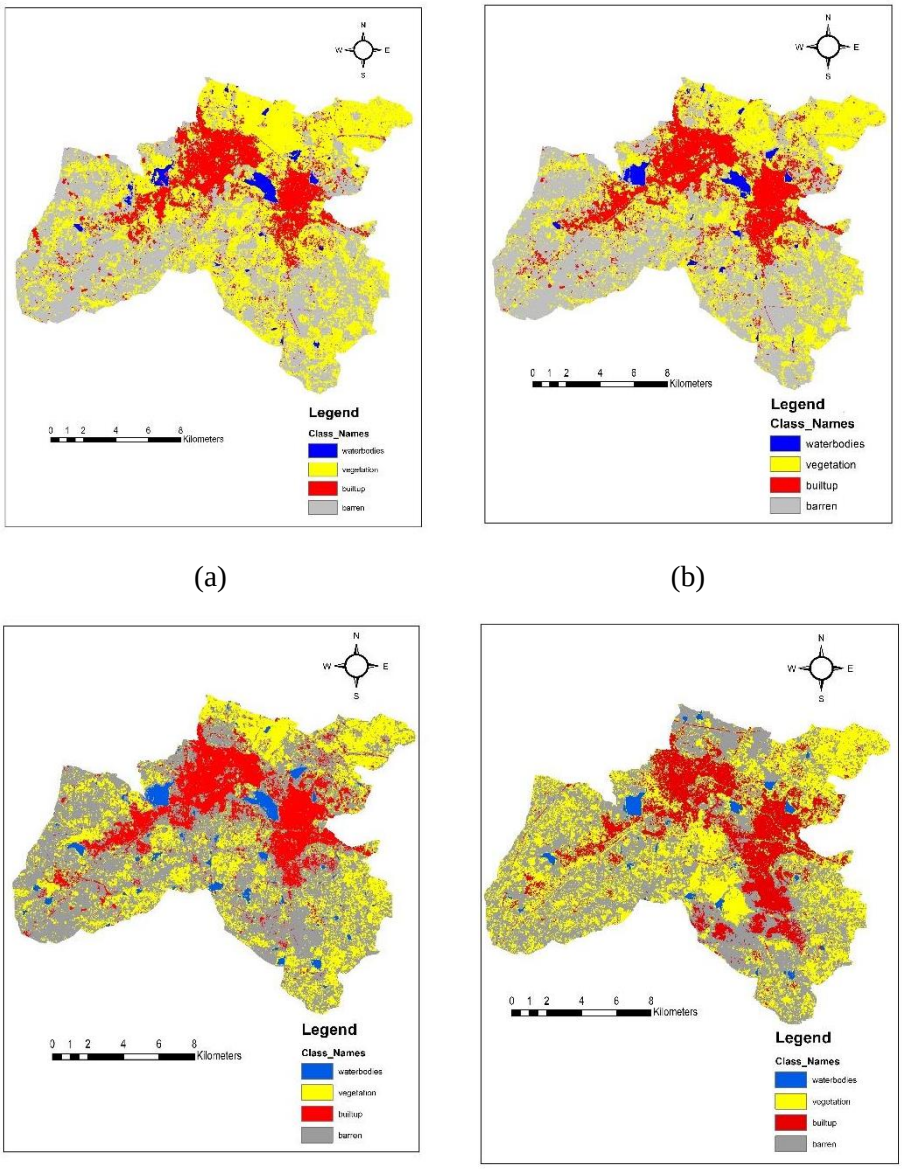

Figure 5.3 LULC of the years (a) 2004, (b) 2006, (c) 2008, (d) 2018

5.1.3 Classification of satellite images

At this stage, to extract the remotely sensed information, a man-machine interactive interpretation is carried out. Maximum likelihood (ML) algorithm, a supervised classification method that has a great potential in image processing because of its ability to simulate varying data, and satellite systems (Roy and Roy 2010), is used to classify the multitemporal Landsat imagery downloaded. A supervised classification groups the pixels into classes that are individual training areas by comparing a set of representative pixels to the spectral properties of each pixel or use the sample specified by the user from the ground. To visually enhance the images, a principal component analysis was performed, to cut back redundancy with the

images, prior to the classification. Polygons around the features are created as per the training samples collected and that areas represent each LULC type. Google Earth imagery, topographic maps, and personal knowledge of the study area helped in gathering the training samples. The raster images were pre-treated in an open source software, Quantum GIS (QGIS). Four LULC types were identified in every raster image for the years 2004, 2006, and 2018, which are shown in Fig. 3, including barren, built-up, vegetation, and waterbodies. To identify the class and group the LULC feature into a type, Anderson et al. (1976) developed a system of land use land cover classification given in USGS as shown in Table 2. However, to suit the study area, the classification system was slightly modified. Post-classification, a change detection technique was fit to deliver a matrix of change, limiting the impacts of sensor and climatic differences between the periods (Adade and Oppelt 2019).

Table 5.2. Description of LULC types

Type of LULC	**Description**
Built Up	Industrial and commercial units, residential areas, mixed urban areas, Transportation facilities
Agriculture	Herbaceous vegetation, shrub and bush areas, mixed forest land
Waterbodies	Lakes, rivers, canals, streams, reservoirs, forest wetland
Barren Land	Sandy areas, Exposed rocks, river banks, mixed grassland with few scattered trees

5.1.4 Markov chain for model calibration and implementation

Markov chain is a stochastic technique in which any future occurrence depends only on the current state and, at the end, forms a sort of chain. LULC raster pictures categorised for distinct dates, i.e. transition from one state of a system at time t + 1, are often used for future prediction using Markov chain. This is because the state of the system at time t can predict the state of the system at time t + 1. This analysis results in three new objects: a transition probability matrix, which stores the probability that each state will change in relation to every other state; a transition area matrix, which stores the expected number of pixels that might change over a predetermined number of time units; and conditional probability images, which express the likelihood that each pixel will have a place in the assigned class in the next ti (Ghosh et al. 2017). Mathematically, one can show how the homogeneous Markov chain model for land use calibration can be demonstrated: One-fourth of an inch One-fourth of Pij L't and one-fourth of Pij 14 appear on page 11 through page 13 of the book. L(t) indicates land use status at time t, while L(t+1) reflects land use status at time t+1. Following the calibration of the model, this

study uses a scenario-bound technique to predict future LULC changes. For the above-mentioned 14-year period, the model was fed LULC simulations for two different historical scenarios: 2004 to 2006 and 2006 to 2018. The Markov chain approach was calibrated and fine-tuned using LULC pictures from 2004 and 2006. Two years are utilised for time 1, 2: 2004 is the first year, and 2006 is the last. The LULC map at time 3 in 2018 is modelled using the differences between two periods, time 1 and time 2. There was a significant improvement in the urban environment because of the socioeconomic changes that took place between 2004 and 2018. In order to simulate the 2018 map, the categorised raster of 2018 is used as a reference, and 20 iterations are executed to verify the results.

5.2 Prediction of future LULC

The following steps are followed in the process of predicting the future LULC

5.2.1 Correlation evaluation

The Pearson correlation coefficient measures the strength of a linear relationship between two sets of data statistically. No linear connection exists when the estimate is 0, but there is a greater linear correlation when the estimate is closer to 1 or 1. The correlation ratio between the four decadal time ranges is shown in Table 3 below. The years between 2006 and simulated 2018 were shown to be closely linked to each other and then to the years between 2004 and 2006.

Table 5.3 Pearsons's Correlation

Initial	Final	Pearson's correlation	2008	2018
2004	2006	0.826546	79.57102	74.69267
2006	2018	0.720344	-	-
2004	2008	0.72836	-	-
2006	simulated 2018	0.996002	-	-

5.2.2 LULC change characteristics of the study area

The accessibility of different terrain types to highways and administrative hubs, as well as socioeconomic conditions and traffic, could play a significant effect in the expansion. Semi-Automatic Classification Plugin in QGIS was used to build the LULC maps in 2004, 2006, and 2018. According to Table 4 (part a), from 2004 to 2006, LULC classes changed by 5.794 for barren; 2.154 built-up; 8.124 vegetation; and 0.0749 waterbodies, which implies an increase in built-up type and a decrease in vegetation, respectively.

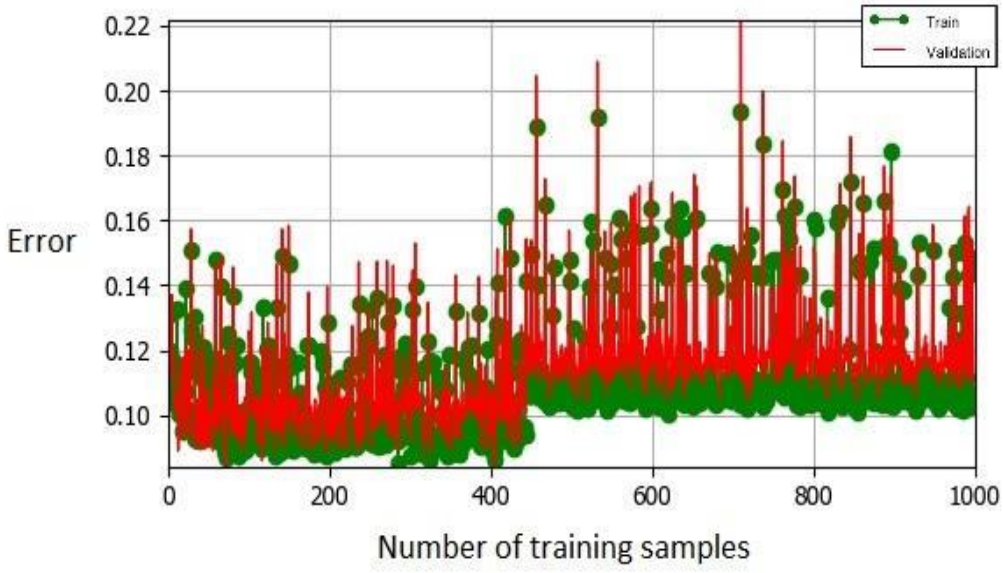

Figure 5.4. Neural Network Learning Curve

From 2006 to 2018, the percentage change in LULC classes is 11.908 for barren, 6.36 for built-up, 4.27 for vegetation and 1.04 waterbodies in Table 4 part B of Section 4. According to the aforementioned data, the rate of LULC change has quickened, with the rate of barren land decreasing at a greater rate and the built-up land increasing at a faster pace, indicating a rapid urbanisation. Many economical activities have been impacted by this shift in land usage. Similar data may be found in Table 4 section C, which provides estimates of the rate of change in LULC classes from 2006 to 2018. The Warangal's built-up expansion is mostly concentrated in two directions: (1) towards the Khilla Warangal, and (2) towards Gopalpur, along the Kakatiya canal in the northeast. Along major highways and national roads, there is a potential growth of agricultural land in the Warangal region.

Table 5.4(a) LULC change statistics from 2004 to 2006

Classes	2004	2006	change	2004(%)	2006(%)	change (%)
Waterbodies	114005700	129940200	15934500	41.456	47.251	5.794
Vegetation	41060700	46986300	5925600	14.931	17.085	2.154
Built up	115124400	93058200	-22066200	41.863	33.839	-8.024
Barren	4808700	5014800	206100	1.748	1.823	0.074

Table 5.4(b) LULC change statistics from 2006 to 2018

Classes	2006	2018	change	2006(%)	2018(%)	Change (%)
Waterbodies	129940200	97191000	-32749200	47.251	35.342	-11.908
Vegetation	46986300	65235600	18249300	17.085	23.722	6.636
Built up	93058200	104684400	11626200	33.839	38.067	4.227
Barren	5014800	7888500	2873700	1.823	2.868	1.044

Table 5.4(c) LULC change statistics from 2006 to simulated 2018

Classes	2006	Simulated 2018	change	2006(%)	simulated_2018 (%)	Change (%)
Waterbodies	129940200	127526400	-2413800	47.251	46.373	-0.877
Vegetation	46986300	48640500	1654200	17.085	17.687	0.601
Built up	93058200	94400100	1341900	33.839	34.327	0.487
Barren	5014800.00	4432500	-582300	1.823	1.611	-0.211

5.2.3 Transition potential modelling in LULC change using artificial neural network

It is possible to compute a transitional potential map using a variety of approaches, including artificial neural network (ANN) and logistic regression (LR). A variety of methods rely on LULC data to model and calibrate LULC change. Use of this strategy is appropriate when the algorithm is dealing with a lot of uncertain or difficult to implement data. As a result, an index from 0 to 1 is generated to describe the terrain. A continuous range, for example, between 0 and 1, is selected depending on the usability of the terrain since fuzzy logic requires it. The interactions between linked neurons and the alteration of the weight connections between them are at the heart of ANN. Additionally, this adjustment is dependent on input data and the network's intended output. "Neural network learning" is the term for this procedure (Fig. 4). Using this information, we were able to create a transition probability matrix for land use types

(see Tables 5, 6, and 7). Vegetation, waterbodies, and arid land all had probability values of at least 0.76 from 2004 to 2006. The built-up class has a transition probability of 0.94%. With a chance of converting from vegetation to built-up land of 0.84% from 2006 to 2018, the transition of diverse land use types has been constant. In terms of transition probabilities, bare and vegetation were the most active, with 0.443 and 0.47 transition probabilities, respectively, that were predominantly turned into waterbodies and built-up with an increase in chance of 0.60.

Table 5.5: Transition probability matrix of LULC classes from 2004 to 2008

	Waterbodies	Vegetation	Built up	Barren
Waterbodies	0.761	0.064	0.169	0.004
Vegetation	0.114	0.788	0.094	0.002
Built up	0.329	0.061	0.602	0.006
Barren	0.101	0.031	0.097	0.768

Table 5.6: Transition probability matrix of LULC classes from 2006 to 2018

	Waterbodies	Vegetation	Built up	Barren
Waterbodies	0.443	0.101	0.441	0.013
Vegetation	0.098	0.844	0.053	0.003
Built up	0.370	0.129	0.472	0.027
Barren	0.101	0.057	0.162	0.678

Table 5.7: Transition probability matrix of LULC classes from 2006 to simulated 2018

	Waterbodies	Vegetation	Built up	Barren
Waterbodies	0.977	0.020	0.002	0
Vegetation	0.011	0.975	0.013	0.00002
Built up	0	0.001	0.998	0
Barren	0	0	0.116	0.883

5.2.4 Prediction of LULC using cellular automata

Using cellular automata to process the ANN results, three sorts of output maps are generated. A transition potential map depicts the likelihood or possibility for a land use/cover class to transition to a different one. Zero (low transition potential) to 100 (high transition potential) are the possible values (high transition potential). For example, the "vegetation to built-up" transition potential and the "barren to waterbodies" transition potential are both derived from LULC classifications. Certaincy raster, which is the difference between two big potentials, is another output type. If there is a substantial difference, then there is more confidence in the anticipated raster, which is based on LULC classes and their transitional potential. For the time years 2004 to 2018 and 2004 to 2052, Fig. 5a and b demonstrate the transitional certainty of the land use categories. To forecast 2018 raster, a cellular automata-based technique was utilised between 2004 and 2006, with a step size of two years and six iterations, as shown in Fig. 6a. The Monte Carlo method is used in the cellular automata approach. To generate kappa statistics, the simulated 2018 raster is compared to the real 2018 LULC categorised raster. LULC for the year 2052 is forecasted using the same technique and increasing the number of iterations after agreement is established through validation. The 2052 LULC raster is shown in Figure 6b. These modifications are necessitated by the fact that the approach relies on pixels that have changed since last year. It is expected that in 2052, the percentage of land covered by barren land would increase, reaching 46.6 percent of the study region, while other land uses will alter at varying sizes.

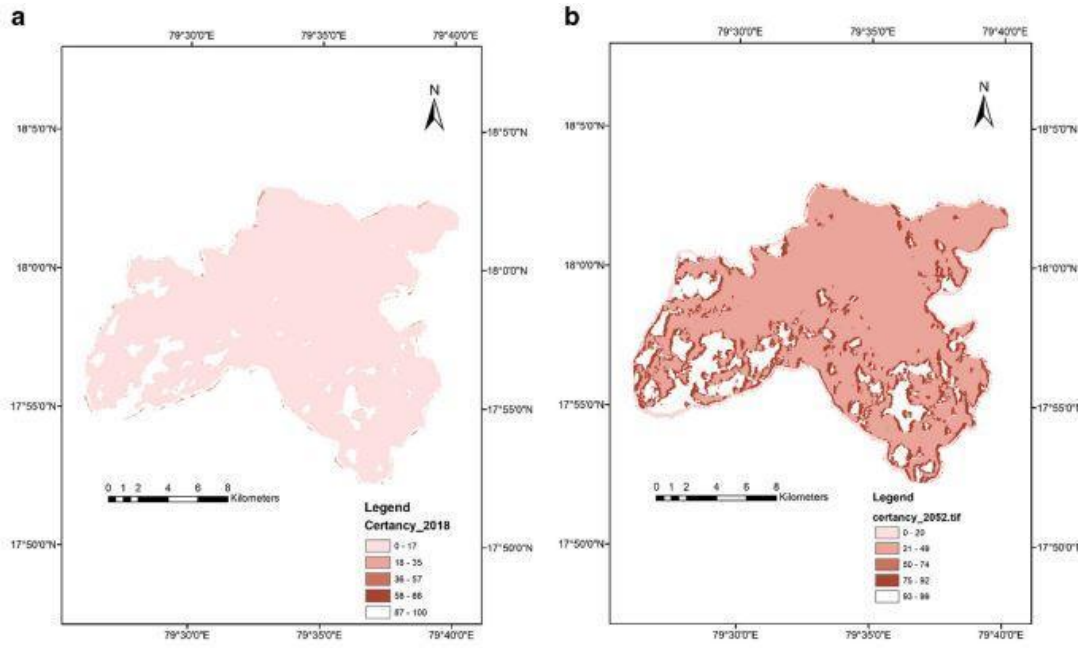

Figure 5.5 Certancy raster for the difference between the two large potentials for the years 2018 and 2052

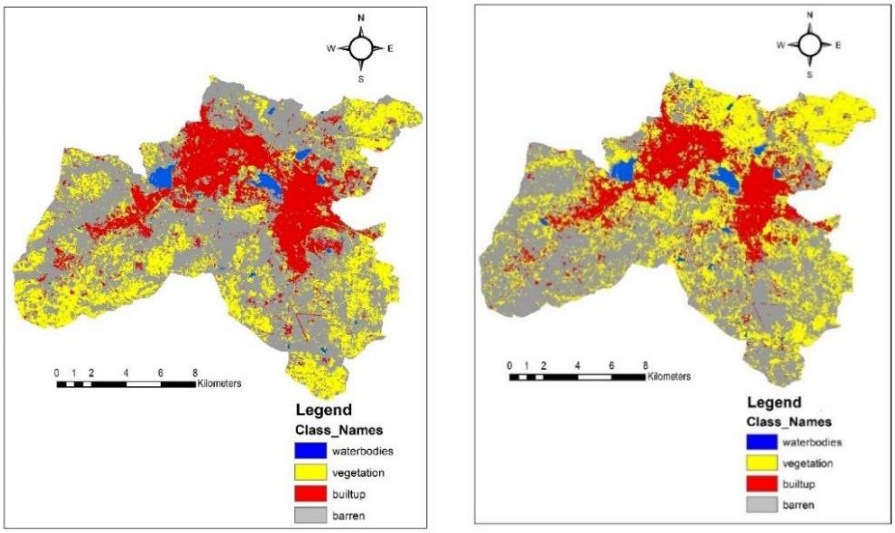

(a) (b)

Figure 5.6. (a) Simulated LULC of 2018, (b) Predicted LULC of the year 2052

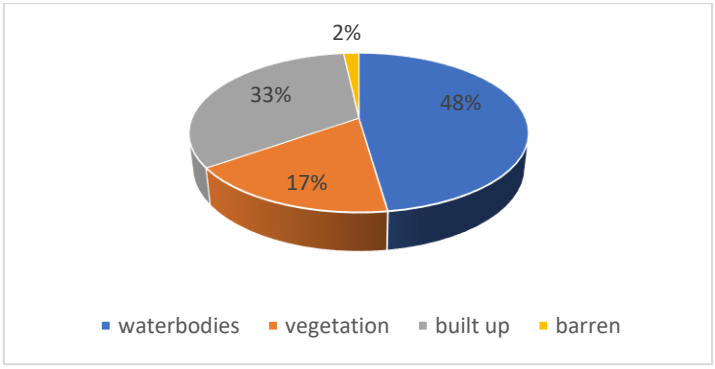

Chart 5.1 Percentage area distribution of future LULC in 2052

5.3 Model validation

Predicting a LULC is only regarded trustworthy for a specific project if it has been validated using the existing datasets. As a result, MOLUSCE certified two LULC rasters, one of which is based on real data from 2018, and the other based on cellular automata simulations of the year 2018. This method was used to forecast the LULC map for 2052 in the same way, except the iterations were given sequentially with respect to the 2004 and 2006 temporal gaps. These four kappa statistics metrics, calculated by the validation module and used to assess the model's accuracy: overall kappa, kappa histogram, kappa location and percentage of correctness, are shown below. Contingency table cell I where piT is the total of all ith row cells, pTj is total of all jth column cells, and c is a raster category count. Comparing real-world classification data with anticipated probabilities, Kappa statistics provides an indication of how well the two datasets match up statistically. There are two Koverall and Klocation metrics that are used to

evaluate the simulation's overall success and location accuracy. There is no agreement when the Kappa statistic reads "0%," but when it reads "100%," it means full agreement. As shown in Table 8, the validated module checked the agreement between the simulated and real-classified 2018 rasters and came up with the following results. Kappa (histogram), Kappa (overall), and Kappa (location) are all 0.933; the percentage of accuracy is 76.229, which indicates that the model is accurate for Warangal, and that the kappa (histogram) estimate is accurate. In order to anticipate the 2052 LULC raster, 23 iterations of the cellular automata module are used as the step size of 2 years. Table 9 shows the raster's expected 2052 validation statistics. Estimated Kappa (histogram), Kappa (overall), and Kappa (location), respectively, are all at 0.911, 0.630, and 0.692, respectively.

Table 5.8 Kappa index of the model validation.

Parameter	Value (%)
Kappa (histogram)	0.700
Kappa (overall)	0.964
Kappa (Location)	0.726
% of Correctness	79.722

5.4 Summary

This research aims to detect and evaluate the LULC change in future using cellular automata-Markov chain based simulation. In other words, the results indicate the capability of open source GIS (Quantum GIS) to run spatial analysis for spatiotemporal land use change study. Hence, it has a big potential for planning environment and adaptive management. Specifically, the application is useful for land use planners and decision-makers to monitor and assess their long-term development. To meet the research objective of the study, data is prepared in QGIS environment. LULC values of the images 2004, 2006, and 2018 were classified into four classes: barren, built-up, vegetation, and waterbodies. These images were used to project the likely changes in 2052. The outcomes of classification indicates a significant growth of some land use land cover mainly barren and vegetation during the period 2006 to 2018 with a stable decrease of other land cover type in the year 2052, especially waterbodies. The result of LULC change projection, which was carried out using CA, suggests that residential area and public building will continue to increase in WMC and this will have an effect on the other land cover types such as agriculture and waterbodies. The distribution of population growth will increase due to the in- crease of residential area and focus of ministries and institutions in WMC as it is in the list of smart cities, so people prefer to live near their place of work. In summary, the methods used here to answer the research questions and achieve the aims of the study have been very good. QGIS provided tools, which played a powerful role in studies of this type, which are very helpful for planner to address the problem, which arise due to environmental change and human activities. This study offers some recommendations to enable them to use land source in a better way; these are as follows.

Chapter 6
Urban flood modelling

6.0 General

An urbanised catchment typically has more impermeable surfaces, which reduces ground infiltration and raises surface runoff. Natural and artificial streams are being changed into an artificial stormwater network because of the growing urbanisation. As urbanisation spreads, natural and man-made streams are being redirected into a man-made stormwater network. Due to the increased frequency and intensity of precipitation, rivers and the existing stormwater drainage system are unable to keep up with the increased volume of rain, leading to urban floods (Li et al., 2015; Duan et al., 2016). In order to support urban planners, precise monitoring of flood inundations and hazard distribution is crucial (Feng et al., 2020). There has been a variety of methods used in the past to identify the most crucial areas for flood control in metropolitan areas. The primary non-structural method currently in use throughout the world is flood modelling, which consists of an integrated hydrologic-hydraulic modelling. Prioritizing the crucial catchments for the deployment of flood mitigation measures in urban contexts has traditionally been done using a variety of approaches. In order to determine the geographical prioritisation in the management of urban floods, Qi et al. (2022) provided a thorough study of source tracking methodology. Hence, in response to the floods in the city of Warangal, we set out to find a model that could accurately represent the inundation. According to the literature for flood modelling, the PCSWMM rainfall-runoff model helps to locate inundating drainage junctions, prioritise the sub-catchments base on the inundation, to create flood risk map. The present study opted for an integrated 1D-2D model, which performs better among 1D, 2D, 1D-1D models to visualize the flood depth and extent (Werner, 2004. The rainfall-runoff model in PCSWMM results helps in identifying inundated drainage junctions and to prepare flood hazard maps. The model's performance was assessed, and the runoff in the storm water drainage network was estimated, using one-dimensional river flow and one-dimensional-two-dimensional drainage overflow modelling.

6.1 Methodology

In the present chapter a complete framework is illustrated to study the flood occurrence due to

This was done in order to facilitate mitigating flood measures in future. The objective of the research is to assist urban planners by demonstrating the significance of flood inundation modelling and hazard.

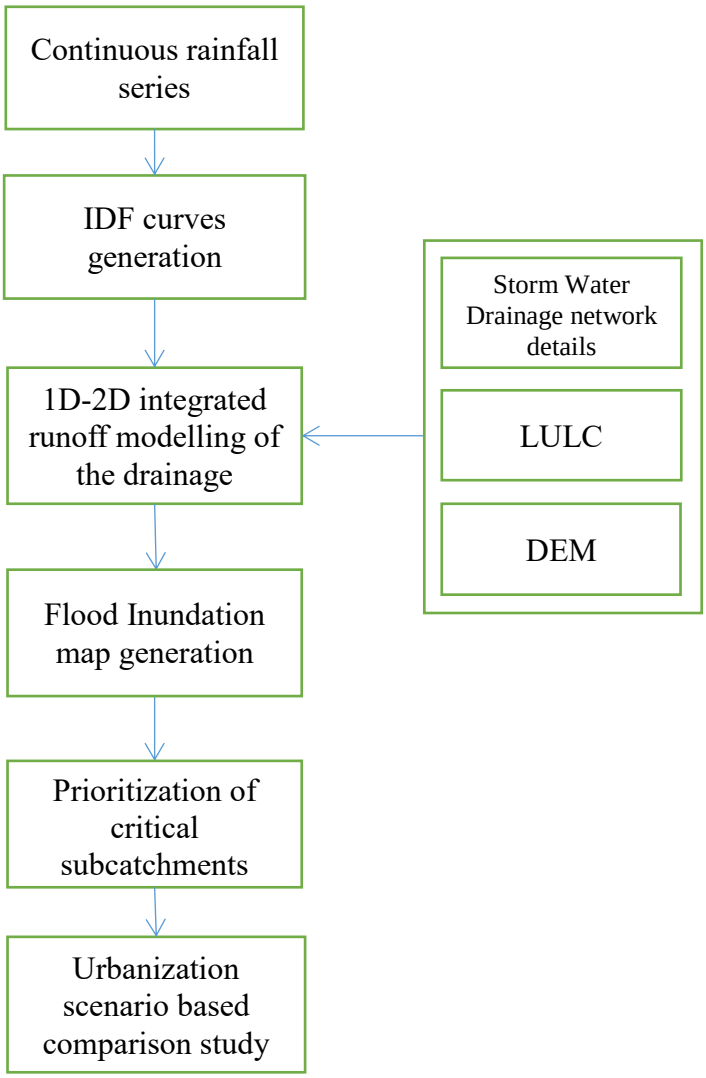

Figure 6.1 Flowchart of methodology.

The overview of the methodology is outlined in the form of a flow chart as shown in Figure 6.1. The steps followed are: (1) Data preparation of both the spatial data like Rainfall series for the continuous events from 2000 to 2019, LULC, DEM and non-spatial data like Storm water drainage network details including subcatchment features, junctions and conduit features, (2) Implementing coupled 1D-2D model using PCSWMM to assess the hydraulic

and hydrological characteristics, (3) to create flood inundation maps (4) to explore the urbanisation-based scenarios in the highly flooded area identified in the previous chapter 4. The results of the present study are validated with geotagged maps, which were taken on site, as the observed data is not available.

6.1.1 Description of the study area

As mentioned in the previous chapter 4, from the flood hazard mapping of WMC as shown in the figure 4.13 the highly vulnerable area Wadepally Lake Catchment was considered for the runoff modelling. Figure 6.2 shows the location of the Wadepally catchment wherein the water flows form the Wadepally Lake at the upstream and flow into Gopalpuram Lake in the downstream. According to data gathered from the public health department, city people encroach upon a number of drains along the study region under consideration. The present situation of drains are critical, they are silted or choked by garbage. Therefore, in the monsoon, due to due inadequacy of carriage capacity the Wadepally lake overflow and inundates the area downstream up to Gopalpuram lake. The same problem is observed in drains downstream of Gopalpuram Lake. Field visit was carried out as shown in figure 6.3 to validate with the ground reality with the local bodies and finalise the extent of study area. Hence, from the field investigations, the catchment of Wadeppaly Lake reach and storm water network around this lake is considered for runoff modelling. The open drains along with existing storm water drains that carry the rainwater are 15km long. Wadepally Lake is one of the three major water supply sources of GWMC located at Greater Warangal Municipal Corporation. In addition, it is located adjacent to NH-202 viz. 100feet wide Road. The storage capacity of Wadepally Tank is about 132 Million Cubic Feet (0.132) TMC. Water spread over an area of about 600 acres. The Catchment area of Wadepally lake and Gopalpuram lake Covers 80 Sq.km.

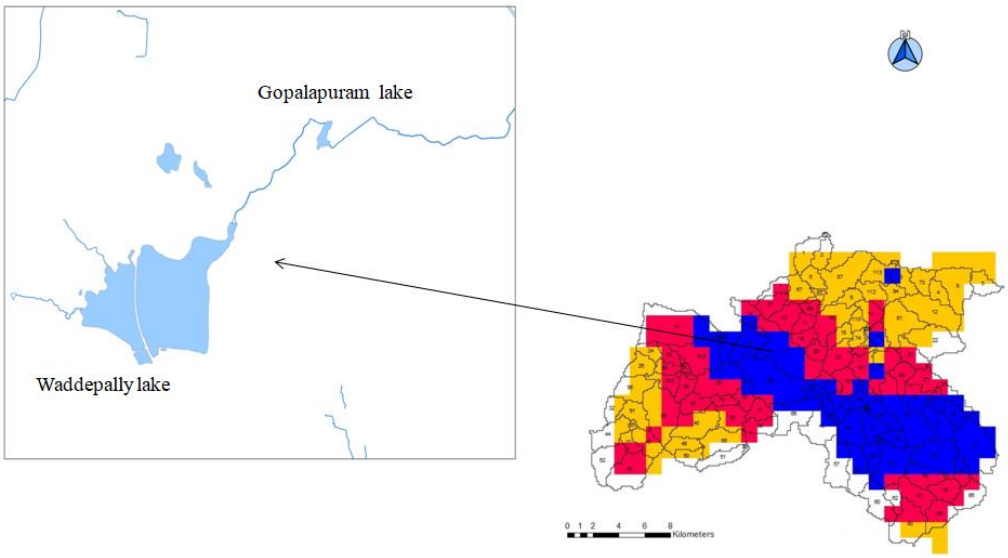

Figure 6.2 Drainage network showing the highly vulnerable area connecting Wadepally Lake and Gopalpuram Lake

Figure 6.3 Geotagged photos of field visit

6.2 Rainfall Frequency Analysis

Rainfall Frequency analysis is a statistical techniques used to develop the relationship between average rainfall intensity, storm duration and return period. Sometimes, the rainfall depth is used in place of the average intensity. Point rainfall data is used to derive Intensity-Duration-Frequency curve and this curve are used in the rational method for urban storm drainage design. In applying the rational method, a rainfall intensity is used which represents the average intensity of a storm of a given frequency for a selected duration. The frequency chosen

should reflect the economics of flood damage reduction. In India frequencies of 1 to 10 years are commonly used for stormwater system design in areas where residential areas to be protected. For commercial and higher value areas, 10 to 20 years or higher return periods are often selected.

6.2.1 IMERG data description

The Global Precipitation Measurement (GPM) mission, which is the TRMM's replacement, was launched in February 2014 as a next-generation satellite precipitation observation system (Hou et al. 2014). As a result, starting in January 2015, a new precipitation product created by GPM satellites, IMERG, has been made accessible to the general public in favour of an outdated precipitation product, TRMM Multi-satellite Precipitation Analysis (TMPA). The GPM satellites can find light precipitation by using a wider spectrum. The NASA IMERG satellite product is available worldwide from 2000 to the present at a half-hourly, 0.1° resolution in three versions: IMERG-Early at a 4-hour latency, available in near real-time but excluding remote sensing data following a satellite pass; IMERG-Late at a 12-hour latency; and IMERG-Final at a 2.5 month latency, which incorporates gauge data to improve product accuracy (Huffman et al., 2019, Tan et al., 2019). In this chapter, IMERG-Early is used with a 20-year time span between 2000 and 2019, a spatial resolution of 0.1°0.1°, and a temporal resolution of 30 min because of its low latency and availability for early warning systems.

6.2.2 Development of IDF relations

The Intensity-Duration-Frequency (IDF) curves describe the relationship between rainfall intensity, duration, and frequency (or its inverse, probability of exceedance). IDF curves are commonly used in hydrologic, hydraulic, and water resource system design. These curves are derived from frequency analysis of continuous rainfall data records. Gumbel's Extreme Value distribution method is used in this study for probability distribution for each selected duration data series. The following periods are considered for design applications: 1 hour, 2 hours, 4 hours, 6 hours, 12 hours, and 24 hours. The observations are fitted to a theoretical Extreme Value (EV) distribution (e.g., Gumbel Type I), and the theoretical distribution is then used to estimate the rainfall events associated with given exceedance probabilities. The derived precipitation depth is used to generate IDF curves with varying return periods.

The following steps were followed in order to develop Intensity- Duration Frequency (IDF) curves.

a. Chow (1951) demonstrated that hydrological studies can be expressed using the hydrologic frequency analysis Equation 6.1. The rainfall (P_T) corresponding of a given return period (T) using the Gumbel's Distribution is given by

$$P_T = \sigma + K.S \qquad \text{Equation 6.1}$$

Where

σ = Average Annual Daily Maximum Rainfall

S = Standard Deviation of Annual Daily Maximum Rainfall

K = Frequency Factor

b. The annual maximum rainfall intensity for specific durations is calculated from rainfall measurements for each year of record (or the annual maximum rainfall depth over the specific durations). Annual maximum values of half-hourly rainfall series for each year of rainfall data were extracted corresponding to 1-hr, 2-hr, 4-hr, 6-hr, 12-hr, and 24-hr time durations as shown in Table 6.1.

Table 6.1 Annual maximum Rainfall intensity for various durations

	Duration					
Year	**1hr**	**2hr**	**4hr**	**6hr**	**12hr**	**24hr**
2000	14.928	14.928	20.243	20.243	22.847	25.977
2001	16.043	16.043	17.478	20.304	26.074	40.510
2002	22.247	22.136	49.670	49.670	61.956	81.065
2003	17.770	12.463	23.211	23.211	23.394	24.627
2004	72.702	39.495	72.702	72.702	72.702	112.429
2005	36.653	23.723	36.653	55.673	55.673	55.676
2006	21.724	21.724	32.973	32.973	35.620	65.219
2007	24.821	18.782	24.821	30.419	30.469	30.790
2008	19.898	15.008	23.526	26.070	40.320	51.669
2009	15.320	15.320	21.858	21.858	21.858	21.858
2010	33.623	33.623	39.884	40.239	40.239	40.239
2011	21.041	21.041	21.041	21.041	21.041	21.114
2012	36.202	29.393	36.260	42.100	42.509	42.509
2013	29.847	29.847	59.884	73.573	74.163	76.204

2014	21.322	21.322	22.012	22.179	27.867	28.058
2015	31.140	31.140	41.805	42.366	54.868	64.806
2016	34.499	34.499	60.204	61.313	61.433	86.868
2017	31.423	31.423	53.068	49.743	56.126	57.043
2018	31.140	31.140	31.701	42.366	42.366	42.371
2019	9.697	9.697	20.439	21.413	28.134	28.258
Mean	27.102	23.637	35.472	38.473	41.983	49.865
Std DEV	13.016	8.222	15.732	17.031	16.865	24.406

c. From each series, mean and standard deviation values were found for each duration .The value of the random variable X_T associated with a given return period, T, is obtained from the following equation 6.2

$$X_T = \ddot{X} + K_T S \qquad \text{Equation 6. 2}$$

Where

X_T = mean of the observations (e.g., arithmetic average of the observations),

S = standard deviation of the observations.

K_T = frequency factor associated with return period T

d. For each duration (e.g., 1hr, 2hr …etc.), the sample mean and sample standard deviations of the series of annual maxima are computed, (x1… xm) (see Table 6.1).

e. The values of location and scale parameters were obtained from equation 6.3 and are shown in Table 6.3.

$$G(x;\mu,\beta) = \frac{1}{\beta} e^{\frac{x-\mu}{\beta}} e^{-e^{\frac{x-\mu}{\beta}}} \qquad \text{Equation 6.3}$$

Where

μ = location parameter

β = is the scale parameter

f. Then, the rainfall values were ranked in increasing order of magnitude. In addition, the plotting positions (Fi) and (Yi) were calculated by making use of equations (6.2 and 6.3).

g. The frequency factors associated with the desired return periods (e.g., 2 yrs, 5yrs, 10yrs, 50yrs, 100yrs) are computed using equation 6.4.

$$K_T = -\frac{\sqrt{6}}{\pi}[0.5772 + \ln\ln(\frac{T}{T-1})]$$ Equation 6.4

Table 6.2 Frequency factors

T (years)	2	5	10	50	100
K_T	0.2857689	1.169498	1.754604	3.042329	3.5867216

h. Finally, the precipitation intensity associated with each return period is to compute. IDF relationship is developed for all return periods and is shown in the Figure 6.4. The fitted IDF relation has R^2 (coefficient of determination) value equal to 0.998 and standard error of 0.012. Design storm intensities derived for different return periods are used in the simulation of runoff later in the next section of the chapter.

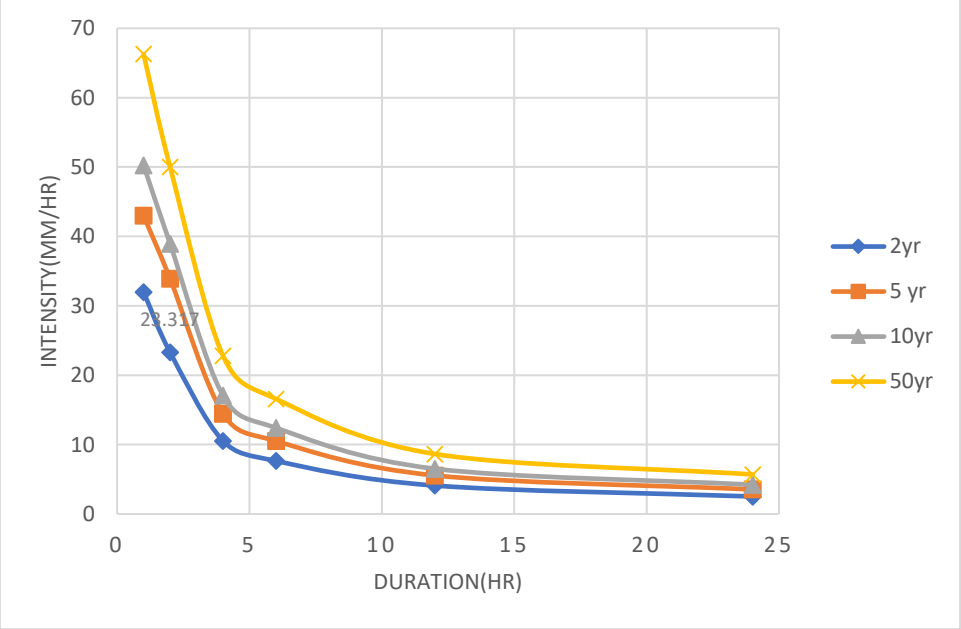

Figure 6.4 Intensity Duration Frequency Curve for the rainfall series of 2000 to 2019

6.3. Model Conceptualization and Parameter for runoff simulation

PCSWMM integrates the full US EPA Storm Water Management Model (SWMM, version 5) engine with Geographic Information System (GIS) capability of simulating single event-based or continuous rainfall-runoff processes for watershed modelling in urban and rural areas. The model contains a wide variety of hydrologic and hydraulic capabilities such as flow routing, evaporation of standing surface water, rainfall interception in depression storage, flow routing through closed and open conduit networks of unlimited size, two-dimensional flood routing, and modelling of backwater, surcharging, and surface ponding, among others. PCSWMM is

a discrete physical-based model that uses momentum, energy, and mass conservation laws to design storm drainage systems that keep vehicles, pedestrians, and urban drainage systems safe from flooding during extreme events.

Traditional one-dimensional (1D) models (either steady or unsteady analysis) typically simulate flow in flood channels and gravity collection networks, but they fall short when it comes to simulating specific phenomena that occur during extreme events, such as street flooding and overbank flow in floodplains. A coupled 1D and 2D PCSWMM model from Computation Hydraulics International (CHI) was used in this study. Because of PCSWMM's fully integrated approach to 1D-2D modelling, the modeller can easily switch between 1D and 2D modelling. One-dimensional-two-dimensional (1D-2D) models connect one-dimensional unsteady flow calculations that simulate linear flow in the subsurface network with two-dimensional flow calculations. The 1D model employs a link-node system, whereas a grid of cells with slope defines the 2D domain and roughness attributes. During severe storms, water flows out of the subsurface system and may gravitate towards a nearby inlet or pond if there is no nearby inlet. Flow may backup or reverse direction due to obstructions or insufficient capacity in the drainage network.

6.3.1 One-Dimensional model description and parameters for River flow modelling

Performing a 1D-flood inundation analysis requires several different steps and layers in PCSWMM. A DEM layer, a transect layer and a flow path or conduits layer is required. Surface runoff happens when the subcatchments cannot take water and move it to the final outfall because the surface is not porous enough. As per the 1D model setup that was shown in the figure 6.5, the routing portion transports the runoff through a system of open or closed pipes, channels, storage units and regulators during a simulation period considered in the study (20 years as mentioned in the section 6.2.4).

The following variables are used in the formulation of PCSWMM: catchment surface area, sub-catchment width, slope, depression storage depth of impervious and pervious area, manning’s constant. The invert heights for each junction or node were assigned as per the Reduced level (RL) provided in the CAD file of storm water drainage network. Conduits are linked to junctions and outfalls in the simulation model. DEM was created from contours with contour interval of 10m, provided by Public health department, Warangal. The study area is delineated into 26 subcatchments from the DEM to capture the effect of spatial variability in

topography in a best way by locating outfalls and identifying the contributing areas. The subcatchments were then connected to the nearest node in the existing storm water drainage network, CAD file that was obtained from the public health department, Warangal. Centroid of the subcatchments were assigned rainfall data using nearest neighbor-based technique. As per the storm drainage network the units considered (shown in the figure 6.6) are 1 outfall at the river downstream that flows between Wadeppaly lake at the upstream and Gopalpuram lake at the downstream, Wadeppaly lake was taken as 1 storage unit in the upstream,1 weir, 73 junction points and 44 conduits joining these nodes.

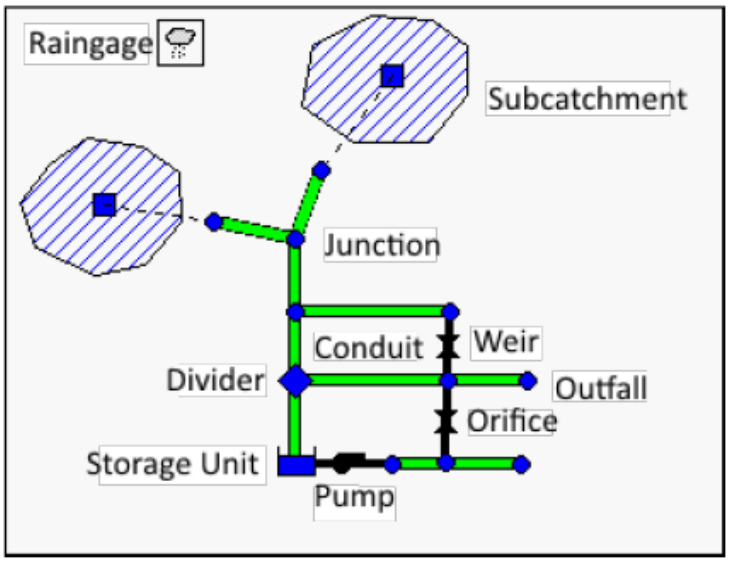

Figure 6.5 1D conceptual model of a stormwater drainage system in PCSWMM (source https://support.chiwater.com)

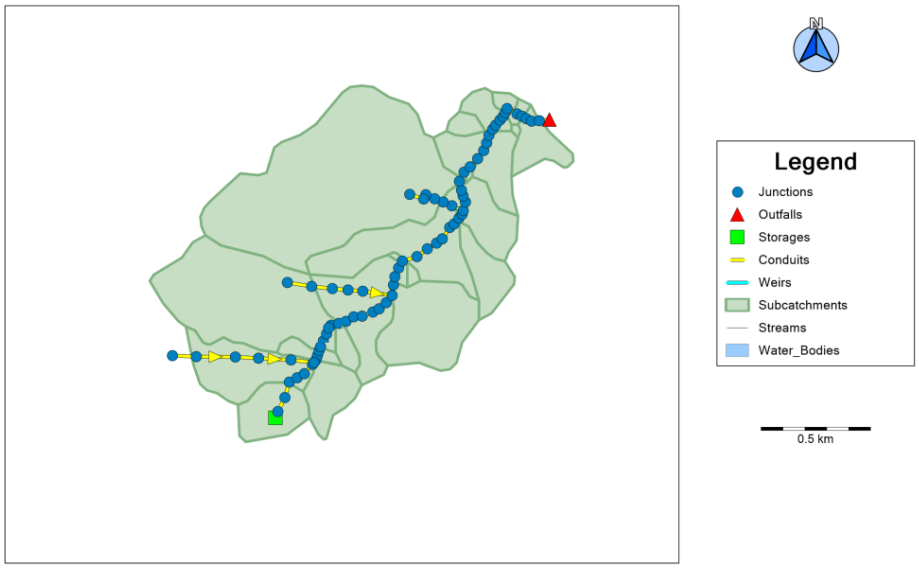

Figure 6.6 1D model Setup

The pressure flow conditions in PCSWMM solve the 1D shallow water equations or Saint-Venant equations and adopt continuity-momentum equations for conduits and junctions (Xu et al., 2018). The process models considered the flow Units in m^3/sec, the Infiltration Method as Green-Ampt hydraulic simulations were used in the flood routing model, which employed the dynamic wave approach. The nanning roughness constant was considered as the calibration parameter in this modeling because it is sensitive to peak runoff from a minimum of 0.035 to a maximum of 0.050 (depending on river surface cover and changed until the optimum values were attained). Sandy loam soil is predominant in the study area. Thus, the depth of the depression storage was estimated as 0.062 inches for impervious and 0.25 inches for pervious surfaces for sandy-loam soil. It shows the various subcatchments that receive and generate runoff (Huber & Dickinson, 1988). Hydrologic input parameters such as flow length, slope, and imperviousness were assigned to each subcatchment. A Transect layer is used to represent the uneven cross-section of the Conduits layer by defining how depth changes as the distance across the cross-section changes. Tools like Transect Creator and Transect Editor were used to build transect layer (as shown in Figure 6.7), which employ elevation data from the DEM layer.

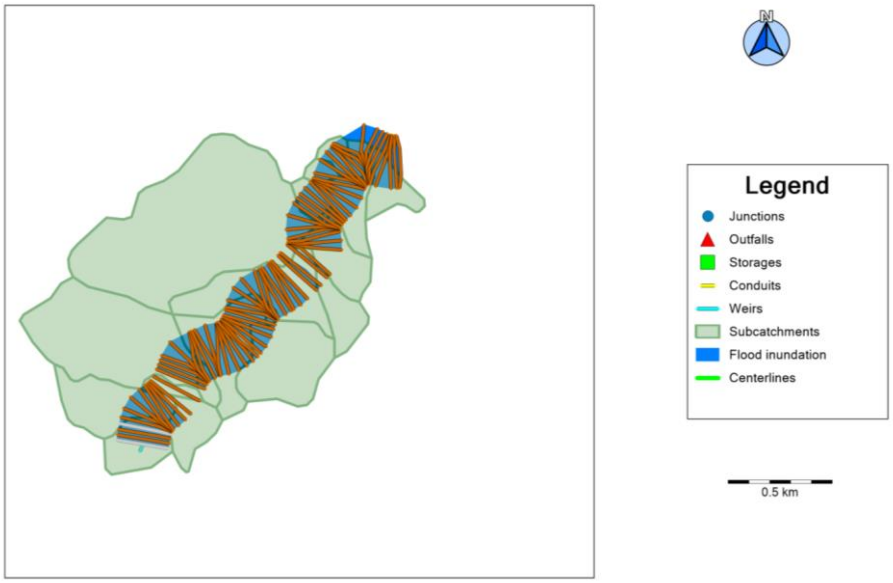

Figure 6.7 Transect layer created for flood inundation

6.3.2 One-Dimensional- Two-Dimensional model description and parameters for drainage overland flow modelling

The modeling of overland flow may be problematic for a strictly 1D modeling as there may be multiple flow pathways around and through obstructions or overland flow path may not be known or undefined. PCSWMM can provide accurate 2D modeling of flood depths, flows and velocities for both urban and rural applications, including river-overland routing of rainfall runoff. An integrated 1D-2D model was created that combines a distributed hydrologic routing model with the 1D hydraulic model for the storm drainage network (as mentioned in the previous section) and a 2D overland flow model. The modelled junctions and conduits of various cross sections are connected to a 2D overland flow model. To measure the overland flow, each subcatchment is put into a nonlinear reservoir model. To model the hydraulic calculations (inflow and outflow) of conduits, a dynamic wave routing model is chosen. For 2D overland flow modeling, the building footprint layer, representing obstructions, in the study area were considered. The layers prepared for the 2D input included the centreline, obstruction (the building footprints of the encroachments) and bounding layers. The layers are then calibrated based on sensitivity analysis of the parameters using SRTC tool. The 2D nodes layer is a point layer used to define the junctions that characterizes the 2D cells by sampling the elevation from a DEM (Figure 6.8). The 2D domain with a hexagonal or rectangular mesh represents each cell by 2D nodes (Figure 6.9).

.

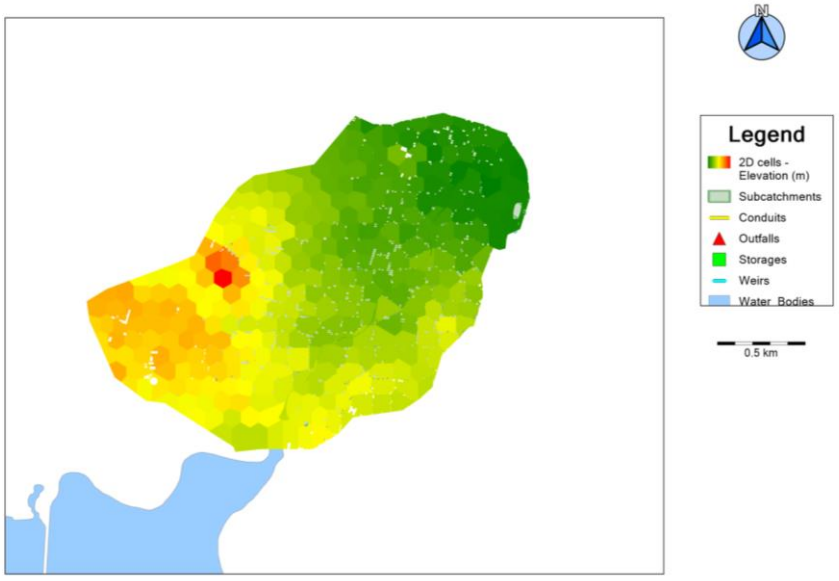

Figure 6.8 2D cell surface elevation

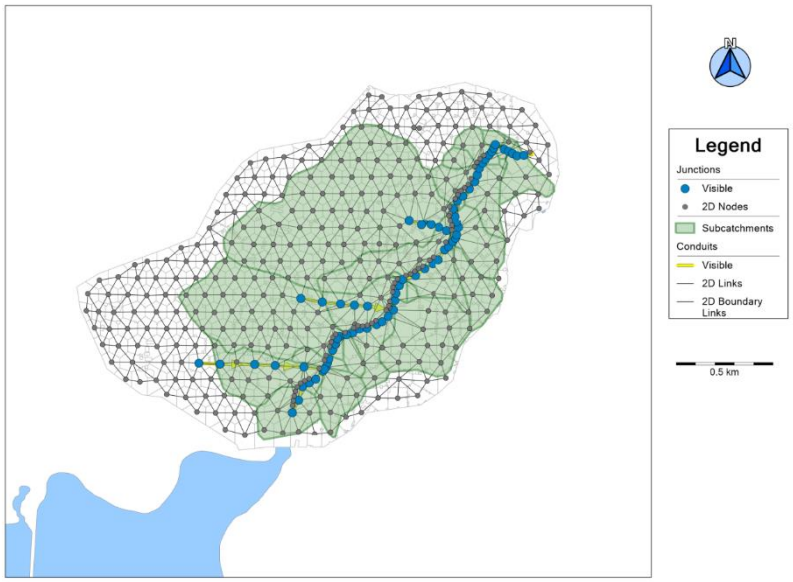

Figure 6.9 2D mesh connected with the 2D nodes

To ensure continuity, 2D nodes are given a small surface area (usually 0.1 m^2), and the surface area in each cell is assigned to the conduits that connect to the node. PCSWMM modifies the conduit lengths and widths in a precise ratio based on the number of links connected to the node. Drains were described as an open channel with a rectangular cross section.

Table 6.3 2D Model parameters

Parameter		Description
Infiltration method		Green Ampt
Manning roughness of	2D mesh	0.05
	impervious surface	0.012
	pervious surface	0.015
2D mesh type		Hexagonal for outer boundary Directional for river channel
Mesh area (m^2)		100
2D mesh resolution		75 m

6.4 Model calibration

In order to perform the sensitivity analysis, we used the SRTC tool. The most sensitive characteristics were found to be the width, slope, imperviousness percentage, and number of curves in the sub-catchment. The correlation coefficient's squared value is used to get the coefficient of determination R2. Accordingly, NSE is considered to be the most acceptable measure of relative inaccuracy or fit because of its simple physical meaning (Legates and McCabe Jr 1999). The NSE is 0.96 and 1.94, whereas RMSE is 0.52/0.53 for calibration and validation correspondingly.

6.5 Urban flood modelling

Depending on how severe a flood is, there are several levels of flood hazard in urban environments. This idea refers to a analysis of related behaviours in various contexts indicating the likelihood of flooding (e.g., flood extent, stormwater flow rate, depth and length of inundation). PCSWMM model is simulated for a design storm condition of 2-year return period and 1-hour duration. The value of intensity is 39.251 mm/hr and given as input at each node/junction from corresponding subcatchments. In the present study, the junctions that are at risk of flooding are now identified using two indicators: one by duration and the other that by depth. The model takes into account the greatest depth produced at a specific conduit junction. Thus, risk map is generated based on depth of water rise at the junction nodes. The 1D nodes under flood risk are shown in the Figure 6.10. The risk analysis shows 40 nodes come under low risk, 25 nodes come under medium risk and 13 nodes come under high risk of flooding. The risk map divided the inundated zones under three classes; Low risk, medium risk and high risk as shown in the table Figure 6.10. Table 6.3 gives the classification of flood risk nodes based on the depth. Figure 6.11 shows the rainfall, runoff and flow readings of highly flooded conduit C31. Table 6.4, Table 6.5 and Table 6.6 shows the Node flooding summary, storage volume summary and Outfall load summary in 1D modelling.

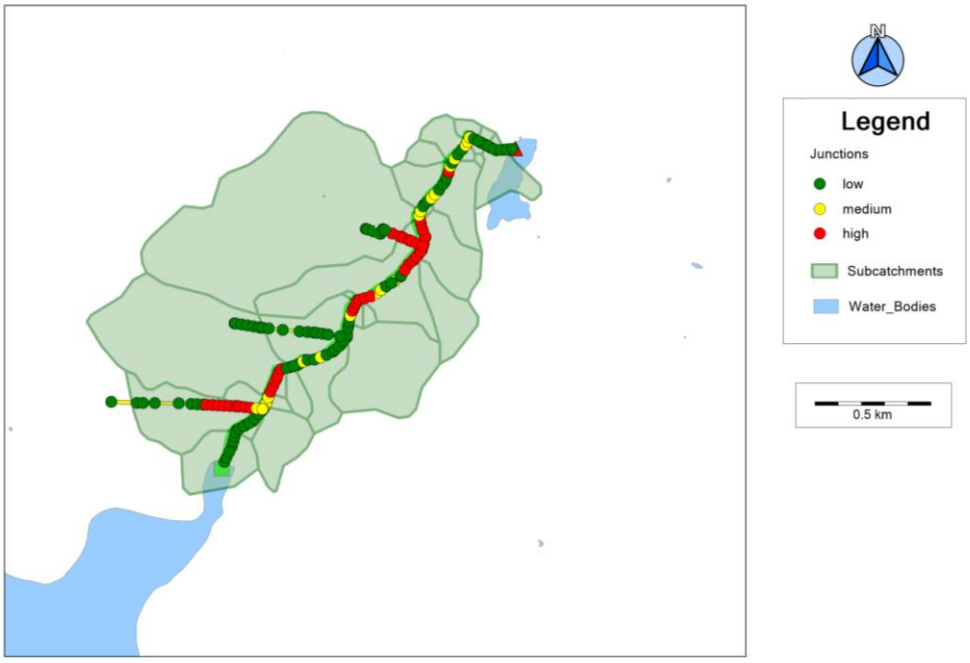

Figure 6.10 1D flood risk map

Table 6.4 Representation of risk type and depth of drains from 1D flood risk map

	Risk type	Depth of drains (m)
	Safe	>4
	Low	3-4
	Medium	2-3
	High	<2

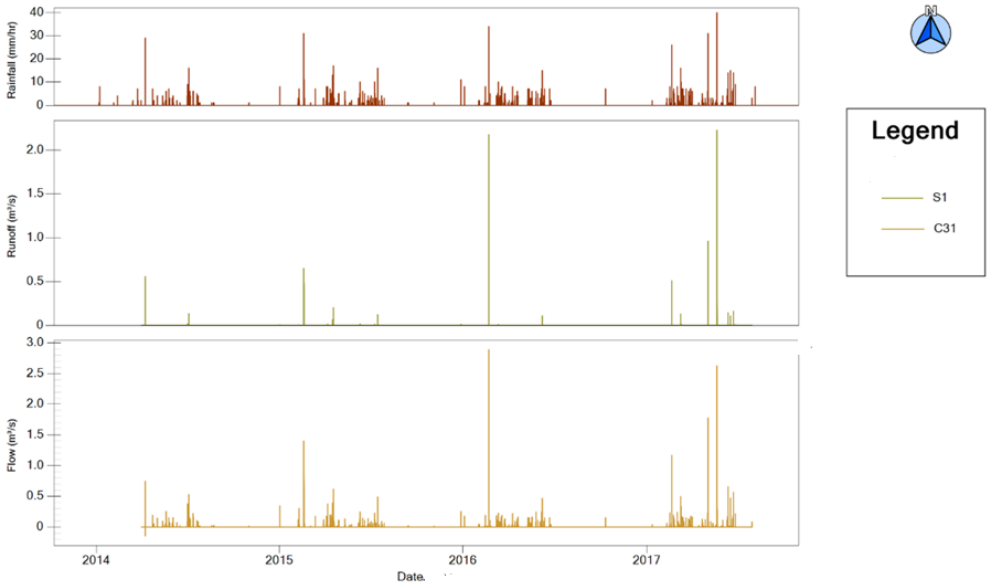

Figure 6.11 Rainfall, flow comparison of flooded conduit C31

Table 6.5 Node flooding summary in 1D modeling

Node	Hours Flooded	Max rate (m3/sec)	Time of max occurrence days hr: mm	Flood volume 10^6 ltr
J31	0.01	207.103	34 18:55	0.257

Table 6.6 Storage volume summary in 1D modeling

Storage Unit	Evaporation Loss (%)	Time of max occurrence (Days hr: min)	Maximum outflow CMS
SU 1	83	25 12:38	0.013

Table 6.7 Outfall loading summary in 1D modeling

Node	Hours Flooded	Max rate (m3/sec)	Time of max occurrence Days hr: mm	Flood volume 10^6 ltr
J31	0.01	207.103	34 18:55	0.257

Once the 1D model is connected to the 2D model is run, max depths for the cells are analyzed to compute the flood extent. The rainfall runoff variation is shown in the Figure 6.11 where

the peaks occur during 2005, 2016, 2017. The simulation results show that most of the junction nodes (J23-24, J29-35, J53-58,) are surcharged and are at high risk to flood. The conduits C31, C3, C8, C20 and C22 are also flooded. The maximum computed water depths in 2D cells are shown in Figure 6.14 while the maximum computed velocities are shown in the Figure 6.13. Most of the flooded nodes fall under minimum depth and max velocities. The integrated 1D-2D flood risk map is shown in the Figure 6.14. The flooded zones are divided into low risk zone, medium risk and high-risk zone. Flow profile for return periods is shown as per the hyetograph-developed gives the occurrence of peak flow for respective return periods.

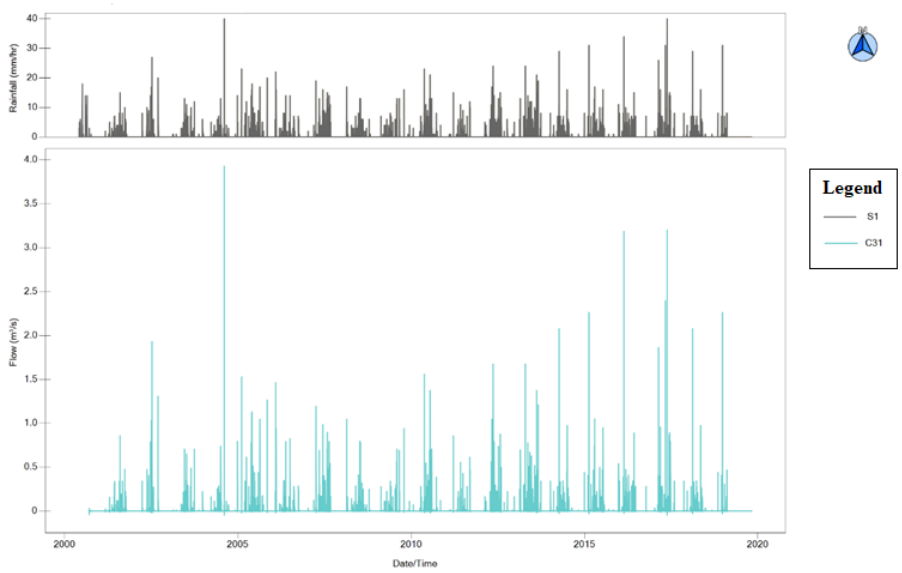

Figure 6.12 rainfall and runoff comparison for 20 years

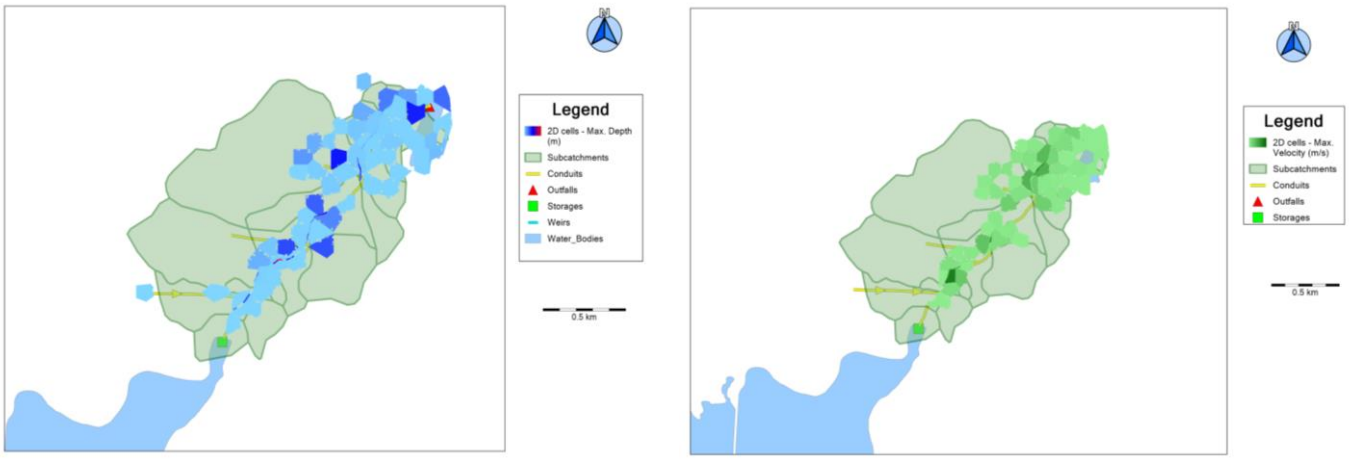

(a) (b)

Figure 6.13 (a) maximum computed water depths in the 2D cells; (b) The maximum computed maximum velocities of the 2D cells.

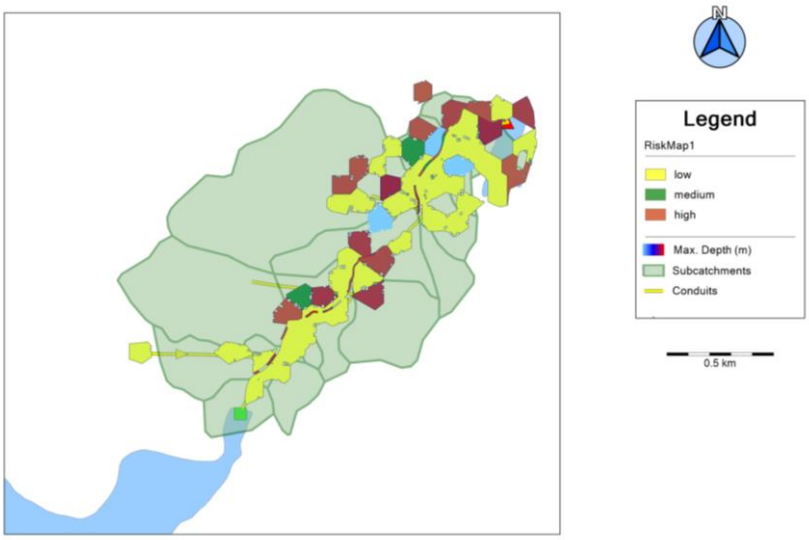

Figure 6.14 Integrated 1D-2D flood risk map

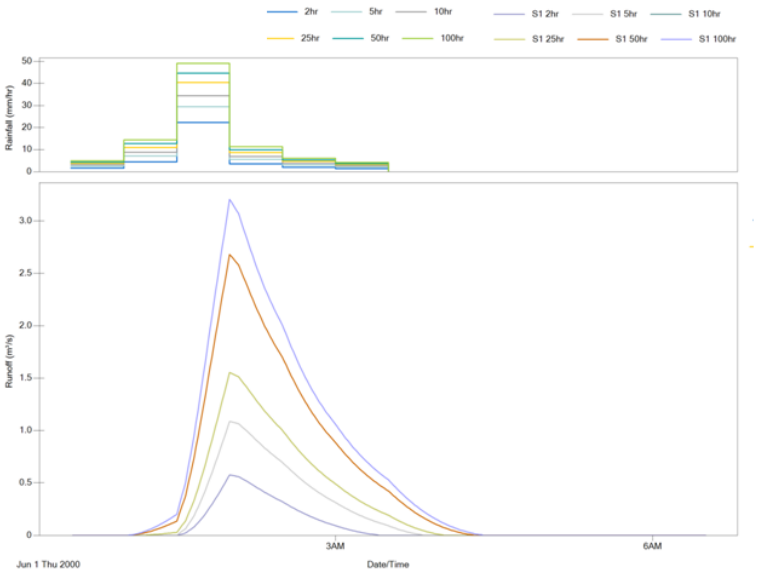

Figure 6.15 Flow profile in the flood conduit

Table 6.8 Output summary

Runoff Quantity Continuity	**Volume (Hectare- m)**	**Depth (mm)**
Total Precipitation	139.007	775.000
Evaporation Loss	0.000	0.000
Infiltration Loss	110.360	615.287
Surface Runoff	31.440	175.287
Final Storage	0.002	0.009
Continuity Error (%)	-0.2011	

6.6 Quantification of urbanization scenarios using PCSWMM

The existing drainage modelling is considered as the reference scenario analysed for the year 2006 as presented in chapter 4. Six urbanization scenarios including past, present and anticipated land use are modelled for the years 2004, 2006, 2008, 2016, 2018, 2052 respectively. Each selected scenario was applied to every subcatchments and hence the percentage imperviousness within every subcatchments was given as per the LULC classes according to the scenario. The calibrated PCSWMM model was used as a tool to simulate the urbanization scenarios. The hydrological effects of the urbanization scenarios were assessed using Flow Duration Curves (FDC), mean discharge (Q-mean). Infiltration and groundwater flow are reduced because of the transition from pervious to impervious surfaces, and so increased runoff is generated. All urbanisation instances show an increased trend in the mean annual runoff compared to baseline (2016).

6.6.1 Impacts of Urbanization on Hydrological modelling

Figure 6.16 depicts how urbanisation has an impact on FDC. The graphs show that when the urbanisation percentage rises, high flows continue to climb while low flows continue to decline. There is no FDC in the "normal scenario." This might be because of rainwater entering the watershed permeating the soil or being held as depression storage on the surface. It may also be partially because all of the land is naturally covered in vegetation, which may lead to zero imperviousness. This outcome may also be influenced by high rates of interception brought on by the presence of natural trees in the watershed and subsequent evapotranspiration. Additionally, it has been noted that extreme flows exceeding 10% of the time will increase from 3.0 m3/s to 5.0 m3/s as urbanisation grows. This demonstrates the negative effects of urbanisation, which raises the risk of floods in the catchment. All flow are clearly intensified by urbanisation, and each peak flow grows as the urbanisation percentage rises.

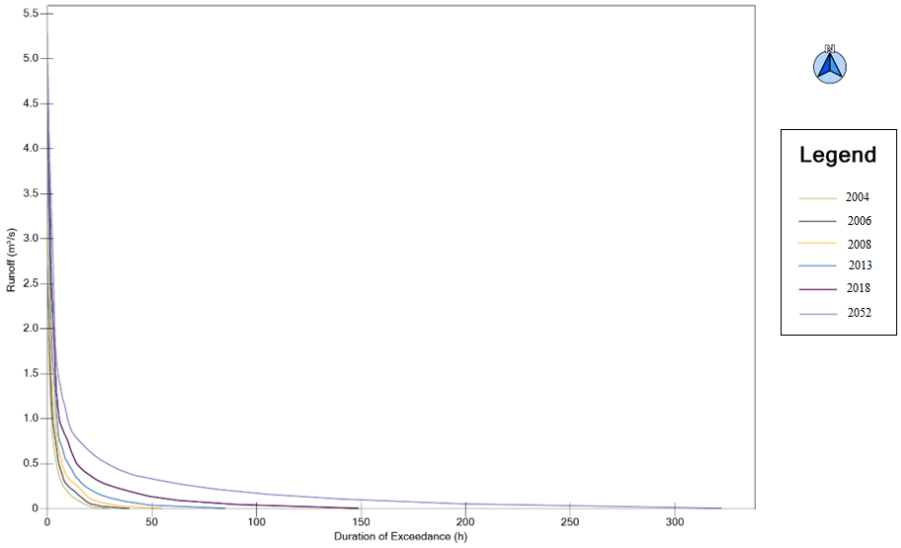

Figure 6.16 Comparison of maximum runoff for all the six scenarios

6.6.2 Impacts of Urbanization on Q-Mean

An indicator of a typical stream conditions is Q-mean (mean of discharge). Comparing present urbanisation and future urbanisation, the mean flow in the Wadepally catchment grew from 0.15 m3/s to 0.65 m3/s. Q-mean as a whole increased with urbanisation, rising from 45% to 322%. The mean flow was trending upward, and this upward trend may have been caused by increased overland flow as urbanisation limits infiltration. Because of these fluctuations in mean flow, stream conditions may deteriorate and new channels may emerge, creating new floodplains and ultimately posing issues for nearby industries and inhabitants.

6.6 Summary

Flood mitigation and reducing its effects both heavily rely on flood inundation modelling. These models forecast the flood extents and inundation depths. This aids in locating the geographic extent of the affected area and allows for the assessment of the risk to life and property. The Wadepally catchment of Warangal city is simulated for the current study's extreme flood event, and maps of flood inundation and flood danger are created. The modelling findings show that the low-lying locations next to water bodies are at a greater danger of flooding. These low-lying locations have developments that are more vulnerable to flooding. Because water tends to flow and collect in places that are topographically at lower elevations, these areas have been encroached primarily for constructing residential colonies and frequently affected by floods during heavy rains.

CHAPTER 7

Sustainable Urban Drainage systems

7.0 General

Stormwater runoff from metropolitan areas is a major cause of flooding and pollution. Rather than allowing water to soak through the soil, impermeable (asphalt/concrete) land use such as roads, parking lots, and sidewalks provide greater runoff to the stormwater drain. In a short amount of time, the stormwater drains are overloaded, causing floods in metropolitan areas. Flooding pollutes stormwater in the event of a combined sewer drainage system. Urban flood management faces a larger challenge when dealing with a flood in an urbanised watershed. Urban runoff and flooding can be mitigated using a variety of stormwater control strategies.

In order to control stormwater overland runoff, which in turn regulates flood volume and flow rate, one of the surface runoff mitigation and treatment approaches is Stormwater Best Management Practice (BMP). Sustainable drainage systems are widely recommended and used in many parts of the world. The terminology for these systems varies from place to place, but the design ideas are the same. In Europe, the Sustainable Urban Drainage System (SuDS) is used to protect public health, keep valuable water sources from being polluted, and keep biological diversity and natural resources safe for the future. In the United States and Canada, SuDS is called Low-Impact Development (SUDS), which is an approach that encourages the interaction of natural processes with the urban environment to keep and rebuild ecosystems for water management. SuDS focuses on keeping natural features and using them along with small-scale hydrological controls to lessen the bad effects of urbanisation. SuDS for urban stormwater runoff is meant to remediate rain where it falls (at the source). Stormwater SuDS is designed to minimise the volume of stormwater entering drainage systems and to attenuate peak discharge (maximum flow rate) by reducing stormwater volume and increasing the discharge duration. As a result, the urban drainage system's overflow is reduced. Hence, urban floods can be mitigated by using SuDS in storm water network. SuDS can be used to manage stormwater runoff at the property level. Many different SuDS elements have been studied for their efficiency in reducing runoff and in this study, four different elements in SuDS were used, including permeable pavement(PP), infiltration trenches(IT), bioretention cells(BC), and rainwater barrel(RB)storage.

With permeable pavements, rainfall can swiftly permeate to an underlying layer of stone through the surface. Reduced runoff can be achieved through full or partial infiltration into the underlying soils. Slight depressions underlain by a gravel layer and planted with indigenous plants make up bioretention cells. They are sized so that they can capture a given quantity of runoff volume from an impermeable ground surface. Stormwater volume is reduced, peak flow is reduced, and stormwater quality is improved thanks to the plants' root systems absorbing some water and nutrients while draining through the soil media and ending up in the stone reservoir below. Excavated trenches are lined with geotextile filter cloth and backfilled with stone aggregates. Designed to receive stormwater, the water flows through the filter fabric and into the underlying soil through the gaps between the stones. Barrels are used to collect rainwater that falls on a roof and store it for later use, such as for irrigation. SUDS practises in urban stormwater management, such as Infiltration trenches, porous pavement, rainwater barrels, and bioretention cells are widely employed to decrease the negative impacts of urban stormwater runoff associated with rising impervious surfaces. Hydrological performance of future SUDS practises can be predicted using computer simulations based on realistic models. Soil and Water Assessment Tool (SWAT), EPA Personal Computer Stormwater Management Model (PCSWMM), U.S. Environmental Protection Agency's (EPA) System for Urban Stormwater Treatment and Analysis Integration (SUSTAIN) and HEC-HMS are some of the most extensively used models. PCSWMM is considered one of the most promising hydrological models for capturing the significantly varied hydrological properties of SUDS in undeveloped and developed urban environments. The PCSWMM was used to model the hydrological performance of the SUDS elements in this study. The concept of SUDS to reduce onsite runoff discharge from the research site are the focus of this investigation.

7.1 Methodology

The aim of the study of this objective is reduction in runoff volume by increasing pervious area percentage, which reduces flooding risk. As the concept of SuDS is applicable to infiltrate and store the rain and runoff that drains into it, various SUDS controls are introduced to reduce the impervious area coverage. In the previous chapter, the PCSWMM storm drainage network is used for the simulation. Each subcatchment is studied and assigned a type of SuDS based on the requirement. SuDS controls within a PCSWMM project is a process that assigns any desired mix and sizing of these

controls to selected subcatchments. The study proposed four SuDS controls, including bioretention cell, infiltration trench permeable pavement and a rain barrel storage facility. As seen in the LULC classification in the chapter 5, the study area is covered by builtup area, which is impervious in nature. The study area is referred to as No-SuDS scenario prior to the introduction of SuDS. Post SuDS development refers to the incorporation of the selected SuDS into both impervious and pervious area.

7.2 Generic SuDS Model

n the PCSWMM model, SuDS controls are represented by a mix of vertical layers that have different properties for each unit of area. This makes it easy to put SuDS in different subcatchments of the study area, even though they cover different amounts of land and have the same design. During a simulation, a moisture balance is maintained to see how much water flows between each SuDS layer. Figure 7.1 shows the typical representation of layers that are used to model a generic SuDS control and the flow path between them.

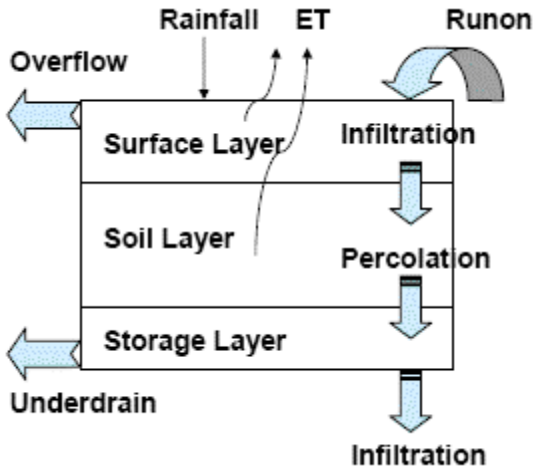

Figure 7.1 SuDS unit layers used in the model.

The possible layers in typical SuDS are as following:

i. The Surface Layer is the ground (or pavement) that includes depressions on the surface where plants are grown in an engineered soil mixture on top of a gravel drainage bed. They store, absorb, and evaporate both rainwater that falls directly on them and water that runs off from surroundings.

ii. Pavement Layer is the porous layer made of concrete or asphalt used in continuous porous pavement systems or in the paver blocks and filler material used in modular systems.

iii. The Soil Layer is the mixture of engineered soil used in bio-retention cells to help plants grow.

iv. The Storage Layer is a bed of gravel and crushed rock that stores water in SuDS controls like bio-retention cells, porous pavement, and infiltration trench systems.

v. The Underdrain System moves water from the gravel storage layer of bio-retention cells, porous pavement systems, and infiltration trenches (usually with slotted or perforated pipes) into a common outlet pipe or chamber. For rain barrels, it is just the drain valve at the bottom of the barrel.

7.2.1 Representation of SuDS controls

i. **Bio retention cells** (Figure 7.2) include depressions on the surface where plants are grown in an engineered mix of soil on top of a gravel drainage bed. They store, infiltrate, and evaporate both rainwater that falls directly on them and water that runs off from other places. The size of a bioretention cell depends on many things, such as the area that drains into it, how well that area drains, how it is used, what kind of soil it is, and more. The size of the bioretention cell needs to be bigger the bigger the drainage area and the more impervious cover there is in that drainage area.

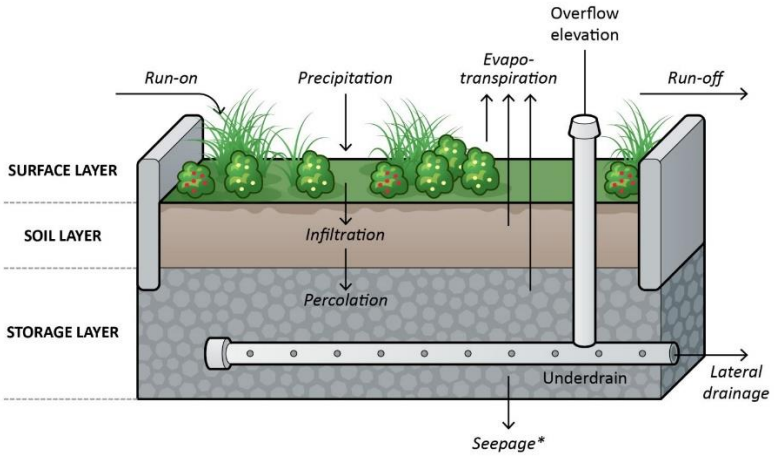

Figure 7.2 Representation of layers in a typical Bioretention cell

ii. **Infiltration trenches** (Figure 7.3) are narrow storage areas beneath granular media that intercepts runoff from upslope impervious areas. Their design function is to

capture and hold runoff for an extended period in order to improve infiltration into the native soil below. To create an underground reservoir, an infiltration trench is provided with a shallow excavated trench lined with a geotextile and backfilled with stone. Stormwater runoff infiltrates the subsoil gradually as it flows into the trench. Extreme rainfall that exceeds the reservoir's capacity may necessitate an overflow.

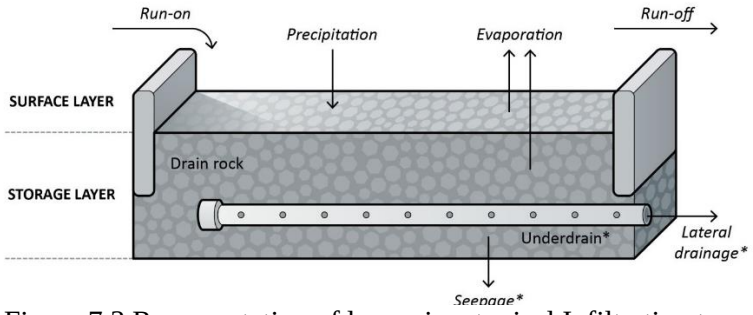

Figure 7.3 Representation of layers in a typical Infiltration trench

iii. **Porous pavement (**Figure 7.4**)** are excavated areas that are filled with gravel and paved with porous concrete or asphalt mix. Normally, all rainfall will immediately pass through the pavement and into the gravel storage layer below, where it will infiltrate into the native soil at natural rates. Impervious paver blocks are placed on a sand or pea gravel bed, with a gravel storage layer beneath. Rainfall collects in the open spaces between the blocks and is carried to the storage zone and native soil below.

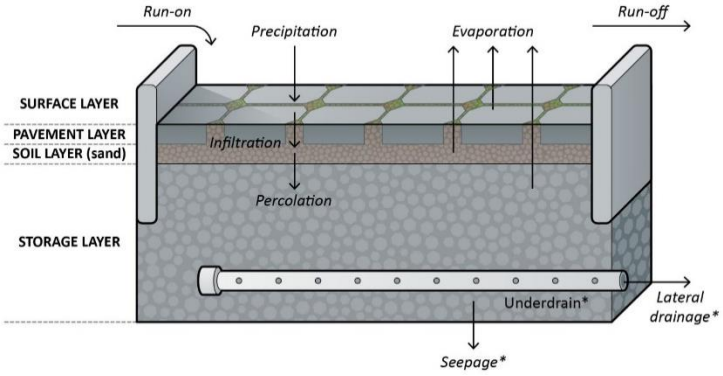

Figure 7.4 Representation of layers in a typical Porous Pavement

iv. **Rain barrels** (Figure 7.5) are containers that collect rainwater from roofs during storms and can either release or reuse it during dry periods. Rain barrels reduce the volume and flow of runoff into sewer or stormwater systems by capturing and storing rainwater. They typically fill up during the first rains of the season and must overflow to a safe disposal location for the duration of the rainy season. Rain barrels work best in garages and outbuildings without basements.

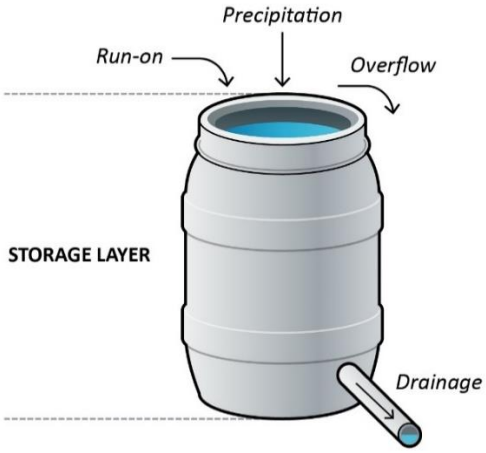

Figure 7.5 Representation of layers in a typical Rain barrel

The Table 7.1 below indicates which combination of layers applies to each type of SuDS control. A portion of the rainfall/runoff storage and water storage evaporation is provided by each SuDS control (except for rain barrels). If an optional impermeable bottom liner is not used, infiltration into native soil occurs in bio-retention cells, porous pavement systems, and infiltration trenches. The overall runoff, infiltration, and evaporation rates computed for the subcatchment as often supplied by PCSWMM represent how well the SuDS controls installed in the subcatchment performed. The hydrological component of the subcatchment where the SuDS is located now receives the surface overflow from SuDS control. Unless another node or subcatchment is provided, flow from the underdrain is directed into the subcatchment's outlet with a SuDS control specified.

Table 7.1 Layers used to model different types of LID units (* means required, 0 mean optional)

LID type	Surface	Pavement	Soil	Storage	Under drain
Bio-Retention Cell	*	-	*	*	0
Infiltration Trench	*	-	-	*	0
Porous Pavement	*	*	-	*	0
Rain Barrel	-	-	-	*	*

7.3 Implementation of SuDS controls in PCSWMM

PCSWMM was used in this study to assess the impacts of urbanization on runoff and flood reduction effects of SuDS practices. PCSWMM allows modeling green infrastructure units like SuDS controls. It is used to model the amount of runoff that comes from the impervious area, mostly. Vertical layers are used to represent SuDS controls and their parameters (such as thickness and infiltration rate) are defined for each unit area of the model. Subcatchments are selected based on the size that can be fitted with these SuDS controls. According to hydrologic features, the whole Wadeppaly catchment is delineated to 23 subcatchments for simulation purposes. The rainfall-runoff process was simulated using a nonlinear reservoir technique, which included infiltration, depression storage, evaporation, and surface runoff. The Curve Number approach was used to mimic infiltration in the model. Two methods can be used to implement SuDS controls in subcatchments.

i. To add one or more controls that will reduce an equivalent quantity of non-SuDS area from an existing subcatchment.
ii. To designate a new subcatchment as a solely SuDS-focused area. To reproduce the ground truth, the first strategy was adopted.

7.3.1 Subcatchments parameters for placing the SuDS controls

When SUDSs are added to a subcatchment, the subcatchments area is the total area of the subcatchment (both non-SuDS and SuDS portions) while the percent imperviousness and width parameters apply only to the non-SuDS portion of the subcatchment. The SuDS Control Editor is used to modify the properties of the SuDS control object's different layers. For each control added, the SuDS Usage Editor is used to specify the size of the control and what fraction of the subcatchments impervious area it captures. The Subcatchment parameters for

different scenarios of SuDS placement for different scenarios are given below. (Table 7.2, 7.3, 7.4)

Table 7.2 Parameters for No LID scenario

Subcatchment	Area (ha)	Imperviousness (%)	Perviousness (%)	Impervious area (ha)	Pervious area (ha)
S1	54.68	55	45	30.074	24.606
S10	8.02	95	5	7.619	0.401
S14	6.74	95	5	6.403	0.337
S15	13.94	95	5	13.243	0.697
S16	4.96	95	5	4.712	0.248
S17	28.15	90	10	25.335	2.815
S19	11.96	99	1	11.8404	0.1196
S21	14.13	50	50	7.065	7.065
S23	10.6	95	5	10.07	0.53

Table 7.3 Subcatchment Parameters for LID placed on impervious area

Subcatchment	Area (ha)	LID in Impervious area (%)	area per unit of LID(ha)	% imperviousness	% perviousness
S1	54.68	10	5.468	50	50
S10	8.02	30	2.406	92.857	7.142
S14	6.74	30	2.022	92.857	7.142
S15	13.94	30	4.182	92.857	7.142
S16	4.96	30	1.488	92.857	7.1428
S17	28.15	35	9.8525	84.615	15.384
S19	11.96	50	5.98	98	2
S21	14.13	20	2.826	37.5	62.5
S23	10.6	30	3.18	92.857	7.142

Table 7.4 Subcatchment parameters for LID placed in pervious area

Subcatchment	Area (ha)	LID in Impervious area (%)	area per unit of LID(ha)	% imperviousness	% perviousness
S1	54.68	5	5.468	61.111	38.888
S10	8.02	1	0.0802	95.959	4.0404
S14	6.74	1	0.0674	95.959	4.0404
S15	13.94	1	0.1394	95.959	4.0404
S16	4.96	1	0.0496	95.959	4.0404
S17	28.15	2	0.563	91.836	8.1632
S19	11.96	0	0	99	1
S21	14.13	15	2.1195	58.823	41.176
S23	10.6	1	0.106	95.959	4.0404

7.3.2 Design parameters in layers of the SuDS controls

To see if SuDS can effectively manage flood in the research region, the scenarios, both before and after the development of SuDS, were modelled. Based on the availability of suitable sites, SuDS controls are placed in the study area. A SuDS storage capacity or overflow components allow surface runoff from impermeable surfaces to flow into and out of them. The attributes of SuDS are defined per-unit-area basis in the model, which is represented as many vertical

layers. Based on (Rossman, 2015) approach, the SuDS parameter values were developed. Once these SuDS have been selected, they can be put in any subcatchment at any desired size using aerial coverage. Design parameters for each layer as specified in Figure 7.1 were given for different SuDS controls

Table 7.5 Design parameters used in IT

Layer	parameter	min	max	unit	values considered
Surface	Berm height	0	300	mm	0
	roughness	0.0012	0.03	Mannings 'n'	0.24
	slope	0	10	%	5
Storage	thickness	900	3650	mm	950
	void fraction	0.2	0.4	-	0.4
	seepage rate	7.2	72	mm/h	72

Table 7.6 Design parameters used in RB

Layer	parameter	units	values considered
Storage	thickness	mm	48
Underdrain	Flow coefficient	mm/hr	1
	Offset height	mm	0
	Flow exponent	-	0.5
	Drain Delay	hrs	6

Table 7.7 Design parameters used in BC

Layer	parameter	min	max	unit	Values considered
Surface	Berm height	150	300	mm	170
	Vegetation volume	0	0.2	fraction	0.1
	roughness	0.04	0.35	Mannings 'n'	0.2
	slope	0	10	%	0.2
Soil	thickness	300	2000	mm	350
	Porosity	0.3	0.55	Volume fraction	0.5
	Field capacity	0.01	0.2	Volume fraction	0.2
	Wilting point	Volume fraction			0.1
	Conductivity	50	140	mm/hr	50
	Conductivity slope	30	55	-	40
	Suction head	50	100	mm	75
Storage	thickness	150	1500	mm	170
	void fraction	0.2	0.4	-	0.4
	seepage rate	7.2	72	mm/hr	0.4

Table 7.8 Design parameters used in PP

Layer	parameter	units	Values considered
Surface	Berm height	mm	170
	Vegetation volume	fraction	0.1
	roughness	Mannings	0.02
	slope	%	2
Soil	thickness	mm	8
	Porosity	Volume fraction	0.25
	Field capacity	Volume fraction	0.2
	Wilting point	Volume fraction	0.1
	Conductivity	mm/hr	0.5
	Conductivity slope	%	10
	Wetting from Suction head	mm	3.5
Pavement	Thickness	mm	150
	Void Ratio	Voids/solids	0.16
	Impervious Surface fraction	mm/hr	0
	Permeability	mm/hr	100
Storage	thickness	mm	12
	void fraction	Voids/solids	0.75
	seepage rate	mm/hr	600
Underdrain flow	coefficient	mm/hr	0.69
	exponent	-	0.5

7.3.3 Design storm

In order to develop the rainfall runoff model to reduce the runoff for the Wadeppaly catchment is considered for the placements of SuDS controls The three scenarios No SuDS, SuDS placed in impervious area and the SuDS placed in pervious area are simulated for 2year and 5 year return period as per the IDF curves generated in the chapter 6. The intensities of 2 year and 5-year return period are 31.991 mm/hr, 57.348 mm/hr, considering the above scenarios runoff is generated and variations area studied.

7.4 Runoff simulation for different scenarios analysis (w.r.t to design storm and combination of SuDS)

SuDS scenarios were simulated using PCSWMM to evaluate the projected runoff volume reduction. The model was re-run for multiple scenarios with the individual SuDS and combined SUDS scenarios in place. As per the table 7.9, the individual placement of Bioretention cell has reduced the volume of runoff by 19 % in subctachment S21 and 33% in

outfall. The mixed combination of four SuDS has also reduced the runoff by 11% in S23 and 22% in outfall. Figure 7.6 shows the peaks in runoff volume for different combinations for a 2-year event. As per the table 7.10, the individual placement of Bioretention cell has reduced the volume of runoff by 19% in conduit c31 and 21% in outfall. The Permeable pavement placement also reduced the volume by 20% in S23. Figure 7.7 shows the peaks in runoff volume for different combinations for a 2-year event. When compared to scenarios, where SuDS is placed in impervious area and pervious area for a 5yr storm event, the results indicate that, No SuDS scenario has the highest runoff values, mixed SuDS scenario followed by the bio retention cell scenario has the highest runoff reduction and its performance remain same in all subcatchments except for S1, S17. Under the infiltration trench scenario, except for subcatchment S10,S15,S23, conduit C31 and Outfall OF all the others have peak flow nearly same to that of no SuDS scenario indicating there is no much effect of infiltration trench. Under permeable pavement w.r.t different subcatchments, peak flow values for SuDS placed in pervious area are more.

Permeable pavement scenarios typically have the biggest impact on lowering flood volume during storms. It has the least amount of storage because it takes up a fifth of the total amount of space that is available (150 mm). Using an infiltration trench with an effective storage depth of 750 mm, it is possible to store all stormwater flow. The infiltration trench is one of the most successful SuDS for lowering flood volume in the three storm events under study, despite having the smallest installed area (0.2 percent). Rain barrel storage, despite its tiny area of 0.5 percent, has the second-highest influence on flood volume reduction in all types of storm events due to the biggest effective storage depth of 1000 mm. Efficiency of the SuDS in reducing runoff volume is influenced by surface area, vertical storage, and drainage area. High catchment area values that are more than the drainage capacity are taken into account by the model. Stormwater can only be temporarily stored in SuDS up to a specific point before the storage layer infiltrates it.

Table 7.9 Runoff comparison within sub catchments for SuDS controls placed in impervious area for 2-year storm event

Subcatchment	NO LID	BC	IT	PP	Mixed
S1	1.077	1.062	1.017	1.059	1.017
S10	0.2358	0.2023	0.2089	0.2091	0.2089
S14	0.1889	0.1857	0.1858	0.1687	0.1859
S15	0.434	0.4211	0.4341	0.4341	0.3509
S16	0.141	0.1369	0.1413	0.1251	0.1414
S17	0.857	0.8358	0.7335	0.8569	0.8353
S19	0.348	0.3484	0.3603	0.3606	0.3118
S21	0.335	0.1763	0.1763	0.1698	0.176
S23	0.329	0.3194	0.329	0.329	0.2685
C31	3.175	2.416	2.901	3.016	2.983
OF	7.539	4.269	6.003	7.273	6.173

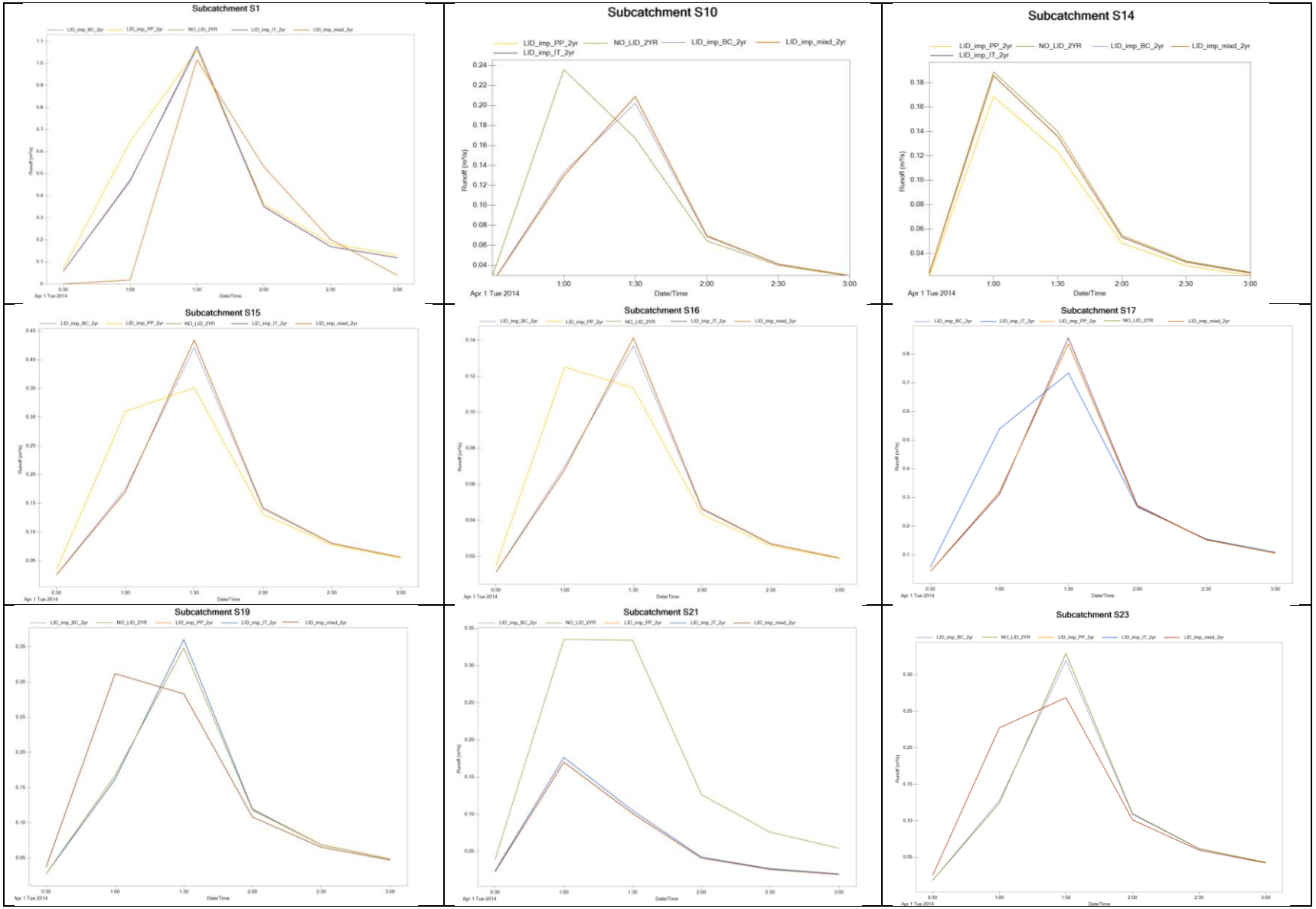

Figure 7.6 Comparison of maximum runoff for all the six scenarios within sub catchments for SuDS controls placed in impervious area for 2 year storm event

Table 7.10 Runoff comparison within sub catchments for SuDS controls placed in impervious area for 5-year storm event

Subcatchment	NO LID	BC	IT	PP	Mixed
S1	1.761	1.649	1.668	1.668	1.059
S10	0.3078	0.2988	0.3078	0.3078	0.2358
S14	0.305	0.305	0.3051	0.1889	0.3052
S15	0.617	0.599	0.6169	0.3509	0.617
S16	0.204	0.198	0.2039	0.1251	0.204
S17	1.228	0.7335	1.228	1.229	1.228
S19	0.3118	0.4974	0.5131	0.5135	0.4974
S21	0.335	0.2831	0.2831	0.2726	0.2726
S23	0.462	0.4489	0.4617	0.2685	0.4619
C31	4.249	2.911	2.416	3.61	3.188
OF	7.135	5.351	4.269	6.161	5.753

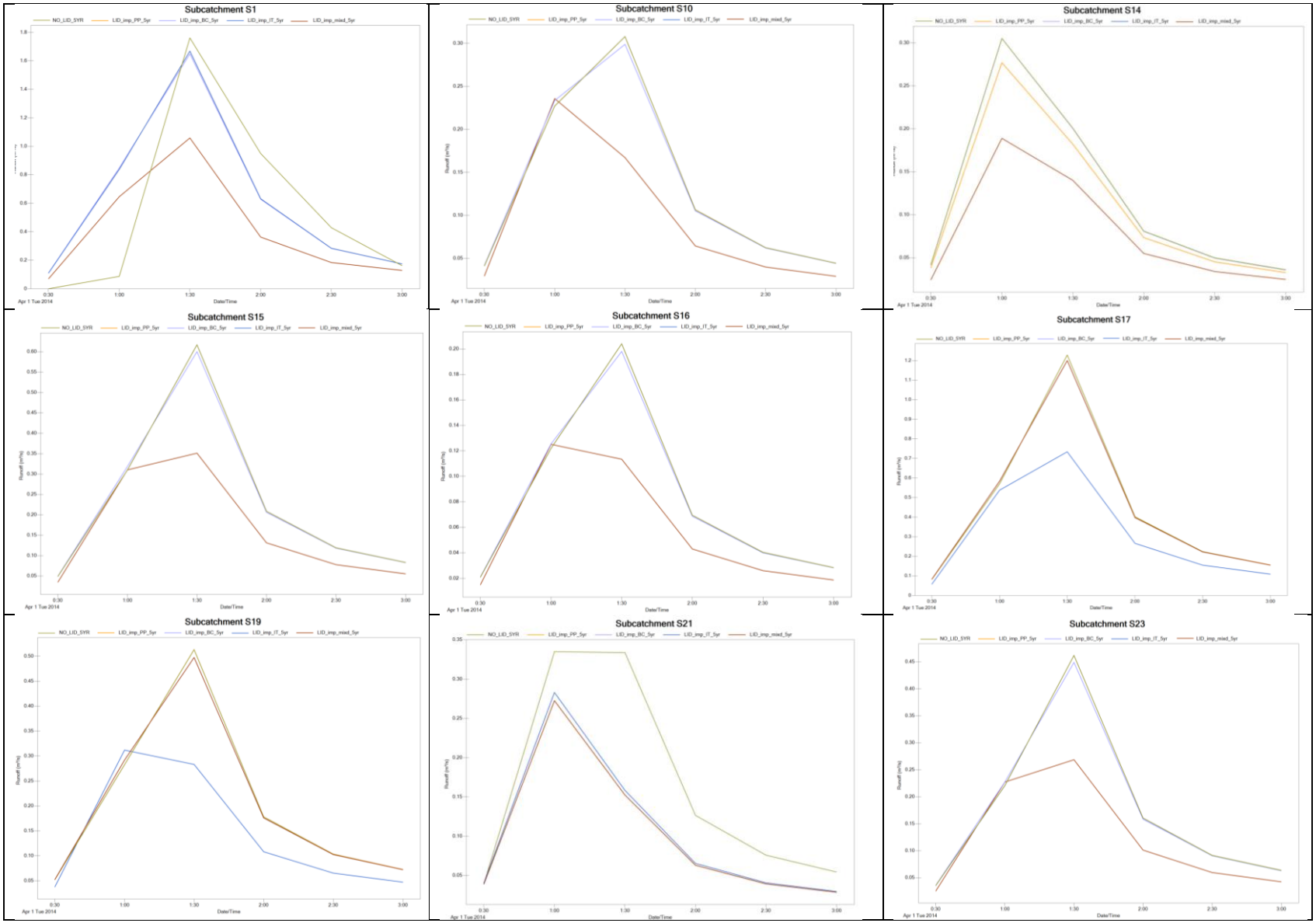

Figure 7.7 Comparison of maximum runoff for all the six scenarios within sub catchments for SuDS controls placed in impervious area for 5-year storm event

Table 7.11 Runoff comparison within sub catchments for SuDS controls placed in pervious area for 2-year storm event

Subcatchment	NO LID	BC	IT	PP	Mixed
S1	1.317	1.296	1.059	1.317	1.296
S10	0.2358	0.2089	0.2161	0.2161	0.2161
S14	0.1889	0.1763	0.1825	0.1825	0.1825
S15	0.3542	0.3542	0.3542	0.3204	0.3509
S16	0.147	0.1423	0.125	0.1471	0.1471
S17	0.923	0.8986	0.9234	0.734	0.9234
S19	0.3661	0.3118	0.3661	0.3118	0.3118
S21	0.335	0.2088	0.2136	0.2137	0.2137
S23	0.3453	0.3349	0.3453	0.2685	0.3349
C31	3.461	2.964	2.416	3.095	3.455
OF	8.89	5.328	8.75	5.519	4.269

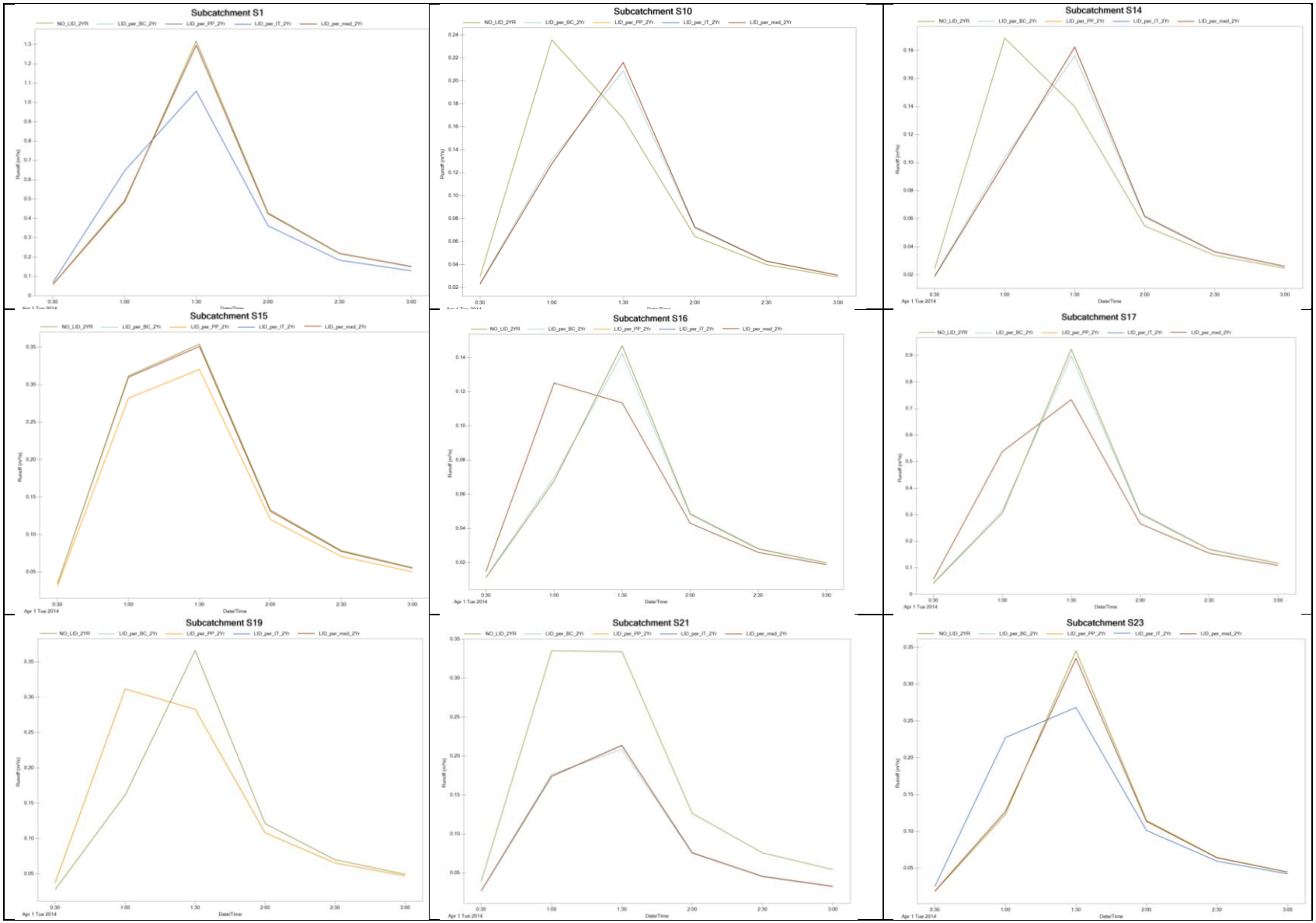

Figure 7.8 Comparison of maximum runoff for all the six scenarios within sub catchments for SuDS controls placed in pervious area for 2-year storm event

Table 7.12 Runoff comparison within sub catchments for SuDS controls placed in pervious area for 5-year storm event

Subcatchment	NO LID	BC	IT	PP	Mixed
S1	1.975	1.946	1.975	1.975	1.059
S10	0.316	0.3066	0.236	0.3163	0.3163
S14	0.256	0.189	0.2645	0.2645	0.2645
S15	0.541	0.541	0.351	0.4902	0.541
S16	0.211	0.2043	0.2107	0.125	0.2107
S17	1.305	1.272	1.305	1.305	0.734
S19	0.521	0.523	0.312	0.523	0.521
S21	0.335	0.3049	0.3113	0.3114	0.3114
S23	0.484	0.4701	0.269	0.4838	0.4701
C31	4.038	3.069	2.416	3.145	3.687
OF	7.096	4.269	6.947	6.924	6.9

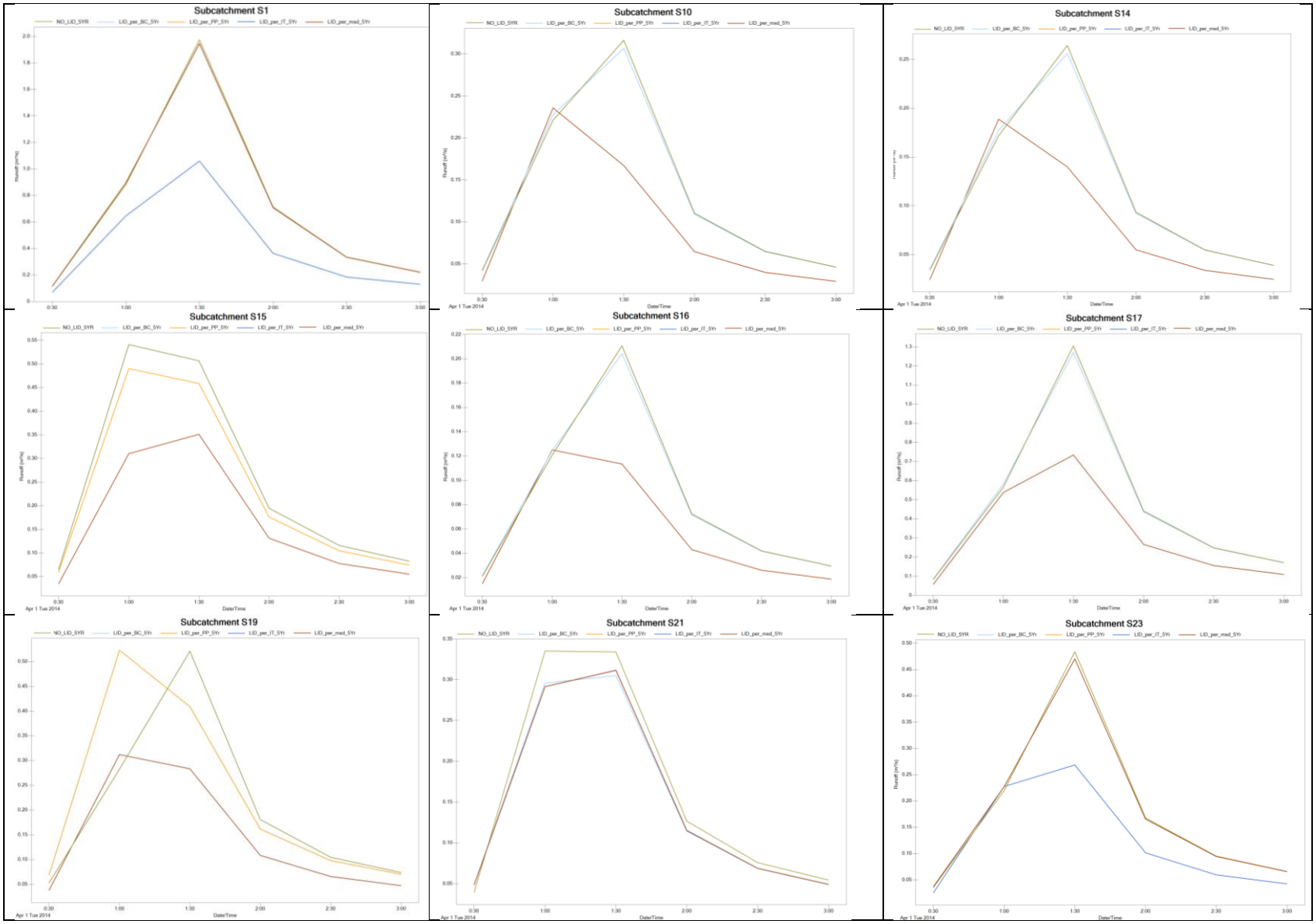

Figure 7.9 Comparison of maximum runoff for all the six scenarios within sub catchments for SuDS controls placed in pervious area for 5-year storm event

7.5 Summary

Runoff from impermeable surfaces is the primary source of stormwater flow from the urban area. Using SuDS procedures on impermeable lots can reduce many of these negative effects. In order to lessen runoff from impermeable surfaces, SuDS are being investigated as an alternative to traditional runoff management strategies. The SuDS material absorbs the collecting runoff, which subsequently seeps into the groundwater. Small local changes can significantly increase the catchment's ability to reduce runoff, lowering the risk of flooding. SUDS has a considerable impact on water runoff in this particular catchment region, with average reductions of 10%, 21%, and 32%, respectively, for the three techniques. When it came to reducing runoff, Bioretention cells outperformed the combinations. When selecting SUDS procedures, cost-effectiveness is critical. In addition to SUDS components, it's important to improve storm drainage systems. When linked to traditional drainage systems, SUDS can control stormwater runoff well in a future with more people living in cities. There are some disavtnages to this study that involve addressing the uncertainties caused by global climate models and a lack of data, as well as taking into account extreme rainfall events in urban flooding applications. In this study, the drainage area is studied on a site-scale instead of a catchment-scale, so the individual SUDS efficiency estimates are very different from those in the literature. The study's conclusion is that adopting many SuDS controls at once is more effective than adopting just one SUDS at a time. One way to keep all of the runoff from the catchment is to make the SUDS storage volume bigger.

CHAPTER 8
Conclusions

8.0. General

From the four phases of the study, it can be summarized that flood hazard mapping gave good results of which area is highly affected with flood. The prediction of LULC using ANN showed accurate results to an extent related to the expansion of urbanization. To assess the existing conditions of the urban drainage a model was developed to show the volume of runoff turning into flood. Finally, the mitigation measure adopted for the reduction of volume of runoff was very helpful at the local level study. The development of a framework will enable global as well as localized units to provide data for periodic maintenance during the times of flood. Based on the four phases of investigation, the following conclusions can be drawn.

8.1 Objective 1

This article analyses the first component of flood risk management that is starting to find out where floods are likely to happen in Warangal Municipal Corporation. This research aimed to map the Flood Hazard zones using GIS and available spatial data sources, where mitigation measures are to be taken. An integrated hierarchical structure through the AHP method with GIS was effectively connected in calculating Flood hazard index for WMC. In developing this model, seven variable that might cause flood were analysed. SWAT, a 2D hydraulic model was used to create rainfall-runoff processes to recreate the impacts of considered rainfall situations. A Flood Hazard map was created by determining the relative weight of flood causative factors. The village administrative boundary was then overlaid on the flood hazard map for each village to determine the villages that are highly prone to flooding. The benefits of this applied technique are found in the ability to incorporate precision, its practical application, advanced yields, and its capacity to keep running for other situations.

8.2 Objective 2

This objective aims to detect and evaluate the Land Use Land Cover and to predict likely the future change in LULC using cellular automata (CA)-Markov chain based simulation. In other words, the results indicate the capability of open-source GIS to run the spatiotemporal analysis for land-use change study. To meet the research objective

of the study, data is prepared in a QGIS environment. LULC values of the images in 2004, 2006, and 2018 were classified into four classes: barren, built-up, vegetation, and waterbodies. These images were used to project the likely changes in 2052. The outcomes of classification indicate a significant growth of barren and vegetation during the period 2006 to 2018 with a stable decrease of other land cover types in the year 2052, especially waterbodies. The result of the LULC change projection, which was carried out using CA, suggests that residential areas and the public buildings will continue to increase in Warangal and this will have an effect on the other land cover types such as agriculture and waterbodies. An accuracy of more than 80% was obtained in all stages. Once the accuracy was achieved, the LULC predicted was then given as input in the rainfall-runoff model and the runoff was simulated.

8.3 Objective 3

The urban flood events during the period 2000 to 2019 in the Wadeppaly catchment were simulated using the PCSWMM model. In urban flood modelling, the surface flow has equal importance to the conveyance flow, which causes the inundation near drains. The study presents a coupled 1D-2D modelling approach that considers both flows in drains and surface flows to find the inundation depths and areas at risk of flooding. Simulations of flow in the open channel and drainage overflow showed that the model was accurate and performed well. The study area is subdivided into 26 subcatchments to best capture the effect of spatial variability in topography, drainage pathways on runoff generation. The routing portion transports this runoff through a system of channels and regulators during a simulation period of 20 years. Surface runoff takes place if water is not taken by the subcatchments and transported to the final outfall due to impervious surface. Based on both 1-D and 1-D–2-D flow analysis, the key findings are presented herein: The simulation results show that most of the junction nodes are surcharged and are at high risk of flooding. The total precipitation depth over the catchment is 775.5 mm and the simulation results show 92 % of rainfall is converted into surface runoff volume and infiltration loss (110.360 and 31.440 in hectares/mm). Thus, a risk map is generated based on the maximum depth of water rise at the junction nodes. The risk is divided into three classes' Low risk, medium risk, and high risk, and the location of flooding nodes is identified. The stormwater runoff simulations are carried out w.r.t the past, present, and future land use. This represents that the drainage

network of the study area is inadequate to carry the extreme storm runoff during critical rainfall events and there is a need of renovating the old drainage lines and constructing new drainage lines to carry the excess. Using the calibrated and validated PCSWMM model, the study also includes a detailed investigation and analysis of how the catchment will change in the future as the climate, land use, and urban drainage systems change.

8.4 Objective 4

A model with different scenarios is develop to analyse the effects of SuDS implications on reduction of runoff in Wadeppaly catchment where the SUDS structural designs are used in conjunction with the conventional drainage system for stormwater management**.** The analysis included four types of SuDS controls namely: Bioretention cell, permeable pavement, Infiltration trench and Rain barrel. The performances of SuDS (in terms of runoff volume reduction) under three scenarios were tested such as No SuDS (considering the natural drainage system), SuDS placed in the impervious area, SuDS placed in the pervious area. All the three scenarios were simulated for a design storm of 2yr and 5yr return periods. The simulations also include placing the SuDS individually and together. When all the scenarios are compared compared to one another the results indicate that the subcatchments S1 followed by S17 has the highest peak flow for the No SUDS placed scenario. Under the Bioretention cell scenario, runoff reduction is considerable and its performance remains the same in all subcatchments except for two subcatchments. Under the infiltration trench scenario, except for one subcatchment, all the others have peak flow nearly the same as that of no SUDS scenario indicating there is no much effect of infiltration trench. The mixed SUDS scenario has the highest reduction in peak flow followed by permeable pavement w.r.t different subcatchments, indicating that this SUDS is on the favourable side of usage. In most of the scenarios, the permeable pavement scenario has the greatest impact in terms of reducing flood volume as it has the least effective storage capacity (150 mm) with the largest possible area. Despite having the smallest area in the entire watershed (0.3%), the Bioretention cell has the most effective storage capacity (284 mm). The Rain barrel has the second most impact on flood volume reduction in all groups of storm events, because of the largest effective storage depth of 1000 mm.

8.5 Specific Contributions made in this Research Work

1. A methodology is developed that demonstrate the integration Remote Sensing, GIS and hydrological model to analyse the urban flooding.
2. A model is developed to analyse of the catchment's response to past, present and future LULC. The transition is studied using Artificial Neural Network, which made the model more reliable.
3. A step towards sustainability is attempted by using a model wherein the Sustainable Urban Drainage Systems were incorporated to study the flood analysis.

8.6 Future Scope of the Investigation

Further study may be attempted in the following focuses:

- Development of 3D model of the city vulnerable to flood.
- Socio economic causative factors can be considered for flood vulnerability assessment in future.
- Instead of using traditional ANNs, deep learning techniques such as (convolution neural network, long short-term memory neural network) which are highly computational can be chosen for big input datasets.
- Due to the lack of observed data available for the study area, discharge-measuring units are to be installed.
- WebGIS platform for real time flood forecast can be developed for the study area.

CHAPTER 9

References

1. Ab Ghani, A. F., Ali, M. B., Dharma lingam, S., & Mahmud, J. (2016). "Digital image correlation (DIC) technique in measuring strain using open source platform Ncorr". In *Journal of Advanced Research in Applied Mechanics*, vol. 26, no. 1, pp. 10-21.

2. Anna Palla, Ilaria Gnecco, Hydrologic modeling of Low Impact Development systems at the urban catchment scale, *Journal of Hydrology*, Volume 528, 2015, Pages 361-368, ISSN 0022-1694, https://doi.org/10.1016/j.jhydrol.2015.06.050.

3. Apel, H., Martínez Trepat, O., Hung, N. N., Chinh, D. T., Merz, B., and Dung, N. V.: Combined fluvial and pluvial urban flood hazard analysis: concept development and application to Can Tho city, Mekong Delta, Vietnam, *Nat. Hazards Earth Syst. Sci*., 16, 941–961, https://doi.org/10.5194/nhess-16-941-2016, 2016.

4. Bapulu, G. V., & Sinha, R. (2005). GIS in Flood Hazard Mapping: A Case Study of Kosi River Basin, India. GIS Development.

5. Balica, S. F., Popescu, I., Beevers, L., & Wright, N. G. (2013). Parametric and physically based modelling techniques for flood risk and vulnerability assessment: A comparison. Environmental Modelling and Software, 41, 84–92. https://doi.org/10.1016/j.envsoft.2012.11.002.

6. CHI 2013. http://chi2013.acm.org/

7. Callistus TENGAN, and Clinton Aigbavboa (2016). Addressing Flood Challenges in Ghana: A Case of the Accra Metropolis, In: Prof CO Aigbavboa and Prof WD Thwala (Eds). 5th International Conference on Infrastructure

Development in Africa (ICIDA 2016), University of Johannesburg, South Africa, 10-12 July 2016, ISBN: 978-0-86970-795-1, pp 498-504

8. Centre for Research on the Epidemiology of Disasters 2015.
9. CFSR Global Weather Data for SWAT 1979-2014 | SWAT | Soil & Water Assessment Tool. (n.d.). https://swat.tamu.edu/data/cfsr
10. Chen AS, Djordjević S, Leandro J, Savić D (2010) An analysis of the combined consequences of pluvial and fluvial flooding. *Water Sci Technol* 62:1491–1498
11. Choubin B, Moradi E, Golshan M, Adamowski J, Sajedi-Hosseini F, Mosavi A. An ensemble prediction of flood susceptibility using multivariate discriminant analysis, classification and regression trees, and support vector machines. *Sci Total Environ*. 2019 Feb 15;651(Pt 2):2087-2096. doi: 10.1016/j.scitotenv.2018.10.064. Epub 2018 Oct 6. PMID: 30321730.
12. Cone, William C., "Stormwater Management Trends: A review of tools, techniques and methods for design and development of the land with implications for sustainable design" (2005). *Landscape Architecture & Regional Planning Masters Projects*. Retrieved from https://scholarworks.umass.edu/larp_ms_projects/11 [5].
13. CRED. 2000-2005 Disasters in numbers. Brussels: CRED; 2016.
14. Dewan, A.M. and Yamaguchi, Y. (2009) Using Remote Sensing and GIS to Detect and Monitor Land Use and Land Cover Change in Dhaka Metropolitan of Bangladesh during 1960-2005. *Environmental Monitoring and Assessment*, 150, 237-249. http://dx.doi.org/10.1007/s10661-008-0226-5

15. Duran, Z. & Musaoglu, Nebiye & Seker, Dursun. (2006). Evaluating urban land use change in the historical peninsula, Istanbul, by using GIS and remote sensing. Fresenius Environmental Bulletin. 15. 806-810.
16. Eckhardt, Rafael & Silveira, Carlos & Rempel, Claudete. (2013). Temporal evolution of land use and land cover - case study in the bom retiro do sul municipality - rs - brazil. Caminhos de Geografia. 14. 150-161.
17. Ellis, J. B., & Viavattene, C. (2014). Sustainable urban drainage system modeling for managing urban surface water flood risk. *Clean - Soil, Air, Water*, 42(2), 153–159. https://doi.org/10.1002/clen.201300225
18. Estoque, R.C., & Murayama, Y. (2015). Intensity and spatial pattern of urban land changes in the megacities of Southeast Asia. *Land Use Policy*, 48, *213-222*.
19. Falconer, R.H. & Cobby, D. & Smyth, P. & Astle, G. & Dent, J. & Golding, Brian. (2009). Pluvial flooding: New approaches in flood warning, mapping and risk management. *Journal of Flood Risk Management*. 2. 198 - 208. 10.1111/j.1753-318X.2009.01034.x.
20. Fang, X., & Su, D. (2006). An integrated one dimensional and two-dimensional urban stormwater flood simulation model. *JAWRA, Journal of the American Water*, 77042, 713–724. Retrieved from http://onlinelibrary.wiley.com/doi/10.1111/j.1752- 1688.2006.tb04487.
21. Gao, h.; Tang, q.; Shi, x.; Zhu, c.; Bohn, t. J.; su, f.; Sheffield, j.; pan, m.; Lettenmaier, d. P.; wood, e. F. Water budget record from variable infiltration capacity (VIC) model. In: wood, e. F. et al. Algorithm theoretical basis document for terrestrial water cycle data records. Princeton: University of Princeton, 2010. p. 120-173.

22. Gersonius, B., Zevenbergen, C., van Herk, S. (2008). Managing flood risk in the urban environment: linking spatial planning, risk assessment, communication and policy. In: Pahl-Wostl, C., Kabat, P., Möltgen, J. (eds) *Adaptive and Integrated Water Management.* Springer, Berlin, Heidelberg. https://doi.org/10.1007/978-3-540-75941-6_14
23. Grillakis, Manolis & Tsanis, I. & Koutroulis, Aristeidis. (2010). Application of the HBV hydrological model in a flash flood case in Slovenia. *Natural Hazards and Earth System Sciences.* 10. 10.5194/nhess-10-2713-2010.
24. Halmy, Marwa. (2015). Land use/land cover change detection and prediction in the north-western coastal desert of Egypt using Markov-CA. *Applied Geography*. 63. 101-112. 10.1016/j.apgeog.2015.06.015.
25. Halmy, Marwa. (2015). Land use/land cover change detection and prediction in the north-western coastal desert of Egypt using Markov-CA. *Applied Geography*. 63. 101-112. 10.1016/j.apgeog.2015.06.015.
26. Hammond, M. J., A. S. Chen, S. Djordjević, D. Butler, and O. Mark. 2015. "Urban Flood Impact Assessment: A State-of-the-Art Review." *Urban Water Journal* 12 (1): 14–29. doi:10.1080/1573062X.2013.857421.
27. Hoang, L. and Fenner, R.A. (2016) System Interactions of Stormwater Management Using Sustainable Urban Drainage Systems and Green Infrastructure. Urban Water Journal, 13, 739-758.https://doi.org/10.1080/1573062X.2015.1036083
28. Messner, F., & Meyer, V. (2006). Flood Damage, Vulnerability And Risk Perception – Challenges For Flood Damage Research.
29. Ian McHarg 1969, Design with nature ,library
30. Ingle, Pravin. (2017). Hydrological modelling using SWAT. 10-15.

31. Jha, A. K., Bloch, R., & Lamond, J. (2011). Cities and Flooding: A Guide to Integrated Urban Flood Risk Management for the 21st Century.
32. Kourtis, Ioannis & Tsihrintzis, Vassilios & Baltas, Evangelos. (2018). Simulation of Low Impact Development (LID) Practices and Comparison with Conventional Drainage Solutions. Proceedings. 2. 640. 10.3390/proceedings2110640.
33. Kundzewicz, Zbigniew & Buda, Su & Wang, Yanjun & Wang, Guojie & Wang, Guofu & Huang, Jinlong & Tong, Jiang. (2019). Flood risk in a range of spatial perspectives – from global to local scales. *Natural Hazards and Earth System Sciences.* 19. 1319-1328. 10.5194/nhess-19-1319-2019.
34. L. Hoang and R.A. Fenner (2016) System interactions of stormwater management using sustainable urban drainage systems and green infrastructure
35. Lawrence Dingman, S. (2015) Physical Hydrology. Waveland Press, Long Grove.Moscrip and Montgomery 1997
36. Matsa, Mark & Muringaniza, Kudakwashe Collins Ralph. (2010). Rate of land-use/land-cover changes in Shurugwi district, Zimbabwe: drivers for change. *JSDA.* 12.
37. Mugume, S. N., & Butler, D. (2017). Evaluation of functional resilience in urban drainag and flood management systems using a global analysis approach. *Urban Water Journal*, 14(7), 727–736. https://doi.org/10.1080/1573062X.2016.1253754
38. Mujib, Muhammad & Apriyanto, Bejo & Kurnianto, Fahmi & Ikhsan, Fahrudi & Nurdin, Elan & Pangastuti, Era Iswara & Astutik, Sri. (2021). Assessment of Flood Hazard Mapping Based on Analytical Hierarchy Process (AHP) and GIS:

Application in Kencong District, Jember Regency, Indonesia. Geosfera Indonesia. 6. 353. 10.19184/geosi.v6i3.21668.

39. Naboureh, A., Rezaei Moghaddam, M.H., Feizizadeh, B. et al. An integrated object-based image analysis and CA-Markov model approach for modeling land use/land cover trends in the Sarab plain. *Arab J Geosci* **10**, 259 (2017). https://doi.org/10.1007/s12517-017-3012-2
40. Nancy B. Grimm, et al. Global Change and the Ecology of Cities Science 319, 756 (2008); DOI: 10.1126/science.1150195.
41. Okirya M., Albert R., Janka O. 2012. Application of Hec-Hms/Ras and GIS Tools in Flood Modeling: A Case Study for River Sironko. Global journal of engineering, design & technology, 1(2), 19–31.
42. Panos, Chelsea & Hogue, Terri & Gilliom, Ryan & Mccray, John. (2018). High-Resolution Modeling of Infill Development Impact on Stormwater Dynamics in Denver, Colorado. 4. 10.1061/JSWBAY.0000863.
43. Prosdocimi I, Kjeldsen TR, Miller JD (2015) Detection and attribution of urbanization effect on flood extremes using nonstationary flood-frequency models. *Water Resour Res* 51:4244–4262
44. Rangari, Vinay & Gongunta, R & Nanduri, Umamahesh & Patel, A. & Bhatt, C M. (2018). 1D-2D MODELING OF URBAN FLOODS AND RISK MAP GENERATION FOR THE PART OF HYDERABAD CITY.
45. Reis, Selçuk. (2008). Analyzing Land Use/Land Cover Changes Using Remote Sensing and GIS in Rize, North-East Turkey. Sensors. 8. 6188–6202.
46. Ronald C. Estoque, Yuji Murayama, Intensity and spatial pattern of urban land changes in the megacities of Southeast Asia, Land Use Policy, Volume 48, 2015,

Pages 213-222, ISSN 0264-8377, https://doi.org/10.1016/j.landusepol.2015.05.017.

47. Semadeni-Davies, A.F., Hernebring, C., Svensson, G., & Gustafsson, L. (2008). The impacts of climate change and urbanisation on drainage in Helsingborg, Sweden: Combined sewer system. *Journal of Hydrology*, 350, 100-113.
48. Tim D. Fletcher, William Shuster, William F. Hunt, Richard Ashley, David Butler, Scott Arthur, Sam Trowsdale, Sylvie Barraud, Annette Semadeni-Davies, Jean-Luc Bertrand-Krajewski, Peter Steen Mikkelsen, Gilles Rivard, Mathias Uhl, Danielle Dagenais & Maria Viklander (2015) SUDS, LID, BMPs, WSUD and more – The evolution and application of terminology surrounding urban drainage, *Urban Water Journal*, 12:7, 525-542, DOI: 10.1080/1573062X.2014.916314
49. Tyler, J., Sadiq, AA. & Noonan, D.S. A review of the community flood risk management literature in the USA: lessons for improving community resilience to floods. *Nat Hazards* 96, 1223–1248 (2019). https://doi.org/10.1007/s11069-019-03606-3
50. Teshome, M.; Devi, A.R. A Review of Recent Studies on Urban Stormwater Drainage System for Urban Flood Management. *Preprints 2020*, 2020100295 (doi: 10.20944/preprints202010.0295.v1).
51. Villarini, G., Vecchi, G. A., Knutson, T. R., and Smith, J. A. (2009), Is the recorded increase in short-duration North Atlantic tropical storms spurious. J. *Geophys. Res.*, 116, D10114, doi:10.1029/2010JD015493
52. Wanhui, Yu., Shuying, Zang., Changshan, Wu., Wen, Liu and Xiaodong, Na (2011). Analyzing and modeling land use land cover change (LUCC) in the Daqing City, China.‖ *Applied Geography*, 31, 600-60.

Publications of the research work

Journals

B Aneesha Satya, M Shashi, Pratap Deva, (2020), "A Pilot Study Of Modeling A City In 3D",*International Journal Of Scientific & Technology Research*, 2020, 9, 3: 2277-8616.

B Aneesha Satya, M Shashi, Pratap Deva, (2020), "Future land use land cover scenario simulation using open source GIS for the city of Warangal, Telangana, India", *Applied Geomatics*, DOI https://doi.org/10.1007/s12518-020-00298.

B Aneesha Satya, Shashi. M, Deva Pratap, (2018) "A geospatial approach to flash flood hazard mapping in the city of Warangal", *Environmental & Socio-Economic Studies*, 2019, 7, 3: 1-13., DOI: 10.2478/environ-2019-0013

Book chapter

B Aneesha Satya, M.Shashi, Deva Pratap, (2019), "Effect of Temporal based Land Use LandCover change pattern on rainfall", Applications of Geomatics in Civil Engineering, Lecture Notes in Civil Engineering 33, https://doi.org/10.1007/978-981-13-7067-0_13,© SpringerNature Singapore Pvt Ltd.

Conferences

B Aneesha Satya, M.Shashi (2022), "Modelling low impact development alternatives for Rainfall runoff reduction using LID concept". International Virtual Conference on Developments and Applications of Geomatics, (DEVA-2022), 29-31 August.

B Aneesha Satya, M.Shashi, Deva Pratap, (2019), "The pilot application of PCSWMM in simulation of urban drainage System -A case study of Warangal city," HYDRO, International Conference on Hydraulics, Water Resources and Coastal Engineering, 18-20 December.

B Aneesha Satya, M.Shashi, Deva Pratap, (2018), "Effect of temporal based land use land cover change pattern on rainfall", An international Conference on Geomatics in Civil Engineering.

B Aneesha Satya, M.Shashi, Deva Pratap, (2017) "Transition Zone identification in the Rural-Urban fringe using High Resolution Satellite Imagery", International

Conference on “Geo- Spatial Technology for Natural Resource Management & Climate Change, National Institute of Rural Development & Panchayat Raj (NIRD & PR), Ministry of Rural Development, Government of India, 21 - 22 December.

B Aneesha Satya, M.Shashi, (2017), “Study of challenge faced by Urban green spaces”, International Conference on Remote Sensing and GIS for applications in Geosciences, Department of Geology Aligarh Muslim University, 12th August 2017.

B Aneesha Satya, M Shashi, (2017). “Urban flood vulnerability impact assessment using microwave data,” International Conference on Urban Geoinformatics, Teri University, New Delhi.

B Aneesha Satya, M Shashi, (2016) “Identification and Mapping of Flash floods in Urban areas using Geospatial Technologies” National Symposium on Recent Advances in Remote Sensing and GIS with Special Emphasis on Mountain Ecosystems, December 7-9, Dehradun, India.